













RESEARCH PAPER



Structure-based optimization of type III indoleamine 2,3-dioxygenase 1 (IDO1) inhibitors

Ute F. Röhrig^{a,†} , Somi Reddy Majjigapu^{a,b,†} , Pierre Vogel^b , Aline Reynaud^c , Florence Pojer^c , Nahzli Dilek^a , Patrick Reichenbach^d , Kelly Ascenção^{a,*} , Melita Irving^d , George Coukos^d , Olivier Michielin^{a,e}  and Vincent Zoete^{a,d} 

^aSIB Swiss Institute of Bioinformatics, Molecular Modeling Group, Lausanne, Switzerland; ^bLaboratory of Glycochemistry and Asymmetric Synthesis, Ecole Polytechnique Fédérale de Lausanne (EPFL), Lausanne, Switzerland; ^cProtein Production and Structure Core Facility, School of Life Sciences, Ecole Polytechnique Fédérale de Lausanne (EPFL), Lausanne, Switzerland; ^dDepartment of Oncology UNIL-CHUV, Ludwig Lausanne Branch, Epalinges, Switzerland; ^eDepartment of Oncology, University Hospital of Lausanne (CHUV), Ludwig Cancer Research-Lausanne Branch, Lausanne, CH-1011, Switzerland

ABSTRACT

The haem enzyme indoleamine 2,3-dioxygenase 1 (IDO1) catalyses the rate-limiting step in the kynurenine pathway of tryptophan metabolism and plays an essential role in immunity, neuronal function, and ageing. Expression of IDO1 in cancer cells results in the suppression of an immune response, and therefore IDO1 inhibitors have been developed for use in anti-cancer immunotherapy. Here, we report an extension of our previously described highly efficient haem-binding 1,2,3-triazole and 1,2,4-triazole inhibitor series, the best compound having both enzymatic and cellular IC₅₀ values of 34 nM. We provide enzymatic inhibition data for almost 100 new compounds and X-ray diffraction data for one compound in complex with IDO1. Structural and computational studies explain the dramatic drop in activity upon extension to pocket B, which has been observed in diverse haem-binding inhibitor scaffolds. Our data provides important insights for future IDO1 inhibitor design.

ARTICLE HISTORY

Received 17 March 2022
Revised 24 May 2022
Accepted 5 June 2022

KEYWORDS

Cancer immunotherapy; structure-based drug design; tryptophan metabolism; X-ray crystallography

Introduction

Immuno oncology provides powerful therapies against cancer in the form of immune checkpoint inhibitors, adoptive cell therapies, monoclonal antibodies, oncolytic viruses, cancer vaccines, and other immuno modulators. However, low response rates due to tumoral immune suppression and resistance remain an unsolved issue¹. L-Trp catabolism along the kynurenine pathway is an important mechanism employed by cancer cells to escape a potentially effective immune response^{2,3}. The rate-limiting step in this pathway is catalysed by indoleamine 2,3-dioxygenase 1 (IDO1) and by tryptophan 2,3-dioxygenase (TDO), with the IDO1 paralogue IDO2 also potentially playing a role^{4,5}. Preclinical data suggests that a combination of IDO1 inhibitors with other anti-cancer agents results in effective anti-tumor immunity^{6–8}. However, in a phase 3 clinical trial of the IDO1 inhibitor epacadostat in combination with pembrolizumab in melanoma patients, the combination failed to increase the overall and progression-free survival when compared to pembrolizumab alone⁹. This failure highlighted the need for a better understanding of the role of the kynurenine pathway, for the development of better IDO1 inhibitors, and for improved trial design^{10,11}. Additional aspects of IDO1 biology are constantly discovered and may influence its role in cancer, such as its signalling activity^{12–14}, regulation by haem

availability¹⁵, nitrite reductase activity in hypoxic tissues¹⁶, involvement in the redox signalling pathways of hydrogen peroxide and singlet oxygen¹⁷, and activation by polysulphides¹⁸. Based on the ongoing interest for IDO1 inhibitors capable of modulating these different pathways and processes selectively, a multitude of small-molecule IDO1 inhibitors have been described^{19,20}, and more than 60 crystal structures of IDO1 have been deposited in the protein data bank (PDB)²¹. These structures with a large diversity of bound cofactors and ligands, including the clinical-stage IDO1 inhibitors epacadostat (**1**, INCB024360, Figure 1A)²³, navoximod (**2**, NLG-919/GDC919)²⁴, EOS200271 (**3**)²⁵, and linrodostat (**4**, BMS-986205)²⁶, yield a wealth of information for inhibitor design²⁷.

We have previously classified IDO1 inhibitors into four types according to their preferential binding and inhibition mechanism²². Type i inhibitors (e.g. 1-methyl-L-tryptophan) preferentially bind to oxygen-bound holoIDO1, type ii inhibitors (e.g. epacadostat) to free ferrous holoIDO1, type iii inhibitors (e.g. navoximod) to free ferric holoIDO1, and type iv inhibitors (e.g. linrodostat) to apoIDO1. Lead optimisation of haem-iron binding type ii and type iii inhibitors has proven difficult due to the selectivity and sensitivity of the haem-ligand interactions to changes in the electronic structure of the ligand²⁸ and due to the small size of the distal haem pocket (pocket A)²⁹, crucial for inhibitor activity. The IDO1

CONTACT Olivier Michielin  Olivier.Michielin@chuv.ch; Vincent Zoete  Vincent.Zoete@unil.ch  SIB Swiss Institute of Bioinformatics, Molecular Modeling Group, Lausanne, CH-1015, Switzerland

*Current address: Chair of Pharmacology, Faculty of Science and Medicine, University of Fribourg, Fribourg, Switzerland

†These authors contributed equally to this work.

 Supplemental data for this article is available online at <https://doi.org/10.1080/14756366.2022.2089665>.

© 2022 The Author(s). Published by Informa UK Limited, trading as Taylor & Francis Group.

This is an Open Access article distributed under the terms of the Creative Commons Attribution License (<http://creativecommons.org/licenses/by/4.0/>), which permits unrestricted use, distribution, and reproduction in any medium, provided the original work is properly cited.

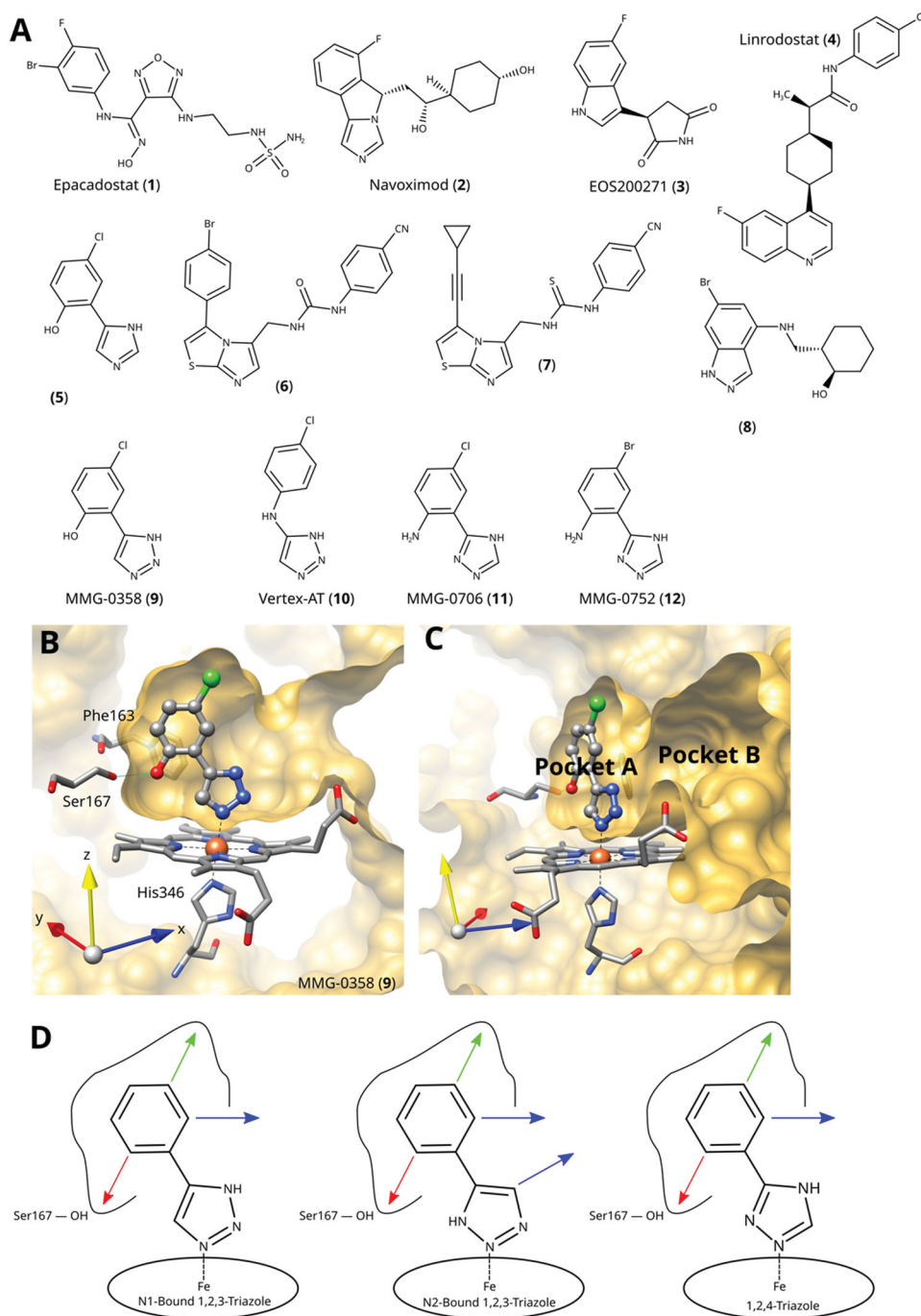


Figure 1. (A) Examples of clinical and other potent IDO1 inhibitors. (B) and (C) Rotated views of the binding pockets A and B in IDO1-active site (PDB ID 6r63²²; ligand MMG-0358). (D) Main lead optimisation strategies pursued in this work. The red arrow denotes a preferentially hydrogen-bonding substituent, the green arrow a hydrophobic substituent, and the blue arrows potential access points to pocket B. As demonstrated before, the acidic hydrogens on the triazole rings are crucial for activity and therefore cannot provide access to pocket B.

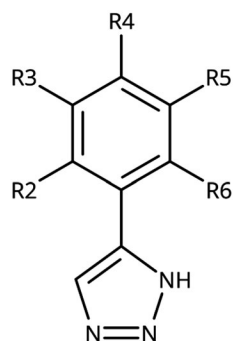
active site further comprises Pocket B, which extends from pocket A towards the entrance of the active site (Figure 1B,C), and whose size and shape are determined by the conformation of the flexible JK-loop²⁷. Although its influence on inhibitor affinity is less pronounced than pocket A, it is of interest for modulation of other compound properties such as specificity, absorption, distribution, metabolism and excretion (ADME), and pharmacokinetics/pharmacodynamics (PK/PD).

Despite the large number of published IDO1 inhibitors, there are only a very limited number of sub-micromolar type ii and type iii inhibitor scaffolds known. Epacadostat (1) binds to the haem iron through an unusual high-affinity hydroxyamidine scaffold,

which was discovered by Incyte^{23,30} and has later been exploited by other groups^{31–38}. Due to its unique tilted iron-binding conformation, it provides a straightforward access to pocket B and allowed the development of numerous nanomolar IDO1 inhibitors with a high selectivity over TDO²⁷. Except for the hydroxyamides, almost all nanomolar haem-binding IDO1 inhibitors are based on a haem-binding free or fused azole scaffold.

Imidazoles are classical haem binders, as present in the haem-binding histidine side chain and in many antifungal drugs, and 4-phenyl-imidazole³⁹ was the first cocrystallized IDO1 inhibitor⁴⁰. Early structure-based optimisation of this chemotype yielded the 2-hydroxy-substituted phenyl derivative as the most active

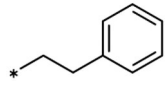
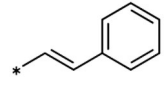
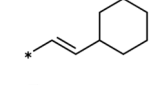
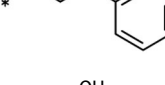
Table 1. 4-Aryl-1,2,3-triazoles with substituted phenyl groups.



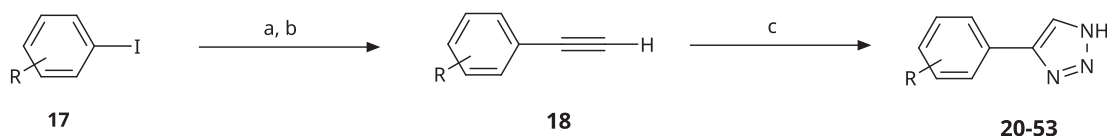
Compound	R2	R3	R4	R5	R6	IC ₅₀ [μ M] (SD ^a)	LE ^b [kcal/mol/HA]
19						10 (1) ²⁸	0.62
20			-OH			>1000	
21						22 ⁵⁸	0.53
22						13 ⁵⁸	0.51
23						280 (20)	0.35
24						34 (-)	0.41
25						>500	
26						>100	
27						>500	
28						>250	
29	-OH					2.3 (0.8) ²⁸	0.64
30				-Cl		0.35 (0.04) ²⁸	0.73
9	-OH			-Cl		0.059 (0.003) ²⁸	0.76
31	-			-Cl		1.5 (0.2) ²⁸	0.61
32	-			-Cl		4.3 ²⁸	0.56
33	-			-		>1000 ²⁸	
34	-OH			-F		0.14 (0.01)	0.72
35	-OH					0.55 (0.05)	0.66
36	-OH					0.25 (0.02)	0.64
37	-OH					0.75 (0.03)	0.56
38	-OH					88 (-)	0.29
39	-OH					160 (-)	0.26
40 ⁶²				-Cl		9.5 (0.8)	0.36

(continued)

Table 1. Continued.

Compound	R2	R3	R4	R5	R6	IC ₅₀ [μ M] (SD ^a)	LE ^b [kcal/mol/HA]
13 ⁶²				-Cl		15 (1)	0.33
41 ⁶²				-Cl		49 (9)	0.29
42 ⁶²				-Cl		260 (50)	0.24
43				-Cl		31 (0.4)	0.29
44	-OH				-OH	13 (3)	0.51
45	-				-OCH ₃	>1000	
46	-Cl			-Cl		6.4 ⁵⁸	0.54
47	-Cl	-Cl				23 ⁵⁸	0.49
48	-Cl		-Cl			31 (0.09)	0.47
49		-Cl	-Cl			51 (4)	0.45
50		-Cl		-Cl		58 (7)	0.44
51	-Cl				-Cl	280 (20)	0.37
52	-Cl		-Cl	-Cl		33 (0.5)	0.44
53	-Cl		-Cl		-Cl	>500	

^aStandard Deviation (SD). ^bLigand Efficiency (LE).



Scheme 1. General synthesis of 4-aryl-1,2,3-triazoles. Reagents and conditions: (a) TMSA, PdCl₂(PPh₃)₂, Et₃N, CuI, dioxane, 45 °C, 5 h. (b) KF, MeOH, rt, 3 h, overall yield 48–85% for 2 steps. (c) TMSN₃, CuI, DMF:MeOH (9:1), 100 °C, 10–12 h, yield 44–85%.

compound⁴¹. Combination of the 2-hydroxy substitution with a 5-chloro substitution led to the most efficient imidazole compound (**5**) with a ligand efficiency (LE) of 0.68 kcal/mol/heavy atom (HA)^{24,28}. In subsequent developments, extending the scaffold to pocket B, a drop in LE was always encountered⁴², but nanomolar activities could be obtained in some 1,5-disubstituted imidazoles^{43,44}. Rigidification of the scaffold to imidazo[5,1-a]isoindole also allowed to retain nanomolar activities^{45–49} and led to the development of navoximod (**2**, Figure 1)²⁴. Independently from the work on imidazo[5,1-a]isoindoles, structural and functional data of imidazo[2,1-b][1,3]thiazole based IDO1 inhibitors was disclosed in 2014 (**6**)⁵⁰. Subsequent work on this fused imidazole scaffold led for example to compound **7** with a good enzymatic activity and a LE of 0.41 kcal/mol/HA⁵¹. However, compounds with this scaffold lack cellular activity^{51–53}.

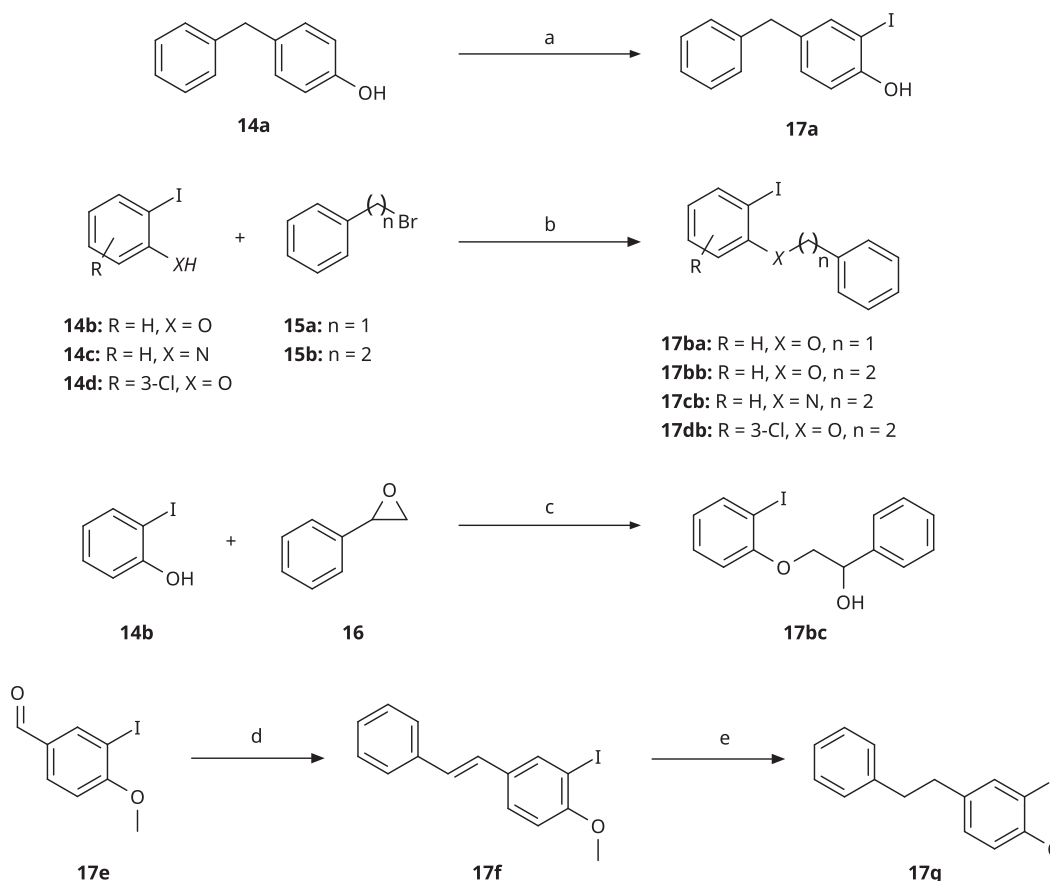
Indazoles are also known haem binders, and the indazol-4-amine scaffold developed by Iomet Pharma⁵⁴ yielded selective nanomolar TDO inhibitors and dual IDO1/TDO inhibitors^{55–57}. X-ray structures of the complexes between IDO1 and some indazol-4-amines such as compound **8** have recently been resolved⁵⁷. These compounds provide access to pocket B while preserving a LE of up to 0.47 kcal/mol/HA.

We have previously discovered 1,2,3-triazoles as highly efficient IDO1 inhibitors and resolved the X-ray structure of MMG-0358 (**9**) in complex with IDO1 (Figure 1)^{22,28,29,58}. Compound **9** forms a direct bond to the haem iron, a hydrogen bond with Ser167 through its hydroxy function, and hydrophobic interactions through its chloro substituent, leading to a LE of 0.76 kcal/mol/HA.

A few 4,5-disubstituted 1,2,3-triazoles with nanomolar activities have been reported⁵⁹, but as we detail below, we failed to reproduce these results. Interestingly, the N-phenyl-1,2,3-triazol-4-amine (**10**) developed by Vertex⁶⁰ demonstrates an IDO1 inhibition mechanism distinct from the 4-phenyl-1,2,3-triazoles despite a similar binding mode²².

1,2,4-Triazole is a common haem-binding scaffold present in many antifungal drugs such as fluconazole, and its direct iron binding in sterol 14 α -demethylase (CYP51) is well documented by structural data. However, these 1-substituted 1,2,4-triazoles have been found to be inactive on IDO1, at variance with imidazole antifungals such as miconazole, which showed some activity⁶¹. However, we recently demonstrated that the 3-substituted 1,2,4-triazole scaffold can provide highly efficient IDO1 inhibitors. Two simple substitutions on the 3-phenyl-1,2,4-triazole scaffold improved its inhibitory activity by more than four orders of magnitude from the millimolar to the low nanomolar range, and we provided structural data for IDO1 binding of MMG-0706 (**11**) and MMG-0752 (**12**, Figure 1)²⁸. These compounds feature a 2-amino, 5-halogen di-substituted phenyl ring and display a LE of 0.80 kcal/mol/HA for the bromo compound, to our knowledge the highest LE reported for IDO1 inhibitors to date. Based on molecular modelling and quantum chemical calculations, we were able to explain the improved activity of the 2-amino substituent versus the 2-hydroxy substituent in this scaffold, due to simultaneous intramolecular and intermolecular interactions²⁸.

Here, we describe our efforts to improve and extend compounds comprising the 1,2,3-triazole and 1,2,4-triazole haem-



Scheme 2. Synthesis of aryl iodides. Reagents and conditions: (a) aq. NH_3 , KI, I_2 , DMF, rt, 1 h, yield 50%. (b) K_2CO_3 , DMF, 80 °C, overnight, yield 50–95%. (c) Cs_2CO_3 , DMF, 100 °C, 24 h, yield 60%. (d) $\text{PhCH}_2\text{P}(\text{Br})(\text{Ph})_3$, $[(\text{CH}_3)_3\text{Si}]_2\text{NNa}$, THF, rt. (e) $\text{N}_2\text{H}_4 \cdot \text{H}_2\text{O}$, $\text{FeCl}_3 \cdot 6\text{H}_2\text{O}$, EtOH, 100 °C, 24 h, overall yield 90% for 2 steps.

binding scaffolds, the best new compound (**144**) demonstrating both enzymatic and cellular IC_{50} values of 34 nM. Although this compound and our previously described compounds such as MMG-0358 (**9**), MMG-0706 (**11**), or MMG-0752 (**12**)^{28,58} are highly efficient both in an enzymatic and in a cellular environment, they are very sensitive to even the smallest changes in their chemical structure, and therefore lack available sites to modulate their ADME and PK/PD properties. Analysing the active site structure of IDO1 and the chemical structures of other known IDO1 inhibitors, it would be natural to extend the compounds from pocket A in the haem distal site to pocket B towards the entrance of the active site (Figure 1D). However, azole ligands are not optimally suited to be extended to pocket B due to their preferred orientation, and this extension often leads to a dramatic decrease in activity for many compounds²⁷. Here, we resolve one new X-ray structure of a previously reported triazole extending to pocket B (**13**, MMG-0472), which validates our docking predictions. Based on this new structural data and the measured activities of almost 100 new compounds, we give recommendations for the development of future IDO1 inhibitors.

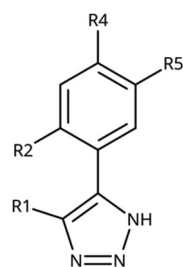
Chemistry

All compounds were synthesised using existing protocols or procedures adapted from the literature. 4-Aryl-1,2,3-triazoles (**20–53**, Table 1) were synthesised according to the method developed by Yamamoto and co-workers⁶³, which involves reaction of ethynyl derivatives (**18**) with trimethylsilyl azide (TMSN₃, Scheme 1). The

ethynyl derivatives were synthesised from iodo substrates (**17**, Scheme 2) by the Sonogashira coupling reaction⁶⁴. Phenols **20**, **39**, and **44** were obtained by demethylation of the corresponding methyl ethers with 48% HBr in water at 100 °C.

5-Substituted 4-aryl-1,2,3-triazoles (Table 2) were obtained according to Scheme 3. Phenyl propynenitrile (**54**) reacted with sodium azide in DMF at 90 °C to produce **62**⁶⁵. Compounds **63** and **68** were obtained from the corresponding aryl benzaldehyde (**55a**, **55b**), nitroethane and ammonium acetate through condensation in presence of acetic acid, followed by dipolar cycloaddition with HN_3 engendered with sodium azide and *p*-toluenesulfonic acid in DMF at 60 °C⁶⁶. The 4,5-diaryl derivative **64** was obtained from 3-chlorobenzaldehyde (**55a**) by reaction with tosylhydrazine (**57**) in ethanol followed by cyclisation with Cs_2CO_3 at 100 °C in DMF⁶⁷. The reaction of ethyl 3-(4-chlorophenyl)propionate (**59**) with sodium azide in DMSO at 60 °C yielded **65**⁶⁸. The reaction of 2-cyanoacetamide (**60**) with aryl benzaldehydes (**55b**, **55c**) in the presence of sodium azide and $\text{Et}_3\text{N} \cdot \text{HCl}$ allowed the formation of triazoles **66** and **67**⁶⁹.

4-Aryl-tether-1,2,3-triazoles (Table 3) were synthesised according to Scheme 4. 4-Arylamino-1,2,3-triazole **78** resulted from treatment of 4-bromoaniline (**69**) with 2-aminoacetonitrile (**70**) and sodium nitrite in 2M HCl at rt first, then by boiling in ethanol⁷¹. Analogues **82**, **83**, **85**, and **86** were derived from the corresponding ethynyl derivative **77** (Scheme 5) and TMSN₃⁶³. Reaction of sulphide **83** with H_2O_2 in the presence of ammonium molybdate in methanol at rt produced sulphone **84**⁷². *O*-methyl oxime **87** was obtained from the corresponding ketone **99** and *O*-methylhydroxylamine hydrochloride in $\text{H}_2\text{O}:\text{EtOH}$ at 70 °C⁷³. The annulated derivative **89** was obtained by

Table 2. 5-Substituted 4-Aryl-1,2,3-Triazoles.

Compound	R1	R2	R4	R5	IC ₅₀ [μM] (SD) ^a	LE ^b [kcal/mol/HA]
61					>1000 ⁵⁸	
62					630 (70)	0.34
63				-Cl	>1000	
64 ⁵⁹				-Cl	>50	
65 ⁵⁹			-Cl		>1000	
66 ⁵⁹			-Cl		800	0.28
67		-OH		-Cl	>1000	
68		-OH		-Cl	220 (7)	0.36

^aStandard Deviation (SD). ^bLigand Efficiency (LE).

treatment of 1,2-indandione-2-oxime (**71**) with hydrazine hydrate and potassium hydroxide at 170–190 °C⁷⁴.

5-Aryl-1*H*-1,2,3-triazoles (Table 4) were obtained according to Scheme 6. Alkynylation of arenecarbaldehyde **90** with ethynylmagnesiumbromide in THF produced the corresponding arylpropargyl alcohol (**91**). The latter underwent dipolar cycloaddition with TMSN₃ in presence of Cul as catalyst (**92a–92u**). Oxidation with pyridinium chlorochromate (PCC) in dichloromethane gave **99–122**^{63,75,76}. Compounds **103–105** were demethylated with 48% HBr in H₂O at 100 °C to produce the corresponding phenols **106–108**. The alkynylation of 4-bromobenzaldehyde with 2-(prop-2-ynoxy)tetrahydro-2*H*-pyran (**93**) in presence of *n*-BuLi in THF at –78 °C yielded the propargyl alcohol **94** after aqueous work-up. **94** was oxidised with MnO₂, followed by hydrolysis to **96** in the presence of pyridinium tosylate (PPTSA). Dipolar cycloaddition of **96** with TMSN₃ (Cul catalyst) in DMF yielded triazole **123**, which was brominated into **124** by reaction with triphenylphosphine and CBr₄ in DMF at rt (Scheme 7A)^{63,77,78}. Triazolomethanamine **126** was obtained from 4-bromobenzoyl chloride and *tert*-butyl prop-2-yn-1-ylcarbamate (**97**), producing ynone **98** in the presence of PdCl₂(PPh₃)₂ as catalyst. **98** reacted with TMSN₃ (Cul catalyst), yielding carbamate **125**. In the presence of trifluoroacetic acid in dichloromethane at rt, carbamate **125** provided the primary amine **126** (Scheme 7B)^{63,79}.

The 3-aryl-1*H*-1,2,4-triazoles (Tables 5 and 6) were prepared according to Scheme 8. Compounds **134–154** and **158–161** were prepared by reaction of the respective carbonitrile **130** with formic acid and hydrazine hydrate in DMF at 90 °C (Scheme 8A)⁸⁰.

The 1,2,4-triazoles **155–157** were obtained from benzamides **132a–132c** through condensation with *N,N*-dimethylformamide dimethyl acetal (DMF-DMA), followed by cyclisation with hydrazine hydrate in acetic acid at 90 °C (Scheme 8B)^{81,82}. The corresponding carbonitriles and benzamides were prepared according to Scheme 9.

Other 1,2,4-triazoles (Table 7) were prepared according to Scheme 10. 3-(4-Bromophenylamino)-1,2,4-triazole (**166**) was synthesised by reaction of 1-bromo-4-iodobenzene (**163**) with 1*H*-1,2,4-triazole-3-amine in the presence of Cul and K₂CO₃ in DMA at 90 °C⁸³. The annulated derivative **168** was synthesised by the S_N2 displacement of 2-chloroacetamide **165** using thiol **164** in the presence of K₂CO₃ in acetone⁸⁴.

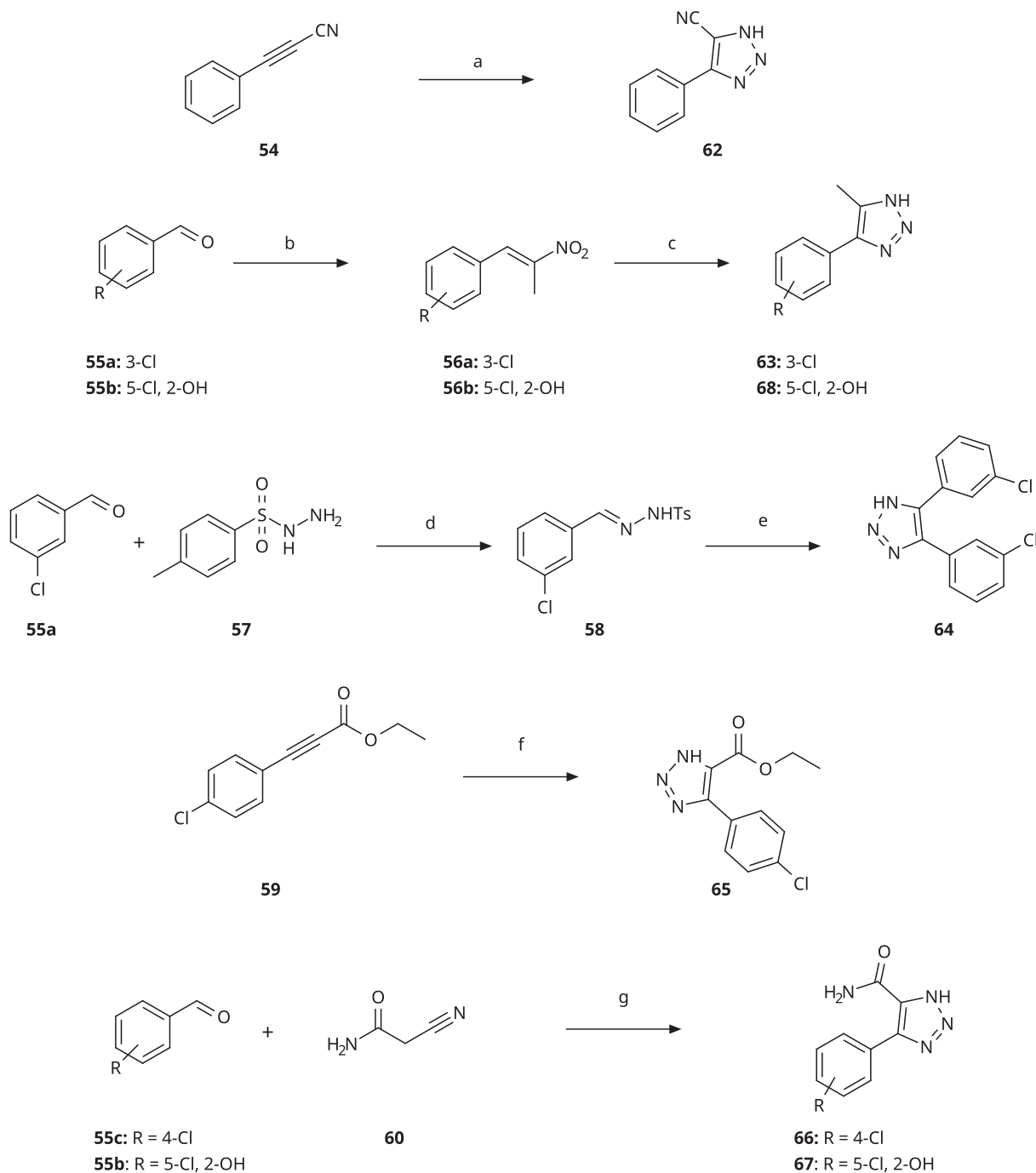
Compounds **9**, **19**, **21**, **22**, **29**, **30**, **31**, **32**, **33**, **46**, **47**, **61**, **81**⁵⁸, **13**, **40**, **41**, **42**⁶², **11**, **12**, **136**, **138**, **169**²⁸, and **10**²² have been described previously by us. Compounds **79**, **80**, **88**, **133**, **139**, **167**, **170**, and **171** were commercially available.

Results and discussion

Structural data

MMG-0472-bound structure

MMG-0472 (**13**, Figure 2) is a 4-phenyl-1,2,3-triazole featuring an extension on the phenyl ring, designed to be located in pocket B. We first described this compound in 2016, when we tested it in cellular assays for hIDO1 and for mIDO2 inhibition. MMG-0472 showed a high cytotoxicity (70% at 200 μM) and was not further pursued for this reason⁶². The mechanism behind this cellular



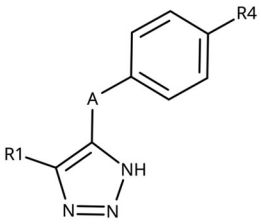
Scheme 3. Synthesis of 5-substituted 4-aryl-(1H)-1,2,3-triazoles. Reagents and conditions: (a) NaN_3 , DMF, 90°C , 3 h, yield 75%. (b) Nitroethane, NH_4OAc , AcOH, reflux, 2 h. (c) NaN_3 , $p\text{TsOH}$, DMF, 60°C , 14 h, overall yield 65–70% for 2 steps. (d) EtOH, rt, 2 h (e) Cs_2CO_3 , DMF, 100°C , 4 h, overall yield 70% for 2 steps. (f) NaN_3 , DMSO, 60°C , 6 h, yield 60%. (g) NaN_3 , $\text{Et}_3\text{N}\cdot\text{HCl}$, DMF, 70°C , 10 h, yield 55–65%.

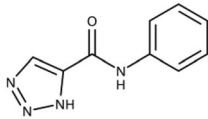
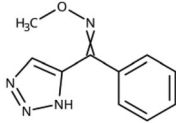
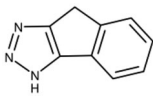
toxicity remains to be clarified and could be due to solubility issues based on our experience with similar compounds. Here, we proceeded to test this compound in the enzymatic assay and found it to be one of the most potent azoles with B pocket extension with an enzymatic IC_{50} value of $14\ \mu\text{M}$ and a LE of $0.33\ \text{kcal/mol/HA}$.

We also investigated compound **13** by X-ray crystallography and obtained diffracting crystals of its complex with IDO1 (PDB ID 7zv3). The $2F_o - F_c$ map of the IDO1 bound ligand clearly shows its electron density in both pockets A and B (Figure 2A). The ligand is non-planar, with the central bond between the triazole ring and

the chloro-phenyl displaying a dihedral angle of 39° . The His346–iron–ligand bond angle is 170° (Figure 2B), deviating by 10° from its optimal value of 180° as determined by density-functional theory calculations on a haem model system (Figure 2C). This deviation probably reflects some strain in the complex. The resolved ligand structure is very close to our docking prediction (Figure 2D) with a root-mean-square distance (RMSD) of $0.3\ \text{\AA}$.

As it can be appreciated from the top view and superimposition with the X-ray structures of triazoles **9**, **11** and **12** (Figure 2D,E), the phenyl ring in compound **13** is rotated away from Ser167 and towards pocket B by about 20° with respect to the phenyl rings of

Table 3. 4-Aryl-tether-1,2,3-triazoles and annulated derivatives.


Compound	A	R1	R4	IC ₅₀ [μM] (SD) ^a	LE ^b [kcal/mol/HA]
10 ⁶⁰	-NH-		-Cl	57 (20)	0.44
78 ⁷⁰	-NH-		-Br	52 (8)	0.45
79	-NH-			>100	
80	-NH-	-phenyl		>250	
81	-CH ₂ -			>1000 ⁵⁸	
82	-O-			>1000	
83	-S-			590 (20)	0.37
84	-SO ₂ -			>1000	
85	-CHOH-			>1000	
86				>1000	
87				>1000	
88				>100	
89				>1000	

^aStandard Deviation (SD). ^bLigand Efficiency (LE).

the other compounds. Therefore, an additional 2-hydroxy substituent on the phenyl ring would not be favourable in these types of compounds, because they would produce a clash between the B-pocket extension and residues 261–265. The structural data for compound **13** thus confirms our previous analysis showing that azole ligands are not optimally suited to extend into pocket B²⁷.

Enzymatic activities

Enzymatic IC₅₀ values were measured with the ascorbate/methylene blue reduction system⁸⁵ in presence of a non-ionic detergent to reduce compound aggregation as described before²⁸. Kynurenine and L-Trp concentrations were determined by HPLC through UV detection. Dose-response curves and Hill slopes can be found in the [Supplementary Information](#) (Figure S2). Generally, IC₅₀ values are slightly lower here than in our first work on 1,2,3-triazoles⁵⁸, as we shortened the incubation time to stop the reaction in its linear phase. If compound solubility allowed, compounds were tested at concentrations up to 1 mM in presence of 5% of DMSO co-solvent.

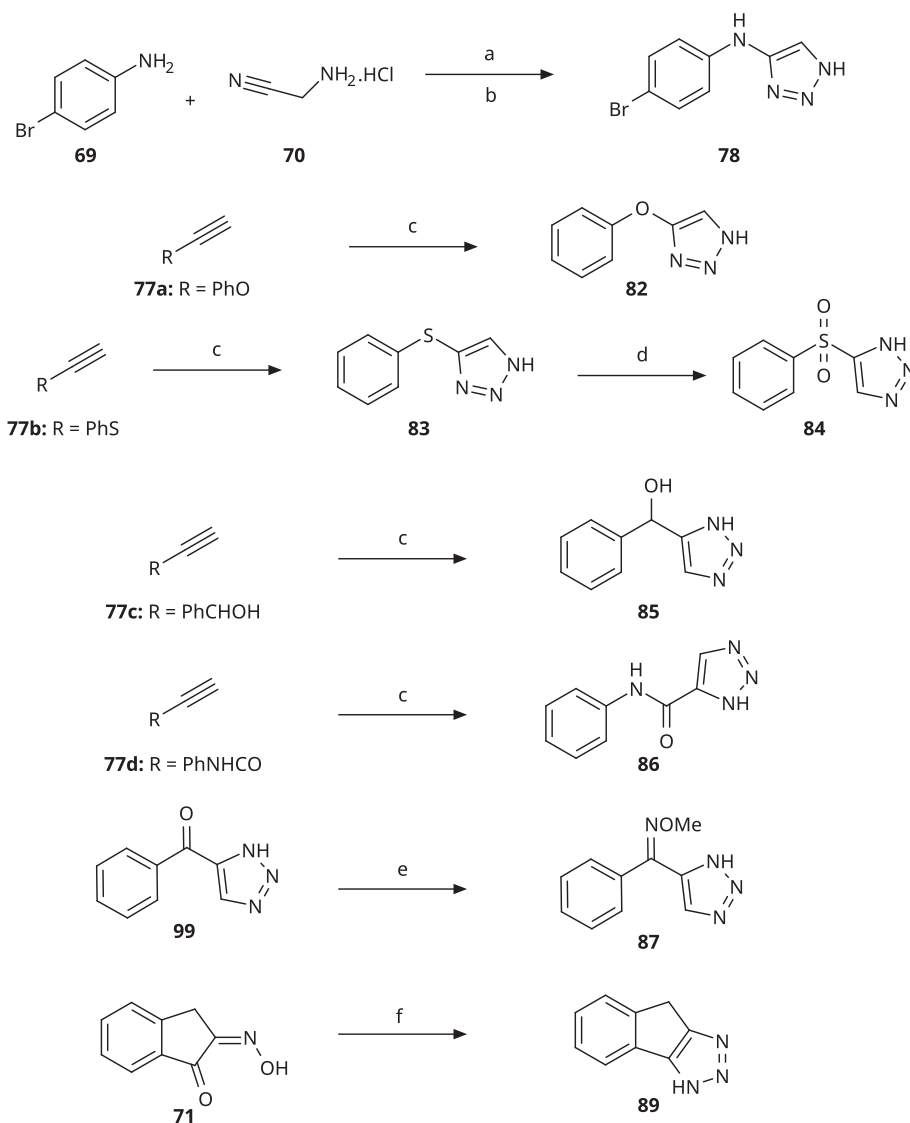
4-Aryl-1,2,3-Triazoles with monosubstituted phenyl groups

We previously showed that 1,2,3-triazoles with *para*-substituted phenyl rings consistently had lower inhibitory activities on IDO1

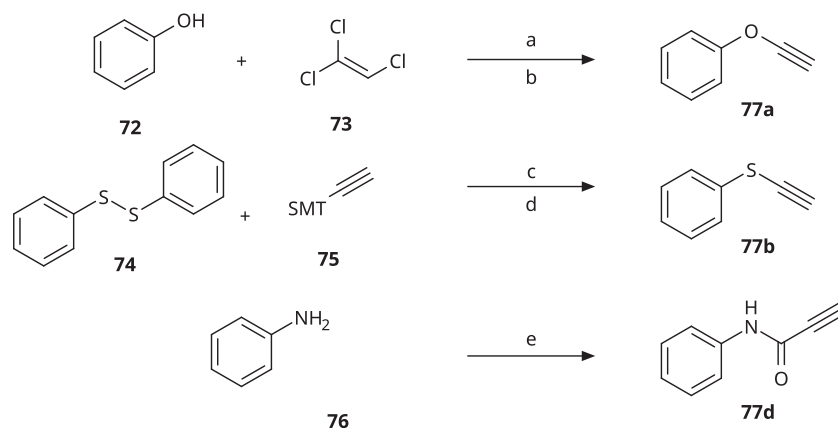
than unsubstituted compounds, their IC₅₀ values increasing from 10 μM (H)²⁸ to 190 μM (F), 530 μM (Cl), 1 mM (CH₃) to above 1 mM (CF₃)⁵⁸ for non-polar substituents. Here, we synthesised and tested one compound with the polar *p*-OH substituent (**20**), which was inactive (Table 1). This result shows that, in agreement with what has been found for imidazoles⁴¹, also polar substituents in this position are unfavourable. This is in agreement with docking predictions, showing little space and hydrophobic groups surrounding *para* substituents (Figure 3A).

On the other hand, we have previously found that non-polar substitutions in *meta* position increased the activity and were most favourable for chloride (0.35 μM)²⁸, while hydroxy (310 μM) and amino (>1 mM) substituents decreased activity⁵⁸. Similar effects were found for substituents in this position in imidazoles^{24,41} and hydroxyamides³⁰. Here, we tested more aliphatic substitutions of different sizes and found the ethyl substituent (**22**, 13 μM, Figure 3B)⁵⁸ to show the best activity, better than methyl (**21**, 22 μM)⁵⁸, *n*-butyl (**24**, 34 μM), and *i*-propyl (**23**, 280 μM, Table 1). For larger substituents, there is not enough space in this position, as suggested by the structural analysis.

Earlier investigations of *ortho* substitutions in the 4-phenyl-1,2,3-triazoles showed that only the hydroxy substituent substantially increased the activity (**29**, 2.3 μM), attributed to the formation of a hydrogen bond with Ser167 in the back of the binding site²⁸. Especially larger substituents, designed for targeting pocket



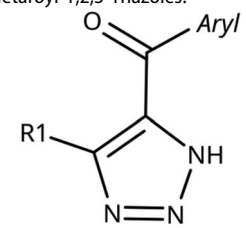
Scheme 4. Aryl-tether-1,2,3-triazoles and annulated derivatives. Reagents and conditions: (a) NaNO_2 , 2M HCl, CH_3COONa , 0 °C-rt, 1 h. (b) EtOH, reflux, overnight, overall yield 70% for 2 steps. (c) TMSN_3 , CuI, DMF:MeOH (9:1), 100 °C, 10–12 h, yield 50–70%. (d) H_2O_2 , $(\text{NH}_4)_2\text{MoO}_4$, MeOH, 0 °C- rt, 14 h, yield 80%. (e) $\text{CH}_3\text{ONH}_2\cdot\text{HCl}$, NaOAc, $\text{H}_2\text{O}:\text{EtOH}$, 70 °C, rt, 15 h, yield 55%. (f) $\text{N}_2\text{H}_4\cdot\text{H}_2\text{O}$, KOH, diethylene glycol, 170–190 °C, 6 h, yield 40%.

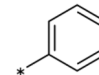
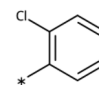
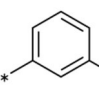
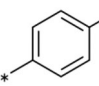
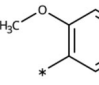
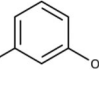
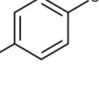
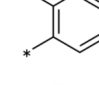
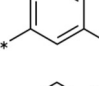
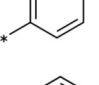
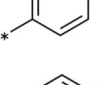
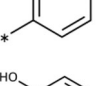
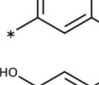
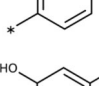
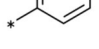


Scheme 5. Synthesis of ethynes. Reagents and conditions: (a) NaOH, DMSO, rt, 4 h. (b) *n*-BuLi, Et_2O , -78 °C-rt, 2h, overall yield 40% for 2 steps. (c) *n*-BuLi, THF, -78 °C-rt, overnight. (d) KF, MeOH, rt, 4 h, overall yield 85% for 2 steps. (e) propiolic acid, DCC, DMAP, Et_2O , rt, 18 h, yield 90%.

B, showed substantially decreased inhibitory activities besides lowering the solubility of the compounds^{58,62}. Here, we show that usage of an ether (**25**, **26**, **27**, Figure 3C) or an amino linker (**28**)

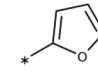
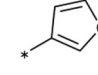
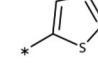
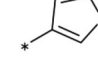
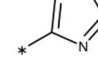
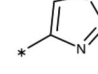
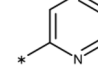
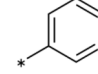
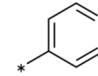
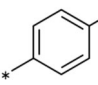
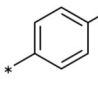
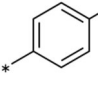
to a large substituent in this position does not yield active compounds either (Table 1). This is also true when introducing a hydroxy group (**27**), expected to increase solubility and allowing

Table 4. 5-Aroyl and 5-Heteroaryl-1,2,3-Triazoles.


Compound	Aryl	R1	IC ₅₀ [μM] (SD ^a)	LE ^b [kcal/mol/HA]
99			430 (60)	0.35
100			>1000	0.20
101			450 (40)	0.33
102			31 (6)	0.44
103			>1000	
104			920 (200)	0.28
105			200 (20)	0.34
106			130 (30)	0.38
107			>1000	
108			>1000	
109			13 (0.8)	0.48
110			190 (10)	0.36
111			370 (30)	0.31
112			11 (0.2)	0.45
113			8.2 (1)	0.46

(continued)

Table 4. Continued.

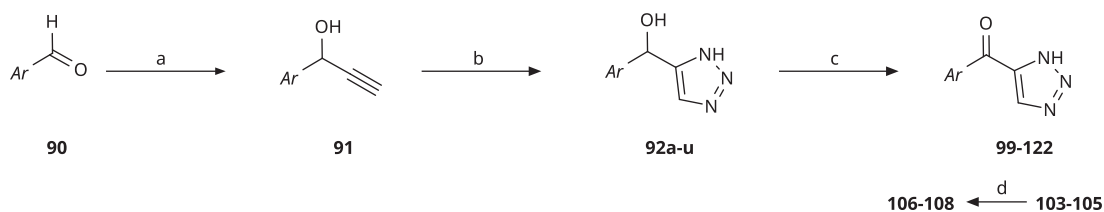
Compound	Aryl	R1	IC ₅₀ [μM] (SD ^a)	LE ^b [kcal/mol/HA]
114			230 (20)	0.41
115			16 (0.7)	0.55
116			17 (1)	0.54
117			68 (3)	0.47
118			82 (6)	0.46
119			510 (100)	0.37
120			>1000	
121			650 (100)	0.33
122			>1000	
123		-CH ₂ OH	>1000	
124		-CH ₂ Br	>1000	
126		-CH ₂ NH ₂	>1000	

^aStandard Deviation (SD). ^bLigand Efficiency (LE).

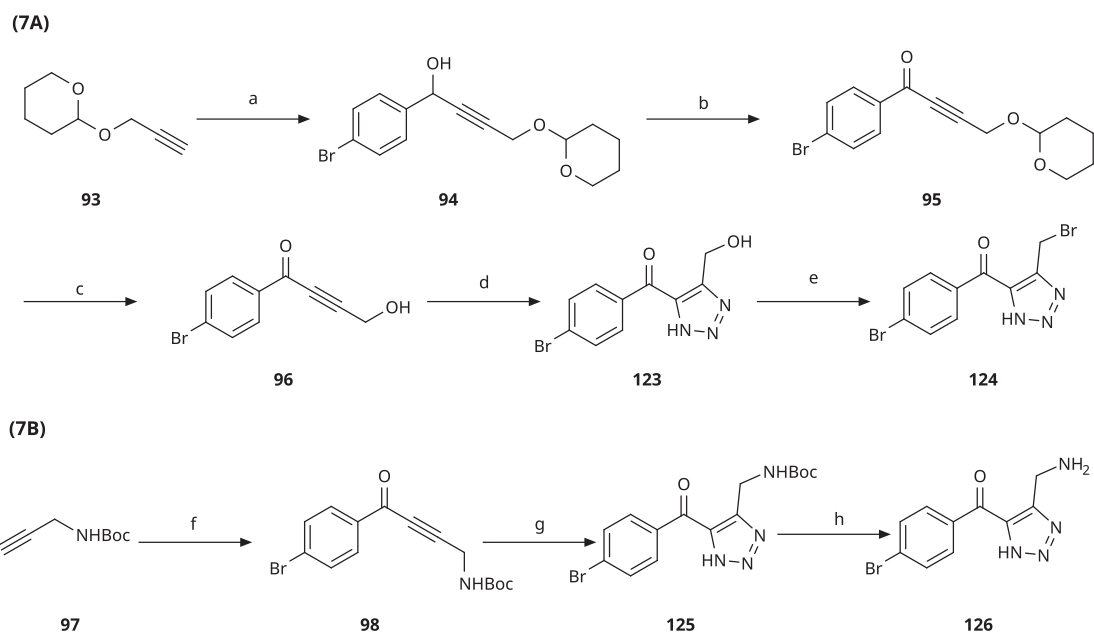
to test the inhibitor at higher concentrations. However, it should be noted that docking predicts that this hydroxy group cannot form favourable interactions within pocket B (Figure 3D).

4-Aryl-1,2,3-Triazoles with double and triple substituted phenyl groups

As described previously, the 2,5-disubstituted compound MMG-0358 (**9**, Figure 1, IC₅₀ = 0.059 μM, LE 0.76 kcal/mol/HA) displayed a very high inhibitory activity, explained by the interactions of its hydroxy substituent with Ser167 and of its chloride substituent with the hydrophobic subpocket around Val125, Cys129, Leu234, and Gly262 as confirmed by X-ray crystallography (Figure 1)^{22,58}. Compounds **31**, **32** and **46** with the 2-hydroxy substituent replaced by amino, methyl, or chloride substituents, were less active but still displayed low micromolar IC₅₀ values, while **33** with inverted polar/non-polar substituents (5-amino-2-methylphenyl instead of 2-amino-



Scheme 6. Synthesis of 5-aryl and 5-heteroaryl-1,2,3-triazoles. Reagents and conditions: (a) ethynylmagnesium bromide, THF, 3 °C-rt, 1 h. (b) TMSN₃, CuI, DMF:MeOH (9:1), 100 °C, 10–12 h, overall yield 55–85% for 2 steps. (c) PCC, DCM, rt, 2 h, yield 35–73%. (d) 48% HBr in H₂O, 100 °C, 14 h, yield 45–50%.



Scheme 7. Synthesis of 4-substituted-5-aryl-(1H)-1,2,3-triazoles. Reagents and conditions: (a) 4-Bromobenzaldehyde, *n*-BuLi, -78 °C to -38 °C, THF, 3 h, yield 88%. (b) MnO₂, DCM, rt, 5 h, yield 97%. (c) PPTSA, EtOH, 50 °C, 4 h, yield 75%. (d) TMSN₃, CuI, DMF/MeOH (9:1), 100 °C, 10–12 h, yield 50%. (e) CBr₄, PPh₃, DMF, rt, 4 h, yield 85%. (f) 4-Bromobenzoyl chloride, PdCl₂(PPh₃)₂, CuI, Et₃N, THF, rt, 1 h, yield 90%. (g) TMSN₃, CuI, DMF/MeOH (9:1), 10 °C, 10–12 h, yield 45%. (h) TFA, DCM, rt, overnight, yield 75%.

5-methylphenyl) was completely inactive⁵⁸. Here, we extended our investigation with 2-hydroxyphenyl derivatives bearing various 5-substituents. 4-Aryl-1,2,3-triazoles with small non-polar 5-substituents up to the size of propyl were inhibitors in the nanomolar range (**34**, **35**, **36**, **37**, LE 0.72 to 0.56 kcal/mol/HA), while analogues with larger substituents such as 5-(2-benzyl) and 5-(2-phenylethyl) (**38**, **39**, LE 0.26 to 0.29 kcal/mol/HA) showed lower activities (Table 1). In our docking approach, only substituents in 5-position up to the size of ethyl docked well (Figure 3E). Other 5-chlorophenyl analogues 2-substituted with longer alkyl chains have been described previously (**13**, **40**, **41** and **42**) but were tested only in a cellular environment on IDO1 and on IDO2⁶². Compound **42** inhibited both human IDO1 and murine IDO2 with a cellular IC₅₀ value of 110 μM. Here, we also measured their enzymatic activities and found them to have a low LE (0.24 to 0.36 kcal/mol/HA). We additionally synthesised and tested 4-[5-chloro-2-(2-phenylethoxy)phenyl]-1,2,3-triazole (**43**), which is also a micromolar inhibitor (31 μM, LE 0.29 kcal/mol/HA, Figure 3F). We also tested two 2,6-disubstituted compounds, **44** (13 μM) and **45** (no inhibition, NI). As in the case of imidazoles⁴¹, the 2,6-di-OH substituted compound is at least 2 orders of magnitude more active than the 2,6-di-OCH₃ substituted compound, but it is less active than the single OH-substituted compound **29**.

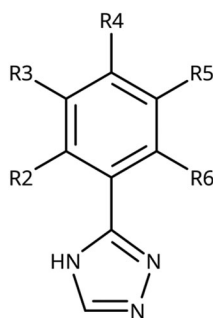
Finally, we synthesised and tested a series of dichloro and trichloro substituted compounds. The most active compound was the

2,5-disubstituted compound **46** (6.4 μM), followed by **47** (23 μM), **48** (31 μM), **52** (33 μM), **49** (51 μM), **50** (58 μM), **51** (280 μM), and **53** (NI). In agreement with the docking predictions, all compounds are less active than the 5-Cl single-substituted compound (**30**, 0.35 μM)²⁸, and the third chloride substituent does not increase activity with respect to the di-substituted compounds.

5-Substituted 4-Aryl-1,2,3-Triazoles

Theoretically, access to the B-pocket could also be achieved through a substitution either of the N3 or the C5 atoms of the 1,2,3-triazole ring (Figure 1D). We explored the possibility of nitrogen substitutions before, without obtaining any active compound⁵⁸. This finding supports the importance of an ionisable NH group in the triazole and the hypothesis that deprotonation of the 1,2,3-triazole is crucial for IDO1 inhibition. Here, we further explored substitution of the C5 atom (Table 2), although this enforces iron binding through the N2 atom (Figure 1D), which has been calculated to be less favourable than binding through the N1 atom^{28,58}. We previously described one compound of this type with a 5-methyl substituent (**61**, NI)⁵⁸. Here, we show that an electron-withdrawing 5-nitrile substitution yielded a slightly active compound (**62**, 630 μM), while combination of the 5-methyl substituent with the 5-Cl substituent on the phenyl ring yielded an

Table 5. 3-Aryl-1,2,4-Triazoles.



Compound	R2	R3	R4	R5	R6	IC ₅₀ [μ M] (SD ^a)	LE ^b [kcal/mol/HA]
133						>1000 ²⁸	
134			-F			>1000	
135				-Br		16 (1)	0.55
136				-Cl		31 (4) ²⁸	0.51
137				-F		160 (20)	0.43
138	-OH					31 (1) ²⁸	0.51
139	-NH ₂					2.0 (0.7) ²⁸	0.65
140	-NH ₂	-F				0.81 (0.2)	0.64
141	-NH ₂	-Cl				29 (3)	0.48
142	-NH ₂				-NH ₂	31 (7)	0.47
12	-NH ₂			-Br		0.020 (0.001) ²⁸	0.80
11	-NH ₂			-Cl		0.035 (0.004) ²⁸	0.78
143	-NH ₂			-F		0.15 (0.006)	0.72
144	-NH ₂		-F	-Br		0.034 (0.004)	0.73
145				-Cl		8.7 (3)	0.49
146				-Cl		420 (90)	0.29
147				-Cl		1.2 (0.04)	0.47
148				-Cl		25 (7)	0.35
149				-Cl		0.49 (0.05)	0.48
150				-Cl		>100	
151				-Cl		>100	
152						>100	
153				-Cl		9.3 (0.3)	0.33
154		-Cl				>1000	

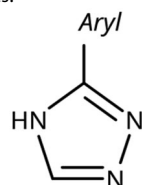
(continued)

Table 5. Continued.

Compound	R2	R3	R4	R5	R6	IC ₅₀ [μ M] (SD ^a)	LE ^b [kcal/mol/HA]
155	-NH ₂			-Br	-CH ₃	63 (10)	0.41
156	-NH ₂			-Cl	-CH ₃	96 (3)	0.39
157	-NH ₂			-Cl	-NH ₂	1.0 (0.02)	0.55

^aStandard Deviation (SD). ^bLigand Efficiency (LE).

Table 6. 3-Hetaryl-1,2,4-triazoles.



Compound	Aryl	IC ₅₀ [μ M] (SD ^a)	LE ^b [kcal/mol/HA]
158		>1000	
159		>1000	
160		16 (7)	0.55
161		10 (2)	0.57
162		250 (10)	0.41

^aStandard Deviation (SD). ^bLigand Efficiency (LE).

inactive compound (**63**, NI). Compounds with this substitution pattern have recently been further explored by Panda and co-workers⁵⁹, who described 11 compounds with nanomolar IC₅₀ values. We synthesised three of the compounds described in this work (original compound numbers: 1d, **64**; 2g, **65**; and 3g, **66**) but could not reproduce the published IC₅₀ values. In our hands, compounds **64** and **65** showed no inhibition of IDO1, although their published IC₅₀ values were 2.51 μ M and 0.39 μ M, respectively⁵⁹. Compound **66**, which has a published IC₅₀ value of 0.62 μ M, showed a weak activity in our tests, with an IC₅₀ value of 800 μ M. The lower activities might be due to higher purities of our compounds and are in line with weak activities measured for other compounds of this type (Table 2). Even combination with the highly activating 2-OH,5-Cl substitutions on the phenyl ring (**67**, **68**) yielded at best a compound with an IC₅₀ value in the high micromolar range.

These compounds cannot meaningfully be docked into the IDO1 active site, the best poses displaying a triazole–haem angle deviating significantly from the optimal angle of 90° (Supporting Information, Figure S1).

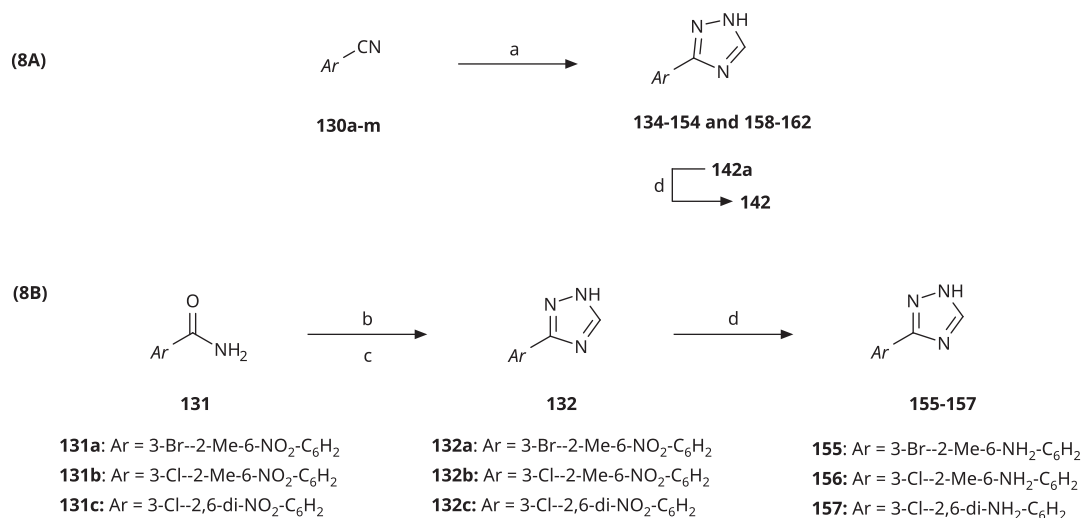
4-Aryl-Tether-1,2,3-Triazoles and annulated derivatives

The 1,2,3-triazole published by Alexandre and co-workers (**10**, Figure 1), which features an amino linker between the triazole

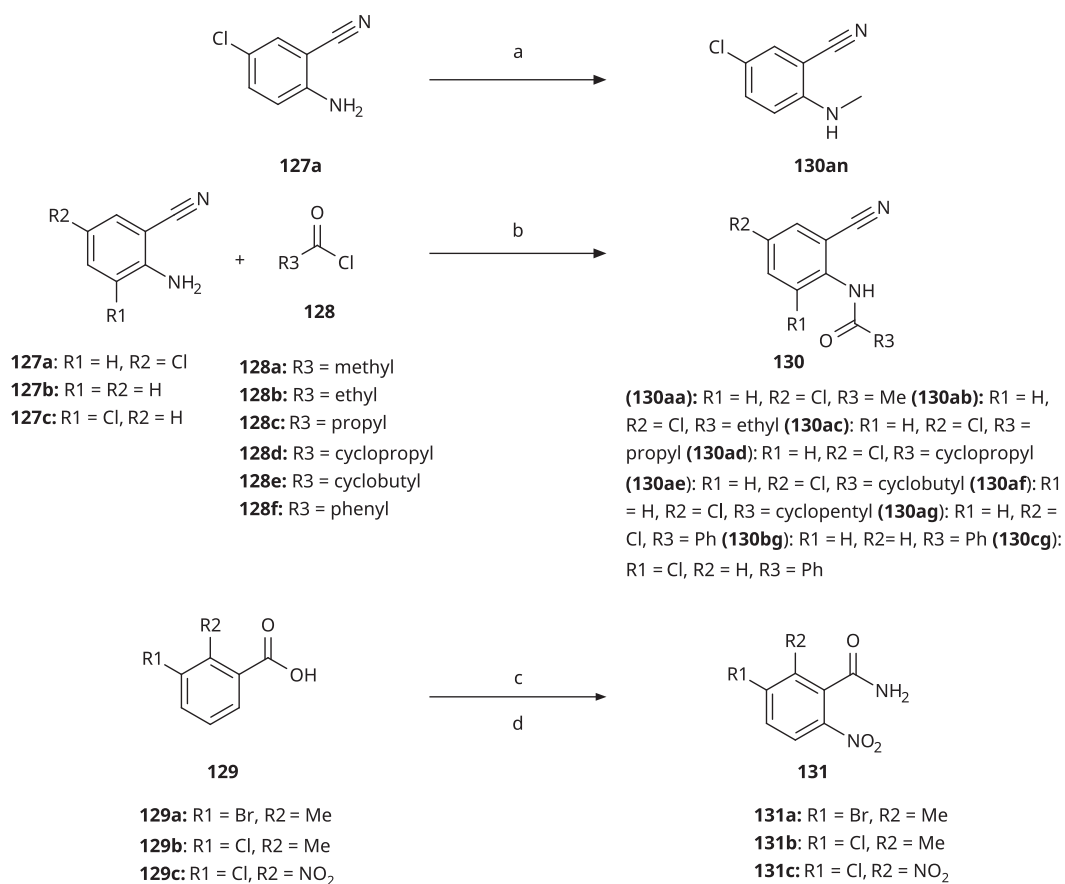
and the 4-chlorophenyl moiety, shows a peculiar behaviour^{60,70,86}. X-ray data demonstrates haem-iron binding and occupancy of pocket A (Figure 4A), but a slow shift of the haem Soret peak in UV-absorption spectra under reductive conditions coupled with haem unbinding and degradation as well as the largely superior activity in cellular assays as compared to enzymatic assays is very distinct from the behaviour of the 4-aryl-1,2,3-triazoles^{22,60}.

Building on these results, we synthesised and tested 1,2,3-triazoles linked to aryl moieties by a one-center tether (N, CH₂, O, S, SO₂, CHOH) or two-atom tether (CONH, Table 3). In our hands, compound **10** displayed an IC₅₀ value of 56 μ M (11.3 μ M in the original publication). 4-(4-Bromophenylamino)-1,2,3-triazole (**78**) showed an inhibitory activity of 52 μ M, whereas the 4-phenylamino analogue (**79**) was not active. These 3 latter compounds dock well into the IDO1 active site, although the phenyl ring adopts a slightly rotated conformation with respect to the X-ray structure (Figure 4B). Compound **80** with an additional phenyl substituent on the C5 of the triazole ring rather docks with the amino linker pointing towards the haem propionate and pocket B but shows no activity in the enzymatic assay (NI, Table 3, Figure 4C), similar to other C5-substituted 1,2,3-triazoles (Table 2).

Replacement of the amino linker by a methylene group (**81**, NI), by an ether group (**82**, NI), by a sulphide group (**83**, 590 μ M, Figure 4D), by a sulfoxide moiety (**84**, NI), by a hydroxymethylene group (**85**, NI) or by a carboxamide group (**86**, NI, Figure 4E) generated inactive compounds except for **83** with the sulphur tether (590 μ M). Compound **87** with a MeON=C linker was synthesised and tested as another possible access point to pocket B but was inactive. The annulated 1,2,3-triazoles **88** and **89** were also inactive. More interesting results were obtained with 5-aryl-1,2,3-triazoles (keto linker), preserving the conjugation and the planarity between the aromatic rings (Table 4). Docking results for compound **99** (430 μ M) suggest that this compound can form a hydrogen bond with Ser167 (Figure 4F), while the keto group simultaneously increases the acidity of the triazole ring. Starting from this 5-benzoyl-1,2,3-triazole scaffold, we explored different single and double substitutions of the phenyl ring, heterocyclic replacements of the phenyl ring, and 4-substitutions of the 1,2,3-triazole ring. Chloro substitutions in 2-position (**100**, NI), 3-position (**101**, 450 μ M) and 4-position (**102**, 31 μ M) of the phenyl ring showed that it was favourable only in the latter, in agreement with the analogous amino-1,2,3-triazole and the docking predictions (Figure 4G)⁶⁰. Similar trends were observed for methoxy substitution in 2-position (**103**, NI), 3-position (**104**, 990 μ M), and 4-position (**105**, 200 μ M). On the other hand, hydroxy substitutions in 2-position (**106**, 125 μ M), 3-position (**107**, NI), and 4-position (**108**, NI) showed that it was favourable only in 2-position. In 4-position, substituent influence was the following: Br (**109**, 13 μ M) > Cl (**102**, 31 μ M) > F (**110**, 185 μ M) > OMe (**105**, 200 μ M) > OH (**108**, NI), similar to what has been found for the 5-position in the 4-phenyl-1,2,3-triazoles. Combination of 2-OH with the 5-Cl substitutions yielded only a moderately active compound (**111**, 365 μ M), as expected by the structure-activity relationship (SAR) of the chloro substituents, but combination of 2-OH with 4-Br (**113**, 8.2 μ M, LE 0.46 kcal/mol/HA) and with 4-Cl (**112**, 11 μ M, LE 0.45 kcal/mol/HA) substantially increased the activities of singly



Scheme 8. Synthesis of 3-aryl-1*H*-1,2,4-triazoles. Reagents and conditions: (a) Formic acid, N₂H₄·H₂O, DMF, 90 °C, 12 h, yield 20–45%. (b) *N,N*-dimethyl formamide dimethyl acetal (DMF-DMA), reflux, 1 h. (c) N₂H₄·H₂O, AcOH, 90 °C, 1.5 h, overall yield 70–80% for 2 steps. (d) SnCl₂·2H₂O, EtOH, 70 °C, 1 h, yield 40–66%.



Scheme 9. Synthesis of aryl carbonitriles and aryl carboxamides. Reagents and conditions: (a) *t*-BuOK, dimethyl oxalate, *N,N*-dimethyl acetamide, 140 °C, 5 h, yield 70%. (b) pyridine, DMAP, rt, 3 h, yield 75–85%. (c) HNO₃, H₂SO₄, rt, 3 h (d) (COCl)₂, NH₄OH, DMF, DCM, reflux, overall yield 70–75% for 2 steps.

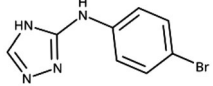
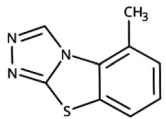
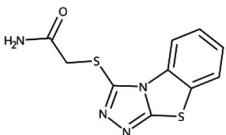
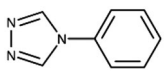
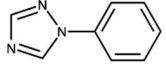
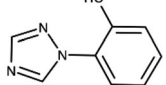
substituted compounds and provided the most active compounds of this type, which remained, however, only in the low micromolar range. In the docked poses, the hydroxy groups of these compounds form a hydrogen bond to Gly262 (Figure 4H). Replacement of the phenyl ring by 5- or 6-membered aromatic heterocycles was mostly beneficial with 5-membered rings (**115**, 16 μM, Figure 4I); **116**, 17 μM; **117**, 67 μM; **118**, 81 μM; **114**, 230 μM; **119**, 515 μM), reaching

a maximal LE of 0.55 kcal/mol/HA for compound **115**. Replacement by 2-(**120**, NI), 3-(**121**, 650 μM), and 4-pyridine (**122**, 1200 μM), however, was detrimental. Substitution of the C4 atom of the 1,2,3-triazole with the aim to reach pocket B were explored combining them with the 4-Br substituted phenyl ring. However, all substitutions, including hydroxymethyl (**123**, NI), aminomethyl (**126**, NI), bromomethyl (**124**, NI), or larger groups (data not shown) yielded inactive

compounds, in agreement with the docking predictions, which do not find low-energy poses for these compounds inside the active site.

In summary, we were able to develop original 5-aryl-1,2,3-triazoles with enzymatic activities in the low micromolar range. However, they did not provide access to pocket B.

Table 7. Other 1,2,4-triazoles.

Compound	Structure	IC ₅₀ [μ M] (SD ^a)	LE ^b [kcal/mol/HA]
166		>1000	
167		>1000	
168		>1000	
169		>1000	
170		870	0.38
171		27	0.52

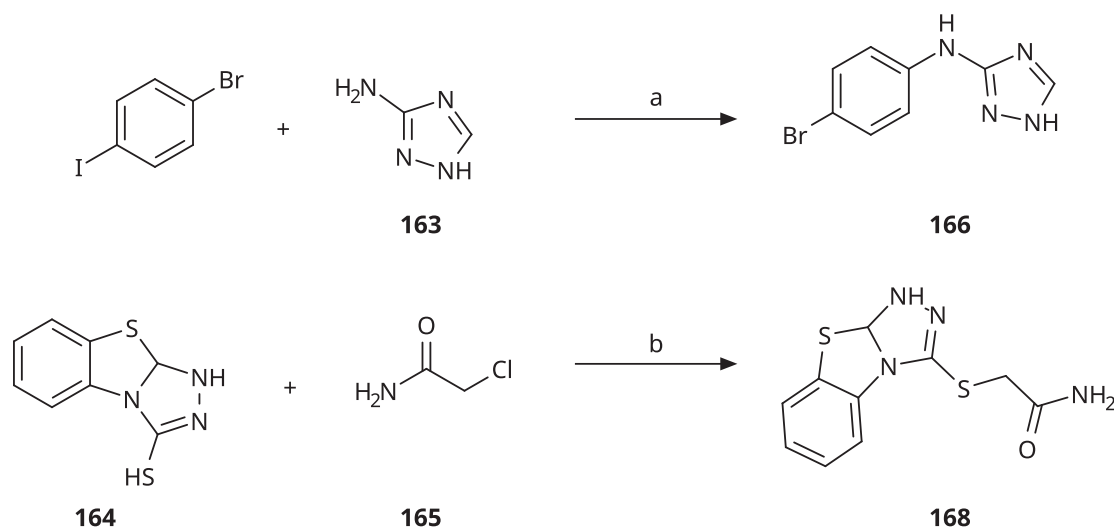
^aStandard Deviation (SD). ^bLigand Efficiency (LE).

3-Aryl-1,2,4-Triazoles

Since we did not find a 1,2,3-triazole providing a convenient access to pocket B while preserving efficiency and potency, we turned in the following to the 1,2,4-triazoles²⁸. For this scaffold, we found previously that 3-(2-aminophenyl)-1,2,4-triazole (**139**) displayed an interesting inhibitory activity of 2 μ M (Table 5). This was better than with the 3-(2-hydroxyphenyl) derivative (**138**, 31 μ M), preferred by the 1,2,3-triazoles. Based on X-ray crystallography and molecular modelling studies, we attributed these results to the simultaneous inter- and intra-molecular hydrogen bonds of the 2-amino substituent in the 1,2,4-triazole, leading to a more favourable planar conformation (Figure 5A). Most important, combination with the 5-chloro substituent (**11**, 0.035 μ M) or the 5-bromo substituent (**12**, 0.020 μ M) yielded highly active compounds with excellent LE of 0.78 and 0.80 kcal/mol/HA, respectively²⁸.

Here, we started by synthesising and testing the *para*-fluorophenyl derivative (**134**), which was found inactive and deterred us from preparing more *para*-substituted phenyl derivatives. Based on the knowledge collected for 1,2,3-triazoles, we tested halogen substitutions in *meta* position. We found that the bromo analogue (**135**, 16 μ M) was more active than the chloro (**136**, 29 μ M) and the fluoro (**137**, 160 μ M) substituted compounds. This was expected based on the size of the hydrophobic sub-pocket in this region and in agreement with the activities found for 1,2,3-triazoles. A 2,6-diamino substituted compound (**142**, 31 μ M, Figure 5C) showed decreased activity with respect to the singly substituted 2-amino compound (**139**, 2.0 μ M). The 2-NH₂,5-F compound was consistently less active (**143**, 0.15 μ M) than its other halogenated counterparts (compounds **11**, **12**).

We synthesised and tested two compounds with 2-amino,3-halo disubstituted phenyl rings. As expected from our structural analysis, **140** (0.81 μ M) and **141** (29 μ M, Figure 5D) are much less active than their 2,5-disubstituted counterparts (Table 5). These compounds cannot offer any synergic effects from interactions of the amino group with Ser167 and the triazole ring on the one hand and the interactions of the halogen with the hydrophobic sub-pocket on the other hand. Methyl substitution of the amino group of compound **11** led to a lower inhibitory activity (**145**, 8.6 μ M). This is in agreement with the structural data and the finding that both hydrogen atoms of the amino group serve as hydrogen bond donors²⁸.



Scheme 10. Synthesis of other 1,2,4-triazoles. Reagents and conditions: (a) K₂CO₃, CuI, *N,N*-dimethyl acetamide, 90 °C, 48 h, yield 39%. (b) K₂CO₃, acetone, reflux, 9h, yield 60%.

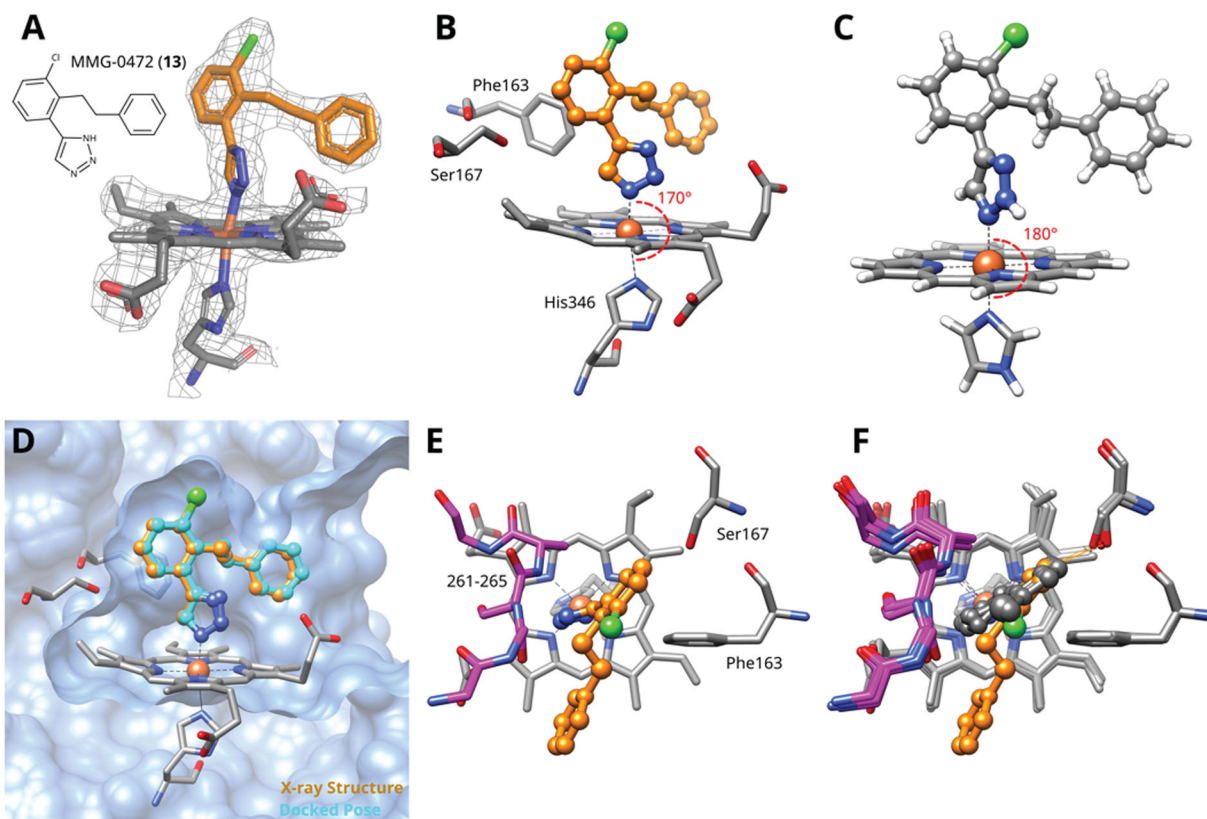


Figure 2. (A) Detail of X-ray structure of compound MMG-0472 (**13**, orange) bound to IDO1 (PDB ID 7zv3). The $2F_o - F_c$ map of the active site is contoured at 1.0σ . (B) Same X-ray structure, highlighting the His346–iron–ligand bond angle of 170° . (C) DFT-optimized model of MMG-0472 binding to haem. The imidazole–iron–ligand bond angle of 180° is highlighted. (D) Superposition of the X-ray structure of MMG-0472 (orange) and its binding pose predicted by docking (cyan). The RMSD between the structures is 0.3 \AA . (E) Top view of MMG-0472 X-ray structure, showing the passage from pocket A to pocket B in-between residues Phe163 on the one side and residues 261–265 (magenta) on the other side. (F) Same view, superimposed with X-ray structures of compounds **9**, **11** and **12** (PDB ID 6r63, 7ah5, 7ah6)^{22,28}.

We also synthesised and tested triple-substituted 3-phenyl-1,2,4-triazoles all having a 2-amino substitution of the phenyl ring. Adding a 4-F substitution to compound **12** only slightly perturbs its activity (**144**, $0.034 \mu\text{M}$). However, adding a 6-methyl substitution to either compound **12** (**155**, $63 \mu\text{M}$, Figure 5E) or **11** (**156**, $90 \mu\text{M}$) reduced the inhibitory activities by more than 3 orders of magnitude. Adding a 6-amino group as in compound **157** ($1 \mu\text{M}$) also strongly reduced the inhibitory activity as compared to compound **11** ($0.035 \mu\text{M}$). This mirrors the results obtained with 2-aminophenyl **139** and 2,6-diaminophenyl derivative **142** and leaves little chance to develop analogues of this type extending to pocket B.

Finally, we investigated amide extensions of the *ortho*-amino group with the hope that the latter could reach pocket B, although structural and functional data suggested this amino group to increase activity by being located in the back of the active site and making two simultaneous hydrogen bonds (Figure 5A). We generally found that amide extensions reduced the compound solubility. With 3-(2-benzamidophenyl)-1,2,4-triazole (**152**), we lost the inhibitory activity completely (Figure 5F). Curiously, introduction of a 5-Cl substituent restored some of the inhibitory activity (**153**, $9.4 \mu\text{M}$, Table 5) albeit at low solubility. Interestingly, the cyclopropanecarboxamide (**149**, $0.49 \mu\text{M}$) and the propenamide (**147**, $1.2 \mu\text{M}$) showed the best inhibitory activities of this series. However, the related cyclobutanecarboxamide (**150**, NI) and cyclopentanecarboxamide (**151**, NI) were inactive as inhibitors and showed strongly reduced solubilities. In the aliphatic series, the butanamide (**148**, $24 \mu\text{M}$) was better than the acetamide (**146**, $425 \mu\text{M}$). Aromatic extensions such as the benzamide (**153**, $9.4 \mu\text{M}$)

led to lower solubilities. However, the latter could be improved by introducing polar groups. Unfortunately, the inhibitory activities of resulting compounds were only in the high micromolar range (data not shown). Summarising, the observed inhibitory activities of the 1,2,4-triazoles bearing 2-amido substituents cannot be rationalised based on structural data. Investigations are rendered complicated by the low solubilities of these compounds.

3-Hetaryl-1,2,4-Triazoles

Replacement of the phenyl ring of parent compound **133** by 4-pyridinyl (**158**, NI, Table 6) and by 2-pyridinyl (**159**, NI) produced inactive compounds. However, 3-(3-aminopyridinyl)-1,2,4-triazole (**160**, $15 \mu\text{M}$, LE 0.55 kcal/mol/HA , Figure 5G) and 3-(3-aminothiophenyl)-1,2,4-triazole (**161**, $10 \mu\text{M}$, LE 0.57 kcal/mol/HA) were low micromolar inhibitors with a similar inhibitory activity as the aniline **139**. Some activity was also found with the chloro-pyrazine derivative **162** ($250 \mu\text{M}$, LE 0.41 kcal/mol/HA). In summary, it is possible to replace the phenyl ring by 5 or 6-membered heteroaromatics, but up to now, no compounds with better activities than the 3-aryl analogues have been found.

Other 1,2,4-Triazoles

To complete our investigation with 1,2,4-triazoles as IDO1 inhibitors, we also tested the derivatives shown in Table 7. 3-(4-Bromophenylamino)-1,2,4-triazole (**166**, NI), an analogue of the 1,2,3-triazole derivative **78**, was found to be inactive. This is not surprising, as **78** only shows an IC_{50} value of $52 \mu\text{M}$, and the 1,2,4-triazoles are generally less active than the corresponding 1,2,3-

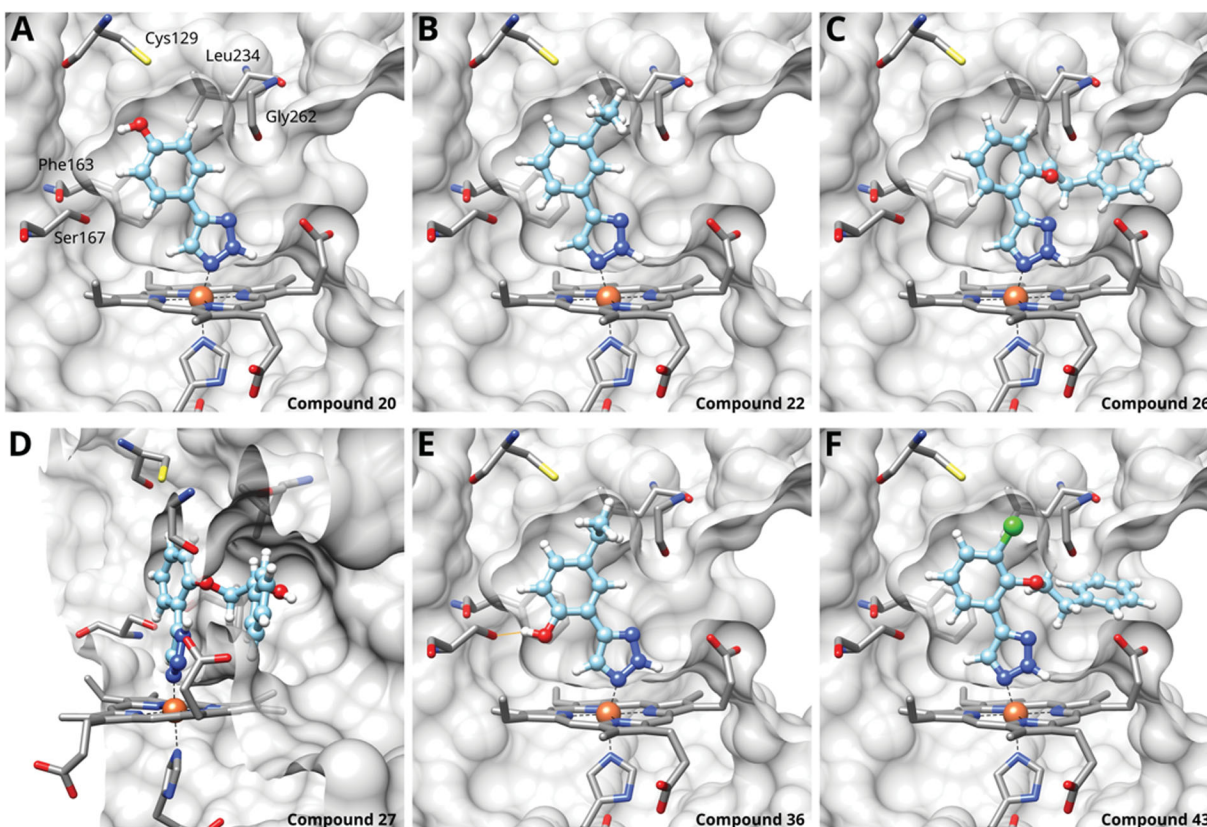


Figure 3. Binding poses of 4-aryl-1,2,3-triazoles predicted by docking. (A) Compound 20: non-optimal pose, the imidazole-iron-triazole bond angle deviates from 180° due to limited space for the *p*-OH substituent. (B) Compound 22: the *m*-ethyl substituent is of good size for the hydrophobic subpocket between Val125, Cys129, Leu234 and Gly262. (C) Compound 26: inactive compound with larger *ortho* substituent using an ether linker. (D) Compound 27: no favourable interactions between hydroxy group and pocket B. (E) Compound 36. (F) Compound 43.

triazoles. The annulated antifungal tryclazole (**167**, NI) and its derivative (**168**, NI, [Figure 5H](#)), designed to extend into pocket B, were inactive, although they dock well into the active site. Their inactivity is probably due to their low iron affinity. We have shown before that 4-phenyl-1,2,4-triazole (**169**, NI) was inactive⁵⁸. However, as we predicted based on quantum chemical calculations²⁸, 1-phenyl-1,2,4-triazole (**170**, 870 μM) showed some activity, which could further be increased by adding an *ortho*-hydroxysubstituent to the phenyl ring (**171**, 32 μM , [Figure 5I](#)), making it about equipotent to the 3-phenyl-1,2,4-triazole **138**. Interestingly, this compound binds to IDO1 in its neutral form, as the 1,2,4-triazole cannot be deprotonated, and might therefore display different properties than the derivatives of **133**, which may bind stronger in their deprotonated form to IDO1.

Cellular activities

We tested the cellular hIDO1 inhibitory activity and toxicity of 30 active compounds at a single concentration ([Figure 6](#) and [Table 8](#)). As some of the aniline derivatives reacted with Ehrlich's reagent (*p*-dimethylaminobenzaldehyde, *p*-DMAB) used to quantify kynurenine, the kynurenine content of these samples was determined by HPLC. To be able to detect also weak inhibition, compounds were tested at the high concentration of 200 μM ([Figure 6A and B](#), filled bars), except for less soluble compounds (**52**, **148**, **149** and **153**), which were tested at a concentration of 50 μM ([Figure 6A and B](#), empty bars). Many compounds showed a good cellular inhibition ([Figure 6A](#)) and a low toxicity ([Figure 6B](#)). It is noticeable that for the compounds tested here, the 1,2,4-triazoles

(orange) generally showed a better cellular inhibition than the 1,2,3-triazoles (black) but also a detectable albeit low toxicity. However, it should be kept in mind that previously tested 1,2,3-triazoles also showed a very good cellular inhibition⁵⁸, and that the toxicity of the 1,2,4-triazoles occurs at a concentration of 200 μM , far above their cellular IC₅₀ value.

Previously determined cellular data for compounds mentioned in this work is given in the [Supporting Information, Table S2](#). Both previously and in the present work, cellular inhibition was observed to be closely related to enzymatic activity for both 1,2,3-triazoles and 1,2,4-triazoles, showing a sigmoidal dependence ([Figure 6C](#)). Three outliers show a lower cellular activity than expected, namely two double-substituted 5-aryl-1,2,3-triazoles (**112**, **113**) and the fluorinated 1,2,4-triazole **143**. On the other hand, three compounds show a higher cellular activity, namely compound **78** of the Vertex scaffold, for which this behaviour has already been documented⁶⁰, the amide 1,2,4-triazole **146**, which might be hydrolyzed to the highly active **11** inside the cell, and the 1,2,3-triazole **42** for unknown reasons.

Here, we determined cellular IC₅₀ values for a selection of three 1,2,4-triazoles ([Figure 6D](#)), and found two of them to display nanomolar activities also in a cellular context. As in the enzymatic assay, the most potent compound is **144** (cellular IC₅₀ value of 0.034 μM), followed by **143** (0.25 μM) and **140** (1.2 μM).

We previously found a good correlation between enzymatic and cellular IC₅₀ values for differentazole compounds^{28,58}. Here, we show this correlation ([Figure 6E](#)) for all 1,2,3-triazole (black) and 1,2,4-triazole (orange) compounds mentioned in this manuscript. The newly determined cellular IC₅₀ values of the 1,2,4-

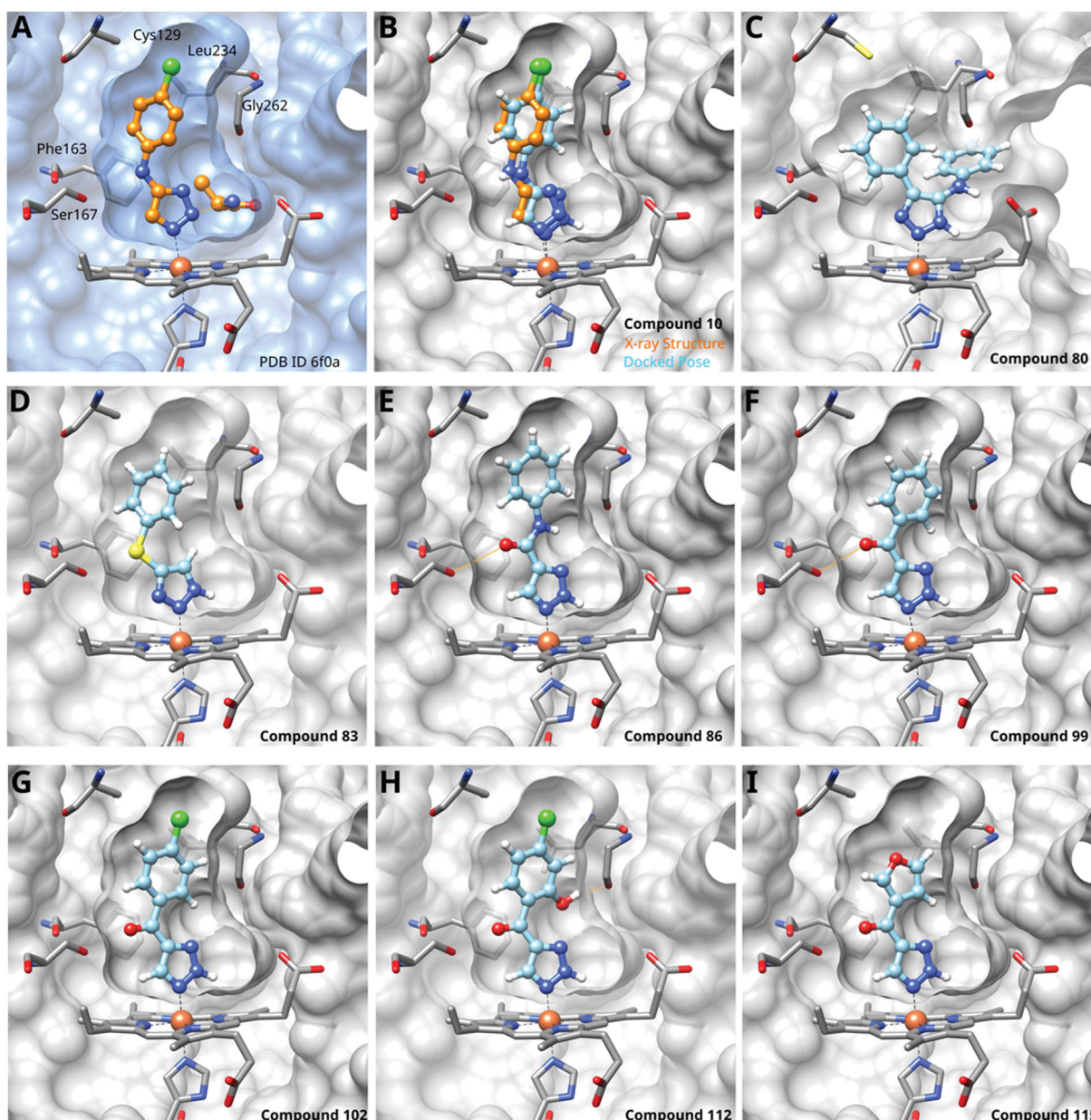


Figure 4. Tethered 1,2,3-triazoles. (A) X-ray structure of compound 10 (PDB ID 6f0a)⁶⁰. (B) Superposition of X-ray structure and of docking pose of 10. Docking poses of (C) compound 80; (D) compound 83; (E) compound 86; (F) compound 99; (G) compound 102; (H) compound 112; (I) compound 115. Hydrogen bonds are shown in orange.

triazoles closely follow this correlation. The only outlier is the original Vertex compound **10**⁶⁰.

Conclusions

In summary, here we described almost 100 new compounds of the 1,2,3-triazole and the 1,2,4-triazole haem-binding series and tested them for their inhibitory activity on IDO1. They provide highly efficient scaffolds for inhibitors binding to pocket A, which are also very potent in a cellular environment and display low cytotoxicities. The best compound (**144**) displays both enzymatic and cellular IC_{50} values of 34 nM and is therefore more potent and efficient *in vitro* than other frequently used IDO1 inhibitors.

We did not measure the activities of these compounds on IDO2 and on TDO to determine their selectivity. However, in our earlier works we found that triazoles such as MMG-0358 with high activities on IDO1 have undetectable activities on TDO ($>100 \mu\text{M}$)⁵⁸. We also found that MMG-0358 has a more than 1000-fold selectivity for IDO1 over IDO2, even though triazoles extending from pocket A to pocket B showed better activity on mouse IDO2 than on human IDO1 in a cellular environment⁶². Based on these observations, it is reasonable to assume that the potent compounds reported here, which are binding only to pocket A, are likely to be highly selective for IDO1 over TDO and IDO2.

Unfortunately, extending these highly efficient compounds into pocket B by one of the attachment points described in Figure 1(D) proved very challenging. We were able to resolve the X-ray structure

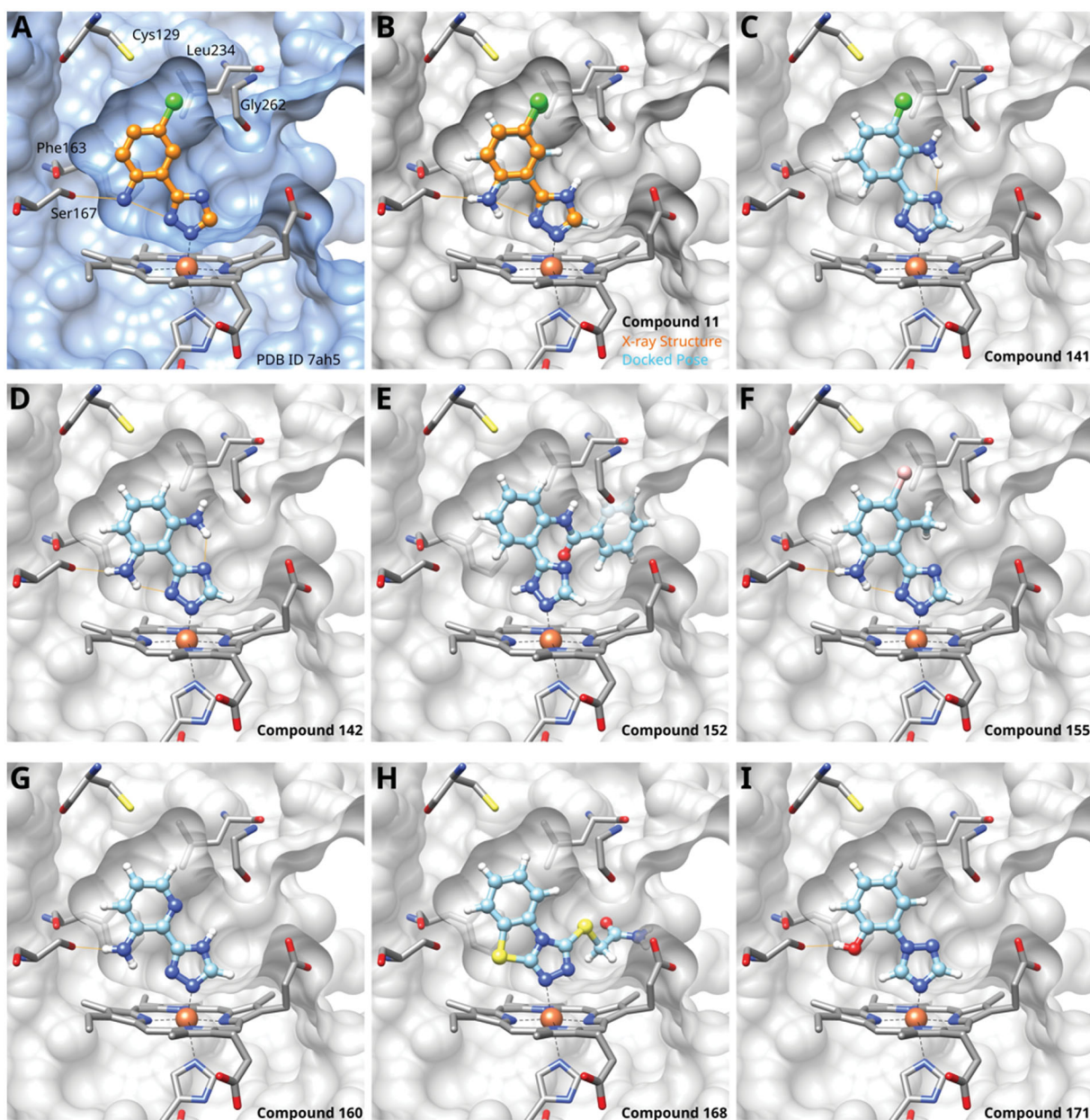


Figure 5. 1,2,4-Triazoles. (A) X-ray structure of compound 11 (PDB ID 7ah5)²⁸. (B) Superposition of X-ray structure and of docking pose of compound 11. Docking poses of (C) compound 141; (D) compound 142; (E) compound 152; (F) compound 155; (G) compound 160; (H) compound 168; (I) compound 171. Hydrogen bonds are displayed in orange.

of the complex of one such compound extending into pocket B (MMG-0472, PDB ID 7zv3). The experimental structure confirms our docking predictions of the binding mode of this compound. However, docking predictions in general are challenging due to the interactions with the haem cofactor in the active site, which is difficult to parameterise classically. For future design of type ii or type iii IDO1 inhibitors, we recommend tackling the issue of addressing pockets A and B simultaneously early on in hit-to-lead optimisation to provide more flexibility for rational compound modifications.

Experimental section

Docking

Docking was performed with our in-house docking code AttractingCavities (AC)⁸⁷, which relies on the physical scoring function of the CHARMM27 force field^{88,89}, while solvation effects are

taken into account by the Fast Analytical Treatment of Solvation (FACTS) model⁹⁰, which has been shown to allow for accurate docking results⁹¹. Ligand force-field parameters were derived with the SwissParam tool⁹². Standard parameters were used, i.e. a cubic search space of 20 Å³ around the IDO1 active site, a rotational angle of 90° for initial ligand sampling, and a N_{Thr} value of 70 for determination of the attractive grid points. For all compounds with an acidic proton, both the neutral and the deprotonated species were docked, and different tautomers were considered. A Morse-like metal binding potential (MMBP) was used to describe the interactions between the haem iron of IDO1 and ligand atoms that display a free electron pair for iron binding⁹³. The protein was kept fixed during the docking. We used seven different IDO1 X-ray structures as targets, chosen for their quality and diversity, namely PDB ID 2d0t⁴⁰ co-crystallized with a smallazole ligand in pocket A, 5whr²⁵ with a resolved JK-loop^C in closed conformation, 6e41⁹⁴ with an analogue of epacadostat in

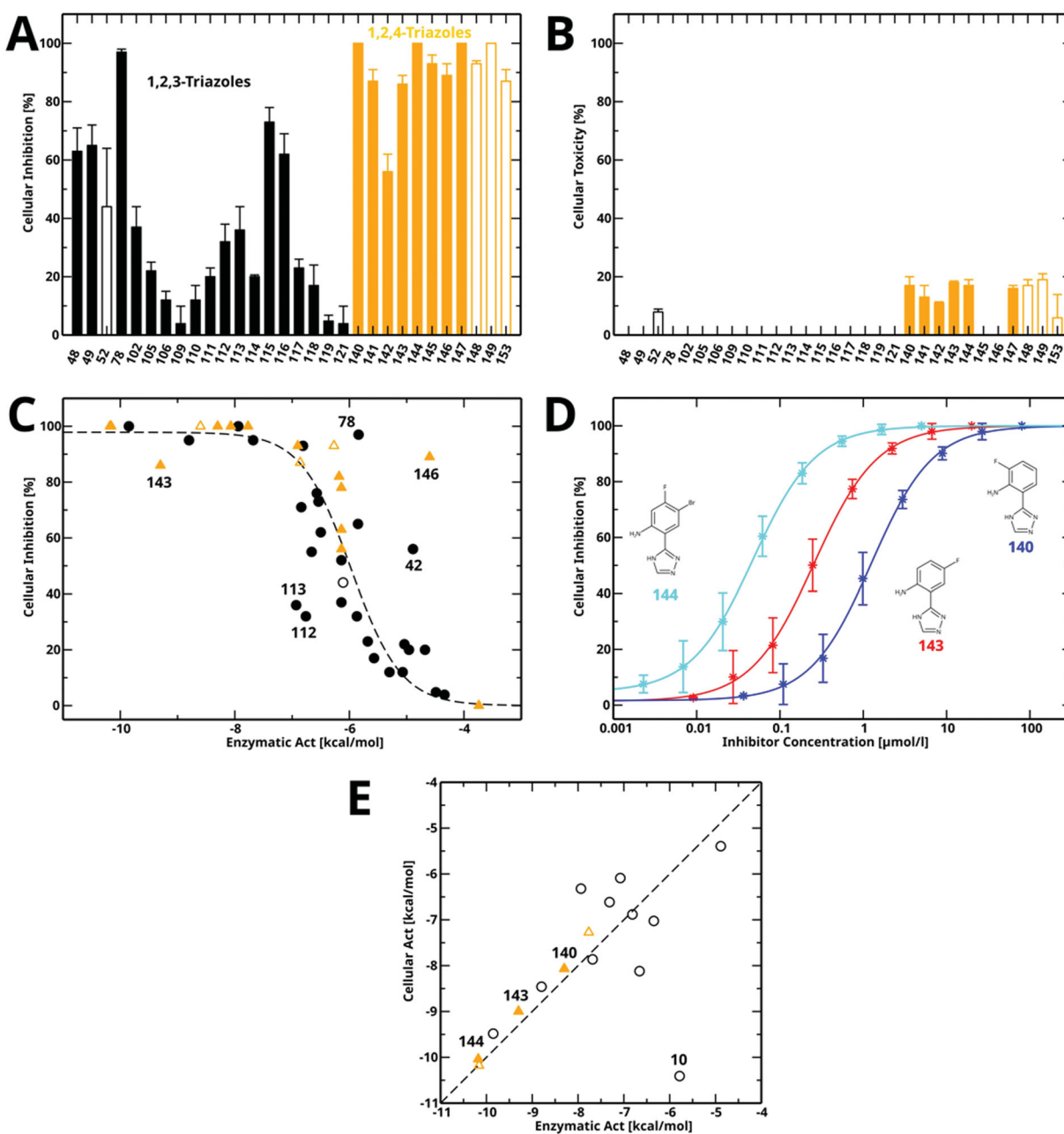


Figure 6. Cellular inhibition and comparison to enzymatic inhibition. (A) Cellular inhibition of kynurenine production at a single compound concentration. Data for 1,2,3-triazole compounds is shown in black, for 1,2,4-triazoles in orange. Values measured at a compound concentration of $200\ \mu\text{M}$ are given in filled bars, values measured at $50\ \mu\text{M}$ in empty bars. (B) Cellular toxicity under the same conditions and using the same colour code as part (A). (C) Cellular inhibition as a function of enzymatic activity ($Act = RT\log(I/C_{50})$). The dashed line is a sigmoidal fit to all data points except for the marked outliers. Compounds measured at a concentration of $50\ \mu\text{M}$ are marked by empty symbols. (D) Cellular dose-response curves of compounds **140**, **143**, and **144** measured in this work. (E) Correlation between cellular activity and enzymatic activity for compounds mentioned in this manuscript. Colour code as in part (A). Filled symbols denote the newly determined data shown in part (D).

pockets A and B, **6kof**⁵¹ with a large azole ligand in pockets A and B, **6o3i**²⁴ with the clinical compound navoximod, **6pu**⁷³² with a hydroxyamidine ligand of peculiar shape, and **7ah4**²⁸ with two small azole ligands in pockets A and D. All ligands were removed before docking.

Density functional theory calculations

Quantum chemical geometry optimizations and charge calculations were carried out in the density functional theory (DFT) framework with the PBE0 hybrid functional⁹⁵ using the Gaussian16 code⁹⁶. Geometry optimizations were carried out with

standard settings and the TZVP basis set⁹⁷. Solvation effects were taken into account by the polarisable continuum model⁹⁸ as implemented in Gaussian16. The histidine-bound haem complex of IDO1 was modelled by an iron-porphin-imidazole system. For the 6-fold coordinated systems, a low-spin complex was assumed, as it has been found experimentally³⁹.

Chemistry

General remarks

All reactions were carried out under nitrogen atmosphere unless otherwise stated. Glassware was oven-dried ($120\ ^\circ\text{C}$), evacuated and

Table 8. Cellular inhibition and toxicity data determined in this work.

Compound	Conc. [μM]	Inh. [%]	Tox. [%]	Cell. IC ₅₀ [μM] (SD ^a)
48	200	63 (8)	0 (0)	
49	200	65 (7)	0 (0)	
52	50	44 (20)	7.9 (1)	
78	200	97 (1)	0 (0)	
102	200	37 (7)	0 (0)	
105	200	22 (3)	0 (0)	
106	200	12 (3)	0 (0)	
109	200	55 (10)	0 (0)	
110	200	12 (5)	0 (0)	
111	200	20 (3)	0 (0)	
112	200	32 (6)	0 (0)	
113	200	36 (8)	0 (0)	
114	200	20 (0.6)	0 (0)	
115	200	73 (5)	0 (0)	
116	200	62 (7)	0 (0)	
117	200	23 (3)	0 (0)	
118	200	17 (7)	0 (0)	
119	200	4.8 (2)	0 (0)	
121	200	3.9 (6)	0 (0)	
140	200	100 (0)	17 (3)	0.81 (0.2)
141	200	82 (7)	13 (4)	
142	200	56 (6)	11 (0.4)	
143	200	86 (3)	18 (0.5)	0.15 (0.06)
144	200	100 (0)	17 (2)	0.034 (0.004)
145	200	93 (3)	0 (0)	
146	200	89 (4)	0 (0)	
147	200	100 (0)	16 (1)	
148	50	93 (1)	17 (2)	
149	50	100 (0)	19 (2)	
153	50	87 (4)	5.9 (8)	

^aStandard Deviation (SD).

purged with nitrogen. Any common reagents, catalysts and solvents that were obtained from commercial suppliers were used without any further purification. For extraction and chromatography, all solvents were distilled prior to use. Thin layer chromatography (TLC) for reaction monitoring was performed on silica gel plates (Merck 60 F254) with detection by UV light (254 nm). Flash chromatography (FC) was conducted using silica gel 60 Å, 230–400 mesh (Merck 9385). Mass spectra were recorded on a Nermag R10-10C instrument in chemical ionisation mode. Electrospray mass analyses were recorded on a Finnigan MAT S50 710C spectrometer in positive ionisation mode. ¹H and ¹³C NMR spectra were recorded with a Bruker-DPX-400 or Bruker-ARX-400 spectrometer at 400 MHz and 100.6 MHz, respectively. Data for ¹H NMR spectra are reported as follows: chemical shift, multiplicity, apparent coupling constant, and integration. Data for ¹³C NMR spectra reported in terms of chemical shift. Chemical shifts are given in parts per million, relative to an internal standard such as residual solvent signals. Coupling constants are given in Hertz. Spectra were analysed with MestreNova. High resolution mass spectra were recorded via ESI-TOF-HRMS or MALDI-TOF-HRMS.

The purity of all final compounds was confirmed to exceed 95% by ¹H NMR showing ¹³C-H satellite signals. Additionally, analytical HPLC purity analysis was carried out for compounds **34**, **113**, **143** and **149** with UV detection at 220 nm, using a PFP propyl column (RESTEK Allure HPLC column, particle size 5 μm , pore size 60 Å, dimensions 150 \times 4.6 mm) with a linear gradient of solvent B (acetonitrile, 0.1% TFA) over solvent A (H₂O, 0.1% TFA) from 0 to 100% in 30 min at a flow rate of 1 mL/min. Typically, 25 μL solution (0.5 mg/mL in 50% ACN/H₂O) was injected for each compound.

Procedures

Synthesis of iodo derivatives

4-Benzyl-2-iodophenol (**17a**)⁹⁹: 4-Benzylphenol (**14a**) (1.1 g, 6.0 mmol) was dissolved in DMF (10 mL), diluted with

concentrated aqueous ammonia (60 mL), and treated with a solution of potassium iodide (5.3 g, 32 mmol) and iodine (1.6 g, 6.3 mmol) in water (20 mL) all at once. After stirring at rt for 1 h, the ammonia was removed under reduced pressure. The remaining solution was neutralised with 1 N HCl in H₂O. After extraction with EtOAc (50 mL), the organic phases were collected, dried over Na₂SO₄, filtered, and concentrated under reduced pressure. The residue was purified by FC (silica gel, EtOAc/hexane) giving **17a** (930 mg, 50% yield) as white solid. ¹H NMR (400 MHz, MeOD) δ 7.50 (d, J = 2.1 Hz, 1H), 7.35–7.23 (m, 2H), 7.18 (td, J = 6.5, 1.7 Hz, 3H), 7.01 (dd, J = 8.3, 2.2 Hz, 1H), 6.76 (d, J = 8.2 Hz, 1H), 3.85 (s, 2H).

1-(Benzyloxy)-2-iodobenzene (**17ba**)¹⁰⁰: To a solution of 2-iodophenol (**14b**) (440 mg, 2.0 mmol) in DMF (6 mL), anh. K₂CO₃ (1.38 g, 10.0 mmol) was added, and the mixture was stirred for 5 min before dropwise addition of benzyl bromide (**15a**) (374 mg, 2.2 mmol). The mixture was stirred at 80 °C for 24 h. After cooling to rt, CH₂Cl₂ (10 mL) and water (10 mL) were added and the mixture was shaken vigorously before extraction with CH₂Cl₂ (2 \times 10 mL). The organic layers were collected, washed with brine (2 \times 10 mL), dried over Na₂SO₄, filtered, and concentrated under reduced pressure. The crude residue of **17ba** (527 mg, 85% yield) was used directly in the next step. ¹H NMR (400 MHz, CDCl₃) δ 5.12 (s, 2H), 6.75 (dt, J = 7.6, 1.3 Hz, 1H, H-5), 6.87 (dd, J = 8.2, 1.1 Hz, 1H, H-6), 7.29 (ddd, J = 8.2, 7.4, 1.5 Hz, 1H, H-4), 7.33–7.46 (m, 3H), 7.55 (d, J = 7.3 Hz, 2H), 7.85 (dd, J = 7.8, 1.6 Hz).

1-Iodo-2-phenethoxybenzene (**17bb**) (CAS [1104274–16–9]): Compound **17bb** was prepared the same way as **17ba** from 2-iodophenol (**14b**) (440 mg, 2.0 mmol) and (2-bromoethyl)benzene (**15b**) (405 mg, 2.2 mmol) in DMF (6 mL), giving **17bb** (583 mg, 90% yield) as colourless oil. ¹H NMR (400 MHz, CDCl₃) δ 7.77 (dd, J = 7.8, 1.6 Hz, 1H), 7.42–7.30 (m, 4H), 7.34–7.21 (m, 2H), 6.78 (dd, J = 8.3, 1.3 Hz, 1H), 6.70 (td, J = 7.5, 1.4 Hz, 1H), 4.21 (t, J = 6.9 Hz, 2H), 3.18 (t, J = 6.9 Hz, 2H).

2-Iodo-*N*-phenethylamine (**17cb**)¹⁰¹: Compound **17cb** was prepared the same way as **17ba** from 2-iodoaniline (**14c**) (440 mg, 2.0 mmol) and (2-bromoethyl)benzene (**15b**) (405 mg, 2.2 mmol) in DMF (6 mL), giving **17cb** (323 mg, 50% yield) as colourless oil. ¹H NMR (400 MHz, CDCl₃) δ 7.65 (dt, J = 7.9, 1.5 Hz, 2H), 7.39–7.18 (m, 1H), 7.18–7.10 (m, 2H), 6.76 (dd, J = 8.0, 1.5 Hz, 2H), 6.53–6.41 (m, 2H), 4.45–4.30 (m, 2H), 2.99 (q, J = 6.8 Hz, 2H).

1-Chloro-3-iodo-2-phenethoxybenzene (**17db**): Compound **17db** was prepared the same way as **17ba** from 2-chloro-6-iodophenol (**14d**) (508 mg, 2.0 mmol) and (2-bromoethyl)benzene (**15b**) (405 mg, 2.2 mmol) in DMF (6 mL), giving **17db** (680 mg, 95% yield) as colourless oil. ¹H NMR (400 MHz, CDCl₃) δ 7.68 (dd, J = 7.9, 1.5 Hz, 1H), 7.40–7.29 (m, 4H), 7.27 (s, 1H), 7.24 (ddt, J = 8.5, 5.3, 2.5 Hz, 1H), 6.78 (t, J = 7.9 Hz, 1H), 4.21 (t, J = 7.4 Hz, 2H), 3.25 (t, J = 7.4 Hz, 2H).

2-(2-Iodophenoxy)-1-phenylethan-1-ol (**17bc**)¹⁰²: 2-Phenyloxirane (**16**) (580 mg, 4.8 mmol, 1.2 eq), 2-iodophenol (**14b**) (880 mg, 4.0 mmol, 1.0 eq), and Cs₂CO₃ (31.9 g, 12 mmol, 3.0 eq) were added to a 100-mL 2-neck round-bottom flask equipped with a condenser and a septum. DMF (8 mL) was added, and the mixture was heated under reflux (110 °C) for 24 h. After cooling to rt, water (10 mL) was added, followed by extraction with EtOAc (3 \times 15 mL). The organic layers were collected, dried over anh. Na₂SO₄, filtered, and concentrated under reduced pressure. The residue was purified by FC (silica gel, EtOAc/hexane) to give **17bc** (0.98 g, 60% yield) as colourless oil. ¹H NMR (400 MHz, CDCl₃) δ 7.80 (dd, J = 7.8, 1.6 Hz, 1H), 7.54–7.47 (m, 2H), 7.46–7.25 (m, 3H), 6.84–6.72 (m, 2H), 5.21 (dt, J = 8.7, 2.9 Hz, 1H), 4.21 (dd, J = 9.3, 3.3 Hz, 1H), 4.02 (t, J = 9.0 Hz, 1H), 3.14 (d, J = 2.6 Hz, 1H).

2-Iodo-1-methoxy-4-phenethylbenzene (**17g**): To a stirred solution of methyl(triphenyl)phosphoniumbromide (1.23 g, 6.7 mmol) in freshly distilled THF (9 mL), sodiumbis(trimethylsilyl)amide (2.19 g, 6.1 mmol) was added under cooling (ice bath), causing the solution to turn yellow. After 1.5 h of stirring at rt, 3-iodo-4-methoxybenzaldehyde (**17e**) (786 mg, 3.0 mmol) was added to the ylide solution and stirring was continued for 4 h. The mixture was acidified using H₂SO₄ (0.1 M, 5 mL) and extracted with CH₂Cl₂ (50 mL). The combined organic phases were dried over Na₂SO₄, filtered, and concentrated under reduced pressure to give 1.84 g (90% yield) of a mixture of (E/Z)-2-iodo-1-methoxy-4-styrylbenzene (**17f**) as a oily solid. ¹H NMR (400 MHz, MeOD) δ 7.99 (d, *J* = 2.2 Hz, 1H), 7.62 (d, *J* = 2.2 Hz, 1H), 7.55 (td, *J* = 8.3, 1.6 Hz, 3H), 7.35 (dd, *J* = 8.4, 6.9 Hz, 2H), 7.30–7.17 (m, 7H), 7.06 (d, *J* = 1.2 Hz, 2H), 6.96 (d, *J* = 8.5 Hz, 1H), 6.80 (d, *J* = 8.5 Hz, 1H), 6.58 (d, *J* = 12.1 Hz, 1H), 6.49 (d, *J* = 12.1 Hz, 1H), 3.90 (s, 3H), 3.84 (s, 3H). The crude olefin mixture (710 mg, 2.1 mmol) was dissolved in ethanol (12 mL) together with FeCl₃·6H₂O (29 mg, 0.11 mmol), immediately followed by the addition of aqueous hydrazine hydrate (1.0 mL, 21.0 mmol). The reaction mixture was stirred at rt for 24 h under air before extraction with CH₂Cl₂ (3 × 5 mL). The organic phases were collected, dried (Na₂SO₄), filtered, and concentrated under reduced pressure. The residue was purified by FC (SiO₂, 10% EtOAc/petroleum ether), affording **17g** (640 mg, 90% yield) as oily solid. ¹H NMR (400 MHz, MeOD) δ 7.55 (d, *J* = 2.1 Hz, 1H), 7.29–7.03 (m, 6H), 6.82 (d, *J* = 8.4 Hz, 1H), 3.82 (s, 3H), 2.93–2.82 (m, 2H), 2.85–2.77 (m, 2H).

General procedure (I) for the preparation of arylethynes

To a stirred solution of commercially available or synthetically prepared iodo derivatives (**17**) (Scheme 1 and 2) (1 eq) mixed with Et₃N (4 eq) in dioxane (4 mL), trimethylsilylacetylene (1.3 eq), PdCl₂(PPh₃)₂ (0.01 eq), and CuI (0.02 eq) were added. The reaction mixture was stirred at 45 °C for 5 h under nitrogen atmosphere. After cooling to rt, the reaction mixture was diluted with Et₂O (5 mL) and washed with brine (5 mL). The organic layer was dried (Na₂SO₄), filtered, and concentrated under reduced pressure. KF (3.6 eq) was added to the residue and the mixture was dissolved in MeOH (5 mL) and stirred for 3 h at rt before concentration under reduced pressure. After addition of CH₂Cl₂ (5 mL) and water (3 mL), the organic layer was collected, dried over MgSO₄, and filtered through a short silica plug to afford the corresponding arylethynes **18** (Scheme 1). Overall yields 65–93%.

Synthesis of arylethynes

1-Butyl-3-ethynylbenzene (**18a**, CAS [2243191–48-0]): Synthesised from 1-butyl-3-iodobenzene (520 mg, 2 mmol) according to the general procedure (I) to afford the title compound as a yellowish oil (269 mg) in 85% yield. ¹H NMR (400 MHz, CDCl₃) δ 7.41–7.29 (m, 2H), 7.25 (td, *J* = 7.4, 0.8 Hz, 1H), 7.19 (dt, *J* = 7.7, 1.6 Hz, 1H), 3.07 (s, 1H), 2.66–2.57 (m, 2H), 1.68–1.56 (m, 2H), 1.37 (h, *J* = 7.4 Hz, 2H), 0.95 (t, *J* = 7.3 Hz, 3H).

1-(Benzyloxy)-2-ethynylbenzene (**18b**)¹⁰³: Synthesised from 1-(benzyloxy)-2-iodobenzene (620 mg, 2 mmol) according to the general procedure (I) to afford the title compound as an oil (291 mg) in 70% yield. ¹H NMR (400 MHz, CDCl₃) δ 7.59–7.47 (m, 3H), 7.41–7.15 (m, 5H), 6.99–6.86 (m, 1H), 5.23 (s, 2H).

1-Ethynyl-2-phenethoxybenzene (**18c**): Synthesised from 1-iodo-2-phenethoxybenzene (648 mg, 2 mmol) according to the general procedure (I) to afford the title compound as an oil (333 mg) in 75% yield. ¹H NMR (400 MHz, CDCl₃) δ 7.46 (dd, *J* = 7.6, 1.7 Hz, 1H), 7.39–7.31 (m, 4H), 7.31–7.23 (m, 1H),

6.95–6.83 (m, 3H), 4.24 (t, *J* = 7.1 Hz, 2H), 3.30 (s, 1H), 3.17 (t, *J* = 7.1 Hz, 2H).

2-(2-Ethynylphenoxy)-1-phenylethan-1-ol (**18d**): Synthesised from 2-(2-iodophenoxy)-1-phenylethan-1-ol (680 mg, 2 mmol) according to the general procedure (I) to afford the title compound as an oil (309 mg) with 65% yield. ¹H NMR (400 MHz, CDCl₃) δ 7.53–7.26 (m, 7H), 6.97 (td, *J* = 7.5, 1.0 Hz, 1H), 6.88 (dd, *J* = 8.4, 1.0 Hz, 1H), 5.18 (dt, *J* = 9.1, 2.8 Hz, 1H), 4.24 (dd, *J* = 9.5, 3.1 Hz, 2H), 4.02 (t, *J* = 9.2 Hz, 2H), 3.34 (s, 1H).

2-Ethynyl-*N*-phenethylaniline (**18e**): Synthesised from 2-iodo-*N*-phenethylaniline (646 mg, 2 mmol) according to the general procedure (I) to afford the title compound as an oil (331 mg) in 75% yield. ¹H NMR (400 MHz, CDCl₃) δ 7.40–7.18 (m, 7H), 6.69–6.59 (m, 2H), 4.72 (s, 1H), 3.46 (td, *J* = 7.1, 5.6 Hz, 2H), 3.34 (s, 1H), 2.96 (t, *J* = 7.2 Hz, 2H).

2-Ethynyl-4-fluorophenol (**18f**)¹⁰⁴: Synthesised from 4-fluoro-2-iodophenol (476 mg, 2 mmol) according to the general procedure (I) to afford the title compound as an oil (231 mg) in 85% yield. ¹H NMR (400 MHz, CDCl₃) δ 7.13–6.97 (m, 2H), 6.91 (dd, *J* = 9.0, 4.6 Hz, 1H), 5.65 (s, 1H), 3.51 (s, 1H).

2-Ethynyl-4-methylphenol (**18g**)¹⁰⁴: Synthesised from 2-iodo-4-methylphenol (468 mg, 2 mmol) according to the general procedure (I) to afford the title compound as an oil (211 mg) in 80% yield. ¹H NMR (400 MHz, CDCl₃) δ 7.20 (d, *J* = 2.2 Hz, 1H), 7.10 (dd, *J* = 8.4, 2.2 Hz, 1H), 6.87 (d, *J* = 8.4 Hz, 1H), 5.65 (s, 1H), 3.46 (s, 1H), 2.27 (s, 3H).

4-Ethynyl-2-methylphenol (**18h**): Synthesised from 4-ethyl-2-iodophenol (496 mg, 2 mmol) according to the general procedure (I) to afford the title compound as an oil (238 mg) in 90% yield. ¹H NMR (400 MHz, CDCl₃) δ 7.35–7.20 (m, 1H), 7.13 (dd, *J* = 8.6, 2.2 Hz, 1H), 6.89 (d, *J* = 8.4 Hz, 1H), 5.66 (s, 1H), 3.46 (s, 1H), 2.58 (q, *J* = 7.7 Hz, 2H), 1.30–1.15 (t, *J* = 7.7 Hz, 3H).

2-Ethynyl-4-propylphenol (**18i**)¹⁰⁵: Synthesised from 2-iodo-4-propylphenol (524 mg, 2 mmol) according to the general procedure (I) to afford the title compound as an oil (202 mg) in 88% yield. ¹H NMR (400 MHz, CDCl₃) δ 7.35–7.17 (m, 1H), 7.10 (dd, *J* = 8.4, 2.4 Hz, 1H), 6.88 (d, *J* = 8.4 Hz, 1H), 5.66 (s, 1H), 3.46 (s, 1H), 2.50 (t, *J* = 7.5 Hz, 2H), 1.75–1.54 (m, 2H), 0.94 (t, *J* = 7.5 Hz, 3H).

4-Benzyl-2-ethynylphenol (**18j**): Synthesised from 4-benzyl-2-iodophenol (620 mg, 2 mmol) according to the general procedure (I) to afford the title compound as an oil (307 mg) in 93% yield. ¹H NMR (400 MHz, MeOD) δ 7.27 (dd, *J* = 8.7, 6.5 Hz, 2H), 7.21–7.12 (m, 4H), 7.03 (dd, *J* = 8.4, 2.3 Hz, 1H), 6.77 (d, *J* = 8.4 Hz, 1H), 4.63 (s, 1H), 3.85 (s, 2H), 3.57 (s, 1H).

2-Ethynyl-1-methoxy-4-phenethylbenzene (**18k**): Synthesised from 2-iodo-1-methoxy-4-phenethylbenzene (676 mg, 2 mmol) according to the general procedure (I) to afford the title compound as an oil (378 mg) in 80% yield. ¹H NMR (400 MHz, MeOD) δ 7.29–7.03 (m, 7H), 6.88 (d, *J* = 8.5 Hz, 1H), 3.83 (s, 3H), 3.55 (s, 1H), 3.33 (p, *J* = 1.6 Hz, 2H), 2.93–2.78 (m, 2H).

1-Chloro-2-ethynyl-3-phenethoxybenzene (**18l**): Synthesised from 1-chloro-2-iodo-3-phenethoxybenzene (676 mg, 2 mmol) according to the general procedure (I) to afford the title compound as an oil (476 mg) in 83% yield. ¹H NMR (400 MHz, CDCl₃) δ 7.42–7.30 (m, 6H), 7.33–7.20 (m, 1H), 7.00 (t, *J* = 7.9 Hz, 1H), 4.39–4.31 (m, 2H), 3.26–3.16 (m, 3H).

1,2,4-Trichloro-5-ethynylbenzene (**18m**, CAS [6546–87-8]): Synthesised from 1,2,4-trichloro-5-iodobenzene (612 mg, 2 mmol) according to the general procedure (I) to afford the title compound as an oil (310 mg) in 76% yield. ¹H NMR (400 MHz, CDCl₃) δ 7.63 (s, 1H), 7.55 (s, 1H), 7.29 (s, 1H), 3.46 (s, 1H).

1,3,5-Trichloro-2-ethynylbenzene (**18n**)¹⁰⁶: Synthesised from 1,3,5-trichloro-5-iodobenzene (612 mg, 2 mmol) according to the general

procedure (I) to afford the title compound as an oil (326 mg) in 76% yield. ^1H NMR (400 MHz, CDCl_3) δ 7.40 (s, 2H), 3.73 (s, 1H).

General procedure (II) for the preparation of 4-Aryl-1,2,3-Triazoles:

To a stirred solution of commercially available or synthetically prepared aryethynes (**18**) (1 equiv) and CuI (0.05 equiv) in DMF/MeOH solution (2 mL, 9:1) under an argon atmosphere, TMSN_3 (1.5 equiv) was added. The resulting solution was stirred at 100°C for 10–12 h. After consumption of the ethynyl substrate, the mixture was cooled to rt, the precipitate was filtered off, and the remaining solution was concentrated under reduced pressure. The crude residue was purified by FC (SiO_2 , EtOAc/petroleum ether) to obtain the desired 4-aryl-1,2,3-triazole.

General procedure (III) for the demethylation of aryl methyl ethers:

The methyl ether (1 eq) was dissolved in 48% HBr in water (4 mL), and the orange solution was heated to 100°C for 14 h under nitrogen atmosphere. The mixture was cooled to rt, diluted with water, and neutralised by the addition of a saturated aq. soln. of NaHCO_3 until the evolution of CO_2 ceased. The organic layer was extracted with EtOAc (2×5 mL), dried over Na_2SO_4 , filtered, and concentrated under reduced pressure to afford a residue that was purified by FC (SiO_2 , EtOAc/petroleum ether) to give the desired phenol.

Synthesis of 4-Aryl-1,2,3-Triazoles

4-(1,2,3-Triazol-4-yl)phenol (**20**)¹⁰⁷: Synthesised from 1-ethynyl-4-methoxybenzene (264 mg, 2.0 mmol) and TMSN_3 (345 mg, 3.0 mmol) using the general procedure (II) to give 4-(4-methoxyphenyl)-1,2,3-triazole (245 mg, 70%) as a white solid. ^1H NMR (400 MHz, CDCl_3) δ 7.92 (s, 1H), 7.76–7.68 (m, 2H), 7.02–6.93 (m, 2H), 3.85 (s, 3H). Using the general procedure (III), 4-(4-methoxyphenyl)-1,2,3-triazole (166 mg, 1.0 mmol) dissolved in 48% HBr in water (4 mL) gave **20** (115 mg, 75%) as a white solid. ^1H NMR (400 MHz, MeOD) δ 8.00 (s, 1H), 7.72–7.59 (m, 2H), 6.95–6.82 (m, 2H), ^{13}C NMR (101 MHz, MeOD) δ 157.82, 127.06, 115.40, HRMS (ESI/QTOF) m/z : calcd for $[\text{M} + \text{H}]^+$ $\text{C}_8\text{H}_8\text{N}_3\text{O}^+$ 162.0662; found, 162.0661.

4-(3-Isopropylphenyl)-1,2,3-triazole (**23**, CAS [2192187-16-7]): Synthesised from 1-ethynyl-3-isopropylbenzene (144 mg, 1.0 mmol) and TMSN_3 (173 mg, 1.5 mmol) using the general procedure (II) to give **23** (84 mg, 45%) as a white solid. ^1H NMR (400 MHz, CDCl_3) δ 7.98 (s, 1H), 7.71 (t, $J=1.8$ Hz, 1H), 7.63 (dt, $J=7.7$, 1.5 Hz, 1H), 7.39 (t, $J=7.7$ Hz, 1H), 7.31–7.23 (m, 1H), 2.99 (p, $J=6.9$ Hz, 1H), 1.31 (d, $J=6.9$ Hz, 6H), ^{13}C NMR (101 MHz, CDCl_3) δ 149.77, 129.65, 128.99, 127.00, 124.30, 123.71, 34.18, 23.95, HRMS (ESI/QTOF) m/z : calcd for $[\text{M} + \text{H}]^+$ $\text{C}_{11}\text{H}_{13}\text{N}_3^+$ 188.1188, found: 188.1185.

4-(3-Butylphenyl)-1,2,3-triazole (**24**, CAS [2192187-22-5]): Synthesised from 1-butyl-3-ethynylbenzene (**18a**) (150 mg, 0.95 mmol) and TMSN_3 (164 mg, 1.43 mmol) using the general procedure (II) to give **24** (153 mg, 80%) as a white solid. ^1H NMR (400 MHz, MeOD) δ 8.15 (s, 1H), 7.68 (d, $J=1.9$ Hz, 1H), 7.64 (dt, $J=7.8$, 1.5 Hz, 1H), 7.36 (t, $J=7.7$ Hz, 1H), 7.21 (dt, $J=7.6$, 1.5 Hz, 1H), 2.74–2.66 (m, 2H), 1.67 (tt, $J=9.2$, 6.9 Hz, 2H), 1.41 (h, $J=7.4$ Hz, 2H), 0.98 (t, $J=7.4$ Hz, 3H), ^{13}C NMR (101 MHz, MeOD) δ 143.49, 128.57, 128.34, 125.61, 123.03, 35.23, 33.44, 29.42, 22.01, 13.00, HRMS (ESI/QTOF) m/z : calcd for $[\text{M} + \text{H}]^+$ $\text{C}_{12}\text{H}_{16}\text{N}_3^+$ 202.1339; found, 202.1342.

4-(2-Benzyloxyphenyl)-1,2,3-triazole (**25**)¹⁰⁸: Synthesised from 1-(benzyloxy)-2-ethynylbenzene (**18b**) (104 mg, 0.5 mmol) and TMSN_3 (87 mg, 0.75 mmol) using the general procedure (II) to give **25** (90 mg, 72%) as a white solid. ^1H NMR (400 MHz, MeOD) δ 8.08 (s, 1H), 7.51–7.42 (m, 2H), 7.43–7.28 (m, 5H), 7.18 (dd, $J=8.4$, 1.1 Hz, 1H), 7.06 (td, $J=7.5$, 1.1 Hz, 1H), 5.23 (s, 2H), ^{13}C NMR (101 MHz, CDCl_3) δ 155.20, 135.99, 130.49, 129.97, 128.98, 128.61, 128.22, 127.86, 121.64, 112.64, 70.91, HRMS (ESI/QTOF) m/z : calcd for $[\text{M} + \text{H}]^+$ $\text{C}_{15}\text{H}_{14}\text{N}_3\text{O}^+$ 252.1131; found, 252.1131.

4-(2-Phenethoxyphenyl)-1,2,3-triazole (**26**): Synthesised from 1-ethynyl-2-phenethoxybenzene (**18c**) (111 mg, 0.5 mmol) and TMSN_3 (87 mg, 0.75 mmol) using the general procedure (II) to give **26** (93 mg, 70%) as a white solid, m.p. $91\text{--}93^\circ\text{C}$. ^1H NMR (400 MHz, CDCl_3) δ 12.03 (s, 1H), 7.98 (s, 1H), 7.81 (s, 1H), 7.46–7.28 (m, 6H), 7.12–7.02 (m, 2H), 4.44 (t, $J=6.6$ Hz, 2H), 3.25 (t, $J=6.6$ Hz, 2H), ^{13}C NMR (101 MHz, CDCl_3) δ 155.12, 137.75, 129.92, 129.01, 128.74, 128.28, 127.04, 121.41, 112.15, 69.00, 35.61, HRMS (ESI/QTOF) m/z : calcd for $[\text{M} + \text{H}]^+$ $\text{C}_{16}\text{H}_{16}\text{N}_3\text{O}^+$ 266.1288; found, 266.1290.

2-(2-(1*H*-1,2,3-triazol-5-yl)phenoxy)-1-phenylethan-1-ol (**27**): Synthesised from 2-(2-ethynylphenoxy)-1-phenylethan-1-ol (**18d**) (120 mg, 0.5 mmol) and TMSN_3 (87 mg, 0.75 mmol) using the general procedure (II) to give **27** (91 mg, 65%) as a white solid, m.p. $153\text{--}155^\circ\text{C}$. ^1H NMR (400 MHz, CDCl_3) δ 8.01 (s, 1H), 7.69 (dd, $J=7.7$, 1.6 Hz, 1H), 7.50–7.42 (m, 2H), 7.42–7.28 (m, 4H), 7.07 (td, $J=7.6$, 1.1 Hz, 1H), 6.99 (dd, $J=8.3$, 1.1 Hz, 1H), 5.20 (dd, $J=9.0$, 3.1 Hz, 1H), 4.38 (dd, $J=9.5$, 3.2 Hz, 1H), 4.08 (t, $J=9.3$ Hz, 1H), ^{13}C NMR (101 MHz, MeOD) δ 156.02, 142.09, 130.21, 128.94, 128.37, 126.99, 121.79, 113.38, 73.96, 72.68, HRMS (ESI/QTOF) m/z : calcd for $[\text{M} + \text{Na}]^+$ $\text{C}_{16}\text{H}_{15}\text{N}_3\text{O}_2\text{Na}^+$ 304.1056; found, 304.1064.

N-Phenyl-2-(1*H*-1,2,3-triazol-5-yl)aniline (**28**): Synthesised from 2-ethynyl-*N*-phenethylaniline (**18e**) (165 mg, 0.75 mmol) and TMSN_3 (130 mg, 1.13 mmol) using the general procedure (II) to give **28** (80 mg, 45%) as a white solid, m.p. $129\text{--}132^\circ\text{C}$. ^1H NMR (400 MHz, MeOD) δ 8.03 (s, 1H), 7.60 (d, $J=7.6$ Hz, 1H), 7.31–7.13 (m, 6H), 6.83 (dd, $J=8.4$, 1.1 Hz, 1H), 6.70 (td, $J=7.5$, 1.1 Hz, 1H), 3.49 (t, $J=7.0$ Hz, 3H), 2.96 (t, $J=7.0$ Hz, 3H), ^{13}C NMR (101 MHz, MeOD) δ 145.50, 139.57, 130.69, 129.11, 128.48, 128.03, 127.78, 125.85, 115.73, 111.04, 44.81, 35.03, HRMS (ESI/QTOF) m/z : calcd for $[\text{M} + \text{H}]^+$ $\text{C}_{16}\text{H}_{17}\text{N}_4^+$ 265.1448; found, 265.1441.

4-Fluoro-2-(1*H*-1,2,3-triazol-5-yl)phenol (**34**): Synthesised from 2-ethynyl-4-fluorophenol (**18f**) (204 mg, 1.5 mmol) and TMSN_3 (259 mg, 2.25 mmol) using the general procedure (II) to give **34** (201 mg, 75%) as a white solid, m.p. $186\text{--}188^\circ\text{C}$. ^1H NMR (400 MHz, MeOD) δ 8.31 (s, 1H), 7.62 (dd, $J=9.6$, 2.8 Hz, 1H), 7.04–6.86 (m, 2H), ^{13}C NMR (101 MHz, MeOD) δ 157.53, 155.20, 150.77, 116.82, 116.73, 115.37, 115.14, 112.71, 112.46, HRMS (ESI/QTOF) m/z : calcd for $[\text{M} + \text{H}]^+$ $\text{C}_8\text{H}_7\text{FN}_3\text{O}^+$ 180.0568; found, 180.0567.

4-Methyl-2-(1*H*-1,2,3-triazol-5-yl)phenol (**35**): Synthesised from 2-ethynyl-4-methylphenol (**18g**) (170 mg, 1.3 mmol) and TMSN_3 (225 mg, 1.95 mmol) using the general procedure (II) to give **35** (171 mg, 75%) as a white solid, m.p. $160\text{--}162^\circ\text{C}$. ^1H NMR (400 MHz, MeOD) δ 8.24 (s, 1H), 7.69–7.58 (m, 1H), 7.04 (dd, $J=8.3$, 2.3 Hz, 1H), 6.85 (d, $J=8.3$ Hz, 1H), 2.32 (s, 3H), ^{13}C NMR (101 MHz, MeOD) δ 152.36, 129.91, 128.66, 127.09, 115.80, 114.63, 19.18, HRMS (ESI/QTOF) m/z : calcd for $[\text{M} + \text{H}]^+$ $\text{C}_9\text{H}_{10}\text{N}_3\text{O}^+$ 176.0818; found, 176.0817.

4-Ethyl-2-(1*H*-1,2,3-triazol-5-yl)phenol (**36**): Synthesised from 4-ethyl-2-methylphenol (**18h**) (146 mg, 1.0 mmol) and TMSN_3 (173 mg, 1.5 mmol) using the general procedure (II) to give **36** (151 mg, 80%) as a white solid, m.p. $71\text{--}73^\circ\text{C}$. ^1H NMR (400 MHz,

MeOD) δ 8.24 (s, 1H), 7.66 (s, 1H), 7.07 (dd, $J=8.3$, 2.2 Hz, 1H), 6.88 (d, $J=8.5$ Hz, 1H), 2.63 (q, $J=7.6$ Hz, 2H), 1.26 (td, $J=7.7$, 1.2 Hz, 3H), ^{13}C NMR (101 MHz, MeOD) δ 152.56, 135.37, 128.73, 126.00, 115.83, 114.74, 114.68, 27.63, 15.08, HRMS (ESI/QTOF) m/z : calcd for $[\text{M} + \text{H}]^+ \text{C}_{10}\text{H}_{12}\text{N}_3\text{O}^+$ 190.0975; found, 190.0977.

4-Propyl-2-(1H-1,2,3-triazol-5-yl)phenol (**37**): Synthesised from 2-ethynyl-4-propylphenol (**18i**) (160 mg, 1.0 mmol) and TMSN_3 (173 mg, 1.5 mmol) using the general procedure (II) to give **37** (152 mg, 75%) as a white solid, m.p. 138–140 °C. ^1H NMR (400 MHz, MeOD) δ 8.24 (s, 1H), 7.64 (s, 1H), 7.05 (dd, $J=8.3$, 2.2 Hz, 1H), 6.88 (d, $J=8.2$ Hz, 1H), 2.65–2.50 (m, 2H), 1.67 (h, $J=7.4$ Hz, 2H), 0.97 (t, $J=7.3$ Hz, 3H), ^{13}C NMR (101 MHz, MeOD) δ 152.60, 133.70, 129.38, 126.63, 115.78, 114.68, 36.80, 24.52, 12.72, HRMS (ESI/QTOF) m/z : calcd for $[\text{M} + \text{H}]^+ \text{C}_{11}\text{H}_{14}\text{N}_3\text{O}^+$ 204.1131; found, 204.1130.

4-Benzyl-2-(1H-1,2,3-triazol-5-yl)phenol (**38**): Synthesised from 4-benzyl-2-ethynylphenol (**18j**) (460 mg, 2.2 mmol) and TMSN_3 (379 mg, 3.3 mmol) using the general procedure (II) to give **38** (441 mg, 80%) as a white solid, m.p. 148–151 °C. ^1H NMR (400 MHz, MeOD) δ 8.23 (s, 1H), 7.75–7.65 (m, 1H), 7.32–7.13 (m, 5H), 7.05 (dd, $J=8.4$, 2.3 Hz, 1H), 6.88 (d, $J=8.3$ Hz, 1H), 3.95 (s, 2H), ^{13}C NMR (101 MHz, MeOD) δ 152.92, 141.64, 132.63, 129.81, 128.40, 128.04, 127.20, 125.58, 115.97, 115.01, 40.57, HRMS (ESI/QTOF) m/z : calcd for $[\text{M} + \text{H}]^+ \text{C}_{15}\text{H}_{14}\text{N}_3\text{O}^+$ 252.1131; found, 252.1137.

4-Phenylethyl-2-(1H-1,2,3-triazol-5-yl)phenol (**39**): Synthesised from 2-ethynyl-1-methoxy-4-phenethylbenzene (**18k**) (544 mg, 2.3 mmol) and TMSN_3 (398 mg, 3.45 mmol) using the general procedure (II) to give 5-(2-methoxy-5-phenethylphenyl)-1H-1,2,3-triazole (282 mg, 44%) as a white solid. ^1H NMR (400 MHz, MeOD) δ 8.15 (s, 1H), 7.79 (s, 1H), 7.30–7.22 (m, 2H), 7.22–7.11 (m, 4H), 7.02 (d, $J=8.5$ Hz, 1H), 3.95 (s, 3H), 2.96–2.90 (m, 4H). Using the general procedure (III), 5-(2-methoxy-5-phenethylphenyl)-1H-1,2,3-triazole (246 mg, 1.2 mmol) dissolved in 48% HBr in water (5 mL) gave **39** (238 mg, 75%) as a white solid, m.p. 157–159 °C. ^1H NMR (400 MHz, MeOD) δ 8.21 (brs, 1H), 7.64 (brs, 1H), 7.32–7.12 (m, 5H), 7.03 (dd, $J=8.3$, 2.3 Hz, 1H), 6.85 (d, $J=8.3$ Hz, 1H), 2.98–2.81 (m, 4H), ^{13}C NMR (101 MHz, MeOD) δ 152.76, 141.71, 132.93, 129.45, 128.21, 127.87, 126.78, 125.45, 115.73, 37.93, 36.90, HRMS (ESI/QTOF) m/z : calcd for $[\text{M} + \text{H}]^+ \text{C}_{16}\text{H}_{16}\text{N}_3\text{O}^+$ 266.1288; found, 266.1293.

4-(3-Chloro-2-phenethoxyphenyl)-1,2,3-triazole (**43**): Synthesised from 1-chloro-2-ethynyl-3-phenethoxybenzene (**18l**) (150 mg, 0.59 mmol) and TMSN_3 (102 mg, 0.89 mmol) using the general procedure (II) to give **43** (120 mg, 68%) as a white solid, m.p. 96–99 °C. ^1H NMR (400 MHz, CDCl_3) δ 7.86–7.71 (m, 1H), 7.46–7.24 (m, 6H), 7.16 (t, $J=7.9$ Hz, 2H), 4.10 (t, $J=6.8$ Hz, 2H), 3.13 (t, $J=6.8$ Hz, 2H), ^{13}C NMR (101 MHz, MeOD) δ 151.89, 138.17, 129.96, 128.90, 128.53, 128.13, 126.77, 126.31, 125.06, 73.32, 36.16, HRMS (ESI/QTOF) m/z : calcd for $[\text{M} + \text{Na}]^+ \text{C}_{16}\text{H}_{14}\text{ClN}_3\text{O}^+$ 322.0718; found, 322.0722.

2-(1H-1,2,3-triazol-5-yl)benzene-1,3-diol (**44**): Synthesised from **45** (130 mg, 0.75 mmol) dissolved in 48% HBr in water (3 mL) using the general procedure (III) to give **44** (93 mg, 70%) as white solid, m.p. 257–259 °C. ^1H NMR (400 MHz, MeOD) δ 8.38 (s, 1H), 7.02 (t, $J=8.2$ Hz, 1H), 6.46 (d, $J=8.1$ Hz, 2H), ^{13}C NMR (101 MHz, MeOD) δ 156.24, 129.03, 106.57, 102.41, HRMS (ESI/QTOF) m/z : calcd for $[\text{M} + \text{H}]^+ \text{C}_8\text{H}_7\text{N}_3\text{O}_2^+$ 178.0616; found, 178.0606.

4-(2,6-Dimethoxyphenyl)-1,2,3-triazole (**45**, CAS [2385145–91-3]): Synthesised from 2-ethynyl-1,3-dimethoxybenzene (324 mg, 2.0 mmol) and TMSN_3 (345 mg, 3.0 mmol) using the general procedure (II) to give **45** (197 mg, 48%) as a white solid. ^1H NMR (400 MHz, CDCl_3) δ 8.34 (s, 1H), 7.35 (t, $J=8.4$ Hz, 1H), 6.74 (d,

$J=8.5$ Hz, 2H), 4.02 (s, 9H), ^{13}C NMR (101 MHz, MeOD) δ 157.60, 132.66, 132.57, 130.45, 103.87, 55.08, HRMS (ESI/QTOF) m/z : calcd for $[\text{M} + \text{H}]^+ \text{C}_{10}\text{H}_{11}\text{N}_3\text{O}_2^+$ 206.0930; found, 206.0940.

4-(2,4-Dichlorophenyl)-1,2,3-triazole (**48**)¹⁰⁷: Synthesised from 2,4-dichloro-1-ethynylbenzene (250 mg, 1.5 mmol) and TMSN_3 (259 mg, 2.25 mmol) using the general procedure (II) to give **48** (272 mg, 85%) as a yellow solid. ^1H NMR (400 MHz, CDCl_3) δ 8.24 (d, $J=8.2$ Hz, 1H), 7.93 (d, $J=8.4$ Hz, 1H), 7.52 (t, $J=2.5$ Hz, 1H), 7.36 (dt, $J=8.5$, 2.5 Hz, 1H), ^{13}C NMR (101 MHz, MeOD) δ 134.29, 132.40, 130.97, 129.62, 127.30, 56.06, HRMS (ESI/QTOF) m/z : calcd for $[\text{M} + \text{H}]^+ \text{C}_8\text{H}_6\text{Cl}_2\text{N}_3^+$ 213.9933; found, 213.9931.

4-(3,4-Dichlorophenyl)-1,2,3-triazole (**49**)¹⁰⁹: Synthesised from 1,2-dichloro-4-ethynylbenzene (170 mg, 1.0 mmol) and TMSN_3 (173 mg, 1.5 mmol) using the general procedure (II) to give **49** (187 mg, 88%) as a yellow solid. ^1H NMR (400 MHz, MeOD) δ 8.25 (s, 1H), 8.06 (d, $J=2.0$ Hz, 1H), 7.81 (dd, $J=8.4$, 2.0 Hz, 1H), 7.62 (d, $J=8.4$ Hz, 1H), ^{13}C NMR (101 MHz, MeOD) δ 144.15, 132.55, 131.53, 130.64, 127.19, 125.05, 47.45, 47.24, 47.03, HRMS (ESI/QTOF) m/z : calcd for $[\text{M} + \text{H}]^+ \text{C}_8\text{H}_6\text{Cl}_2\text{N}_3^+$ 213.9933; found, 213.9928.

4-(3,5-Dichlorophenyl)-1,2,3-triazole (**50**, CAS [55751–17-2]): Synthesised from 1,3-dichloro-5-ethynylbenzene (170 mg, 1.0 mmol) and TMSN_3 (173 mg, 1.5 mmol) using the general procedure (II) to give **50** (175 mg, 82%) as a yellow solid. ^1H NMR (400 MHz, MeOD) δ 8.29 (s, 1H), 7.84 (d, $J=2.0$ Hz, 2H), 7.42 (q, $J=1.6$ Hz, 1H), ^{13}C NMR (101 MHz, MeOD) δ 143.94, 135.32, 133.74, 127.46, 123.88, HRMS (ESI/QTOF) m/z : calcd for $[\text{M} + \text{H}]^+ \text{C}_8\text{H}_6\text{Cl}_2\text{N}_3^+$ 213.9933; found, 213.9932.

4-(2,6-Dichlorophenyl)-1,2,3-triazole (**51**, CAS [2385230–51-1]): Synthesised from 1,3-dichloro-2-ethynylbenzene (170 mg, 1.0 mmol) and TMSN_3 (173 mg, 1.5 mmol) using the general procedure (II) to give **51** (160 mg, 75%) as a yellow solid. ^1H NMR (400 MHz, MeOD) δ 7.95 (s, 1H), 7.58–7.49 (m, 2H), 7.45 (dd, $J=8.9$, 7.2 Hz, 1H), ^{13}C NMR (101 MHz, MeOD) δ 135.87, 130.82, 128.08, HRMS (ESI/QTOF) m/z : calcd for $[\text{M} + \text{H}]^+ \text{C}_8\text{H}_6\text{Cl}_2\text{N}_3^+$ 213.9933; found, 213.9927.

4-(2,4,5-Trichlorophenyl)-1,2,3-triazole (**52**): Synthesised from 1,2,4-trichloro-5-ethynylbenzene (**18m**) (340 mg, 2.0 mmol) and TMSN_3 (345 mg, 3.0 mmol) using the general procedure (II) to give **52** (395 mg, 80%) as a yellow solid, m.p. 190–192 °C. ^1H NMR (400 MHz, CDCl_3) δ 8.20 (s, 1H), 8.09 (s, 1H), 7.56 (s, 1H), ^{13}C NMR (101 MHz, DMSO) δ 140.90, 131.74, 131.59, 130.85, 130.49, 130.18, 129.72, HRMS (ESI/QTOF) m/z : calcd for $[\text{M} + \text{H}]^+ \text{C}_8\text{H}_5\text{Cl}_3\text{N}_3^+$ 247.9544; found, 247.9536.

4-(2,4,6-Trichlorophenyl)-1,2,3-triazole (**53**): Synthesised from 1,3,5-trichloro-2-ethynylbenzene (**18n**) (170 mg, 1.0 mmol) and TMSN_3 (173 mg, 1.5 mmol) using the general procedure (II) to give **53** (198 mg, 80%) as a yellow solid, m.p. 236–238 °C. ^1H NMR (400 MHz, MeOD) δ 7.97 (s, 1H), 7.66 (s, 2H), ^{13}C NMR (101 MHz, DMSO) δ 136.31, 135.32, 128.67, HRMS (ESI/QTOF) m/z : calcd for $[\text{M} + \text{H}]^+ \text{C}_8\text{H}_5\text{Cl}_3\text{N}_3^+$ 247.9544; found, 247.9538.

Synthesis of 5-Substituted 4-Aryl-1,2,3-Triazoles

4-Phenyl-1H-1,2,3-triazole-5-carbonitrile (**62**)⁶⁵: To a strongly stirred solution of NaN_3 (195 mg, 1.5 mmol) suspended in DMF (4 mL) at 90 °C, a second solution of phenylpropynenitrile (**54**) (255 mg, 2.0 mmol) in DMF (2 mL) was added dropwise through an addition funnel over 10 min. The mixture was stirred for 1 h at 90 °C before cooling to rt and removing the solvent under reduced pressure. Water (6 mL) was added, and the aqueous layer was extracted with CH_2Cl_2 to remove the oil and to give a transparent light colored solution. Finally, the aqueous solution was acidified with 10%

HCl resulting in a light yellow precipitate which was washed with iced water to yield the crude product. The residue was purified by FC (SiO₂, CH₂Cl₂/MeOH) to obtain **62** (255 mg, 75% yield) as white solid. ¹H NMR (400 MHz, MeOD) δ 7.93 – 7.77 (m, 2H), 7.52 – 7.39 (m, 3H), 5.38 (brs, 1H), ¹³C NMR (101 MHz, MeOD) δ 147.13, 130.16, 128.97, 126.41, 126.16, 116.65, 112.66, HRMS (ESI/QTOF) *m/z*: calcd for [M + H]⁺ C₉H₆N₄⁺ 171.0671; found, 171.0667.

4-(3-Chlorophenyl)-5-methyl-1,2,3-triazole (**63**): 3-Chlorobenzaldehyde (280 mg, 2.0 mmol), nitromethane (180 mg, 2.4 mmol) and ammonium acetate (93 mg, 1.2 mmol) were added to 2 mL of glacial acetic acid. The resulting solution was heated under reflux for 2 h before pouring the reaction mixture into ice water. The yellow solid thus formed was collected by filtration to give the crude product 1-chloro-3-(2-nitroprop-1-en-1-yl)benzene (**56a**)^{66,110}. The crude product (197 mg, 1.0 mmol) and NaN₃ (98 mg, 1.5 mmol) were stirred in DMF (3 mL), and *p*-TsOH (87 mg, 0.5 mmol) was added to the mixture at rt. The mixture was stirred at 60 °C under air for 1 h. After completion of the reaction, the mixture was cooled to rt, quenched with H₂O (5 mL) and extracted with EtOAc (3 × 10 mL). The organic layers were collected, dried over anhydrous Na₂SO₄, filtered, and concentrated under reduced pressure. The residue was purified by FC (silica gel, EtOAc/hexane) to afford **63** (135 mg, 70%) as white solid, m.p. 161–163 °C. ¹H NMR (400 MHz, CDCl₃) δ 11.42 (brs, 1H), 7.73 (t, *J* = 1.8 Hz, 1H), 7.62 (dt, *J* = 7.4, 1.6 Hz, 1H), 7.46 – 7.31 (m, 2H), 2.55 (s, 3H), ¹³C NMR (101 MHz, MeOD) δ 134.37, 132.79, 130.00, 127.53, 126.48, 124.94, 8.94, HRMS (ESI/QTOF) *m/z*: calcd for [M + H]⁺ C₉H₈ClN₃⁺ 194.0485; found, 194.0482.

4,5-Bis(3-chlorophenyl)-1,2,3-triazole (**64**)⁶⁷: To a stirred solution of 3-chlorobenzaldehyde (420 mg, 3 mmol) in ethanol (6 mL) *p*-toluenesulfonyl hydrazide (**57**) (615 mg, 3.3 mmol) was added, and the solution was stirred for 2 h at rt. After completion of the reaction, the solvent was removed under reduced pressure. The obtained solid residue was washed with ethanol and dried under reduced pressure to afford N'-(3-chlorobenzylidene)-4-methylbenzenesulfonohydrazide (**58**)⁷⁷, ¹H NMR (400 MHz, CDCl₃) δ 8.36 (bs, 1H), 7.91 (s, 1H), 7.89 (s, 1H), 7.73 (s, 1H), 7.59 (t, *J* = 1.8 Hz, 1H), 7.49 – 7.25 (m, 5H), 2.44 (s, 3H). The residue (**58**) (440 mg, 1.4 mmol) was dissolved in DMF (5 mL), Cs₂CO₃ (764 mg, 2.2 mmol) was added, and the mixture was heated to 100 °C, monitoring the progress of the reaction by TLC. The reaction mixture was cooled to rt and diluted with cold water. After extraction with EtOAc, the organic layers were collected, dried (anhydrous Na₂SO₄), filtered, and concentrated under reduced pressure. The residue was purified by FC (silica gel, EtOAc/hexane) to give **64** (285 mg, 70%) as white solid. ¹H NMR (400 MHz, CDCl₃) δ 8.62 (s, 2H), 7.90 (t, *J* = 1.9 Hz, 2H), 7.72 (dt, *J* = 7.4, 1.5 Hz, 2H), 7.52 – 7.35 (m, 4H), ¹³C NMR (101 MHz, MeOD) δ 134.38, 131.99, 130.02, 129.30, 128.40, 127.74, 127.38, 126.22, HRMS (ESI/QTOF) *m/z*: calcd for [M + H]⁺ C₁₄H₁₀Cl₂N₃⁺ 290.0246; found, 290.0246.

Ethyl 4-(3-chlorophenyl)-1*H*-1,2,3-triazole-5-carboxylate (**65**)⁵⁹: To a stirred solution of ethyl-3-(4-chlorophenyl)propionate (**59**) (209 mg, 1.0 mmol) in DMSO (2 mL), NaN₃ (182 mg, 2.8 mmol) was added, and the solution was stirred under reflux at 70 °C for 6 h. After completion of the reaction, the mixture was cooled to rt and quenched with water. After extraction with EtOAc, the organic layer was collected, washed with brine, dried (anhydrous Na₂SO₄), filtered, and concentrated under reduced pressure. Purification by FC (silica gel, EtOAc/hexane) produced **65** (150 mg, 60%) as white solid. ¹H NMR (400 MHz, MeOD) δ 7.83 (dd, *J* = 8.4, 1.7 Hz, 2H), 7.51 (dd, *J* = 8.5, 1.6 Hz, 2H), 4.39 (qd, *J* = 7.1, 1.4 Hz, 2H), 1.36 (td, *J* = 7.2, 1.4 Hz, 3H), ¹³C NMR (101 MHz, MeOD) δ 160.72, 135.17,

130.52, 128.08, 61.10, 13.00, HRMS (ESI/QTOF) *m/z*: calcd for [M + H]⁺ C₁₁H₁₁ClN₃O₂⁺ 252.0534; found, 252.0535.

4-(4-Chlorophenyl)-1*H*-1,2,3-triazole-5-carboxamide (**66**)⁶⁹: To a stirred solution of 4-chlorobenzaldehyde (**55c**) (280 mg, 2.0 mmol), 2-cyanoacetamide (**60**) (169 mg, 2.0 mmol), and Et₃N·HCl (566 mg, 5.0 mmol) in DMF (3 mL), NaN₃ (390 mg, 6.0 mmol) was added. The mixture was stirred at 70 °C for 10 h before cooling to rt and adding water (20 mL) and 10% HCl solution (1 mL). After extraction with EtOAc (2 × 30 mL), the organic layer was collected, washed with water (3 × 50 mL) and brine solution (1 × 50 mL), dried (anhydrous Na₂SO₄), filtered, and concentrated under reduced pressure. The residue was subject to FC (SiO₂, CH₂Cl₂/MeOH) to obtain **66** (288 mg, 65% yield) as white solid, ¹H NMR (400 MHz, MeOD) δ 7.92 (d, *J* = 8.3 Hz, 2H), 7.47 (d, *J* = 8.3 Hz, 2H), ¹³C NMR (101 MHz, MeOD) δ 163.78, 134.64, 130.54, 128.25, HRMS (nanochip-ESI/LTQ-Orbitrap) *m/z*: calcd for [M + Na]⁺ C₉H₇ClN₄O₂Na⁺ 245.0201; found, 245.0196.

4-(4-Chloro-2-hydroxyphenyl)-1*H*-1,2,3-triazole-5-carboxamide (**67**): Synthesised from 5-chloro-2-hydroxybenzaldehyde (**55b**) (314 mg, 2.0 mmol), 2-cyanoacetamide (**60**) (169 mg, 2.0 mmol), and Et₃N·HCl (566 mg, 5.0 mmol), and NaN₃ (390 mg, 6.0 mmol) using the same procedure as for **66** to give **67** (260 mg, 55% yield) as a white solid, m.p. 260–262 °C. ¹H NMR (400 MHz, MeOD) δ 7.68 – 7.57 (m, 1H), 7.31 (ddd, *J* = 8.7, 2.7, 1.4 Hz, 1H), 6.96 (dd, *J* = 8.7, 1.5 Hz, 1H), ¹³C NMR (101 MHz, MeOD) δ 164.84, 154.03, 137.63, 130.39, 130.37, 124.01, 118.10, 116.86, HRMS (ESI/QTOF) *m/z*: calcd for [M + Na]⁺ C₉H₇ClN₄O₂Na⁺ 261.0150; found, 261.0159.

4-Chloro-2-(5-methyl-1,2,3-triazol-4-yl)phenol (**68**): Synthesised from 5-chloro-2-hydroxybenzaldehyde (**55b**) (312 mg, 2.0 mmol), nitromethane (180 mg, 2.4 mmol), and ammonium acetate (93 mg, 1.2 mmol) according to the same procedure as used for **63** to afford **68** (136 mg, 65%) as white solid, m.p. 149–151 °C. ¹H NMR (400 MHz, CDCl₃) δ 7.56 (d, *J* = 2.5 Hz, 1H), 7.25 (dd, *J* = 8.8, 2.6 Hz, 1H), 7.05 (d, *J* = 8.7 Hz, 1H), 2.69 (s, 3H), ¹³C NMR (101 MHz, MeOD) δ 170.80, 158.40, 149.45, 145.46, 138.72, 120.68, 19.07, HRMS (ESI/QTOF) *m/z*: calcd for [M + H]⁺ C₉H₉ClN₃O⁺ 210.0429; found, 210.0431.

Synthesis of 4-Aryl-Tether-1,2,3-Triazoles and annulated derivatives

N-(4-Bromophenyl)-1,2,3-triazol-4-amine (**78**)⁷¹: 4-Bromo aniline (335 mg, 2.62 mmol) was dissolved in hydrochloric acid (6.03 mL of 2 M, 12.06 mmol), diluted with water (8 mL) and cooled to 0 °C. Sodium nitrite (181 mg, 2.62 mmol) was added and the mixture was stirred at 0 °C for 20 min before slowly adding a solution of 2-aminoacetonitrile monohydrochloride (**70**) (243 mg, 2.62 mmol) in water (3 mL). The mixture was stirred for 10 min at 0 °C before adding sodium acetate (3.02 g, 37.0 mmol) and allowing the mixture to warm to rt, where it was stirred for 1 h. The precipitate was collected by filtration and washed with water to afford 2-(3-(4-chlorophenyl)triazol-2-en-1-yl)acetonitrile. The residue (238 mg, 1.0 mmol) was dissolved in EtOH (7 mL) and heated under reflux for 4 h. The mixture was allowed to cool to rt and concentrated under reduced pressure. The crude compound was triturated with CH₂Cl₂ to produce a cream solid which was purified by FC (40% EtOAc in petroleum ether) to afford **78** (167 mg, 70%) as a white solid. ¹H NMR (400 MHz, MeOD) δ 7.39 (s, 1H), 7.35 – 7.25 (m, 2H), 7.19 (m, 2H), ¹³C NMR (101 MHz, MeOD) δ 148.34, 142.56, 131.44, 121.80, 116.57, 110.61, HRMS (ESI/QTOF) *m/z*: calcd for [M + H]⁺ C₈H₈BrN₄⁺ 238.9927; found, 238.9933.

4-(Phenoxy)-1,2,3-triazole (**82**): Synthesised from (ethynyloxy)-benzene (**77a**) (130 mg, 1.1 mmol) and TMSN₃ according to the

general procedure (II) to afford **82** (124 mg, 70%) as a white solid. ^1H NMR (400 MHz, CDCl_3) δ 11.08 (bs, 1H), 7.44–7.34 (m, 3H), 7.29 (s, 1H), 7.24–7.14 (m, 2H), ^{13}C NMR (101 MHz, MeOD) δ 158.33, 156.97, 129.48, 123.62, 117.16, HRMS (ESI/QTOF) m/z : calcd for $[\text{M} + \text{H}]^+$ $\text{C}_8\text{H}_8\text{N}_3\text{O}^+$ 162.0662; found, 162.0666.

4-(Phenylthio)-1,2,3-triazole (**83**): Synthesised from ethynyl(phenyl)sulfane (**77b**) (176 mg, 1.3 mmol) and TMSN_3 according to the general procedure (II) to afford **83** (154 mg, 67%) as a white solid. ^1H NMR (400 MHz, CDCl_3) δ 7.72 (s, 1H), 7.42–7.24 (m, 5H), 3.42 (s, 2H), ^{13}C NMR (101 MHz, MeOD) δ 135.18, 128.91, 128.52, 126.57, HRMS (ESI/QTOF) m/z : calcd for $[\text{M} + \text{H}]^+$ $\text{C}_8\text{H}_8\text{N}_3\text{S}^+$ 178.0433; found, 178.0436.

4-(Phenylsulfonyl)-1H-1,2,3-triazole (**84**)¹¹¹: To a stirred solution of compound **83** (60 mg 0.34 mmol) in methanol (2 mL), H_2O_2 (0.1 mL, 2.7 mmol) and a catalytic amount of ammonium molybdate (7 mg, 0.04 mmol) were added and allowed to stir at rt for 14 h, monitoring the progress of the reaction by TLC. After completion of the reaction, the solvent was removed under reduced pressure. The obtained solid products were dissolved in CH_2Cl_2 (2 mL) and water (2 mL), and the aqueous phase was extracted with CH_2Cl_2 (2×4 mL). The combined organic layers were washed with brine, dried over Na_2SO_4 , filtered, and concentrated under reduced pressure. The residue was purified by FC to give **84** (57 mg, 80%) as a white solid. ^1H NMR (400 MHz, CDCl_3) δ 8.17 (s, 1H), 8.09 (dd, $J=7.3, 1.8$ Hz, 2H), 7.69–7.61 (m, 1H), 7.57 (dd, $J=8.5, 6.9$ Hz, 2H), ^{13}C NMR (101 MHz, MeOD) δ 148.22, 140.70, 133.77, 129.19, 127.44, HRMS (ESI/QTOF) m/z : calcd for $[\text{M} + \text{Na}]^+$ $\text{C}_8\text{H}_7\text{N}_3\text{O}_2\text{SNa}^+$ 232.0151; found, 232.0154.

Phenyl(1,2,3-triazol-4-yl)methanol (**85**)¹¹²: Synthesised from 1-phenylprop-2-yn-1-ol (**77c**) (198 mg, 1.5 mmol) and TMSN_3 according to the general procedure (II) to afford **85** (184 mg, 70%) as a white solid. ^1H NMR (400 MHz, CDCl_3) δ 7.57 (s, 1H), 7.51–7.31 (m, 5H), 6.08 (s, 1H), ^{13}C NMR (101 MHz, MeOD) δ 142.64, 128.16, 127.49, 126.22, 68.31, HRMS (ESI/QTOF) m/z : calcd for $[\text{M} + \text{Na}]^+$ $\text{C}_9\text{H}_9\text{N}_3\text{ONa}^+$ 198.0640; found, 198.0638.

N-Phenyl-1H-1,2,3-triazole-4-carboxamide (**86**): Synthesised from *N*-phenylpropiolamide (**77d**) (145 mg, 1.0 mmol) and TMSN_3 according to the general procedure (II) to afford **86** (94 mg, 50%) as a white solid. ^1H NMR (400 MHz, CDCl_3) δ 8.28 (s, 1H), 7.71 (d, $J=8.0$ Hz, 2H), 7.44–7.35 (m, 2H), 7.17 (td, $J=7.3, 1.1$ Hz, 1H), ^{13}C NMR (101 MHz, MeOD) δ 159.40, 142.22, 137.70, 128.50, 124.37, 120.71, 120.59, HRMS (ESI/QTOF) m/z : calcd for $[\text{M} + \text{Na}]^+$ $\text{C}_9\text{H}_8\text{N}_4\text{ONa}^+$ 211.0590; found, 211.0588.

Phenyl(1H-1,2,3-triazol-4-yl)methanone *O*-methyl oxime (**87**): To a stirred solution of phenyl(1H-1,2,3-triazol-4-yl)methanone (**99**)¹¹³ (50 mg, 0.29 mmol) in H_2O (2 mL), and EtOH (1 mL), *O*-methylhydroxylamine hydrochloride (65 mg, 0.82 mmol) and NaOAc (104 mg, 1.28 mmol) were added. The flask was equipped with a reflux condenser and heated to 70 °C for 2 h. After cooling to rt, the mixture was extracted with EtOAc (3×5 mL). The organic layers were combined, dried over Na_2SO_4 , filtered, and concentrated under reduced pressure. Purification by FC gave **87** (32 mg, 55%) as amorphous solid. ^1H NMR (400 MHz, CDCl_3) δ 8.16 (s, 1H), 7.67–7.59 (m, 2H), 7.54–7.42 (m, 3H), 4.20 (s, 3H), ^{13}C NMR (101 MHz, DMSO) δ 148.52, 138.55, 137.27, 135.12, 129.65, 129.08, 128.47, 62.86, HRMS (ESI/QTOF) m/z : calcd for $[\text{M} + \text{H}]^+$ $\text{C}_{10}\text{H}_{11}\text{N}_4\text{O}^+$ 203.0927; found, 203.0926.

3,8-Dihydroindeno[1,2-d][1,2,3]triazole (**89**)⁷⁴: 1,2-Indandione-2-oxime (**71**) (161 mg, 1.0 mmol), hydrazine hydrate (97 mg, 3.0 mmol) and potassium hydroxide (168 mg, 3.0 mmol) were dissolved in diethyleneglycol (3 mL) under nitrogen atmosphere. The reactions mixture was heated to 170–190 °C and maintained at this temperature for 6 h. Upon completion of the reaction, the

mixture was cooled to rt, and water (5 mL) and EtOAc (10 mL) were added. EtOAc (10 mL) was added, the phases were separated, and the aqueous phase was further extracted with EtOAc (3×10 mL). The combined organic phases were washed with brine, dried over Na_2SO_4 , filtered, and concentrated under reduced pressure. The residue was purified by FC to yield **89** (63 mg, 40%) as a white solid. ^1H NMR (400 MHz, CDCl_3) δ 7.84 (dt, $J=7.6, 1.1$ Hz, 1H), 7.57 (dp, $J=7.3, 1.0$ Hz, 1H), 7.47–7.33 (m, 2H), 3.83 (d, $J=0.8$ Hz, 3H), ^{13}C NMR (101 MHz, MeOD) δ 153.40, 146.94, 131.79, 127.05, 126.00, 120.16, 27.32 HRMS (ESI/QTOF) m/z : calcd for $[\text{M} + \text{H}]^+$ $\text{C}_9\text{H}_8\text{N}_3^+$ 158.0713; found, 158.0716.

Synthesis of ethynes **77a**, **77b**, **77d**

(Ethynyloxy)benzene (**77a**)¹¹⁴: A mixture of phenol (**72**) (940 mg, 10.0 mmol) and NaOH powder (400 mg, 10 mmol) in DMSO (10 mL) was stirred at rt for 2 h before slowly adding trichloroethylene (**73**) (0.91 mL, 10.0 mmol). The mixture was stirred at rt until completion of the reaction. Then, water (25 mL) and CH_2Cl_2 (50 mL) were added, the phases were separated, and the aqueous phase was further extracted with CH_2Cl_2 (3×50 mL). The combined organic phases were washed with brine, dried over Na_2SO_4 , filtered, and concentrated under reduced pressure. The crude residue was used in the next step without purification. To a solution of the residue (752 mg, 4.0 mmol) in dry Et₂O (32 mL) at –78 °C, a solution of *n*-BuLi (2.5 M in hexane, 6.4 mL 16.0 mmol) was added under nitrogen atmosphere. After addition, the mixture was warmed to –20 °C over 1 h and stirred at this temperature for 1 h, before adding water (10 mL) and warming the mixture to rt. The phases were separated and the aqueous phase was extracted with CH_2Cl_2 (3×15 mL). The combined organic phases were washed with brine, dried over Na_2SO_4 , filtered, and concentrated under reduced pressure. The residue was purified by FC (silica gel, EtOAc/hexane) to provide **77a** (189 mg, 40%) as a brown oil. ^1H NMR (400 MHz, CDCl_3) δ 7.45–7.36 (m, 2H), 7.40–7.26 (m, 2H), 7.19 (m, 1H), 2.12 (s, 1H).

Ethynyl(phenyl)sulfane (**77b**)¹¹⁵: To a solution of TMS-acetylene (**75**) (655 mg, 3.0 mmol) in 10 mL THF at –78 °C, *n*-BuLi (2.5 M in hexane, 1.1 mL, 3.0 mmol) was added dropwise and stirred for 1.5 h. A solution of diphenyl disulphide (**74**) (324 mg, 3.3 mmol) in 2 mL THF was added dropwise, and the mixture was warmed to rt over 2 h before adding H_2O (5 mL). After extraction with Et₂O (3×10 mL), the organic layer was collected, washed with brine, dried over Na_2SO_4 , filtered, and concentrated under reduced pressure to yield the TMS-protected thioethyne. For deprotection, the thioethyne (412 mg 2.0 mmol) was stirred for 3 h at rt with KF (441 mg, 7.6 mmol) in MeOH (10 mL). After concentration under reduced pressure, CH_2Cl_2 (5 mL) and water (3 mL) were added. The organic layer was collected, dried (MgSO_4) and filtered through a short silica plug to afford **77b** (192 mg, 85%) as a brown oil. ^1H NMR (400 MHz, CDCl_3) δ 7.51–7.44 (m, 2H), 7.42–7.33 (m, 2H), 7.30–7.22 (m, 1H), 3.28 (s, 1H).

N-Phenylpropiolamide (**77d**)¹¹⁶: Propiolic acid (350 mg, 5.0 mmol) and DCC (1.03 g, 5.0 mmol) were combined in 15 mL of CH_2Cl_2 . The solution was stirred for 10 min before adding aniline (**76**) (466 mg, 5.0 mmol) and DMAP (7.5 mg, 0.06 mmol) in dry CH_2Cl_2 at 0 °C under nitrogen atmosphere. After complete addition, the mixture was stirred at rt for 18 h. The reaction mixture was filtered and washed with 1 N HCl (5 mL) and a saturated solution of sodium chloride (2×50 mL). The organic phase was separated, dried over Na_2SO_4 , filtered, and concentrated under reduced pressure. The residue was purified by FC (silica gel, EtOAc/hexane) to provide **77d** (652 mg, 90%) as a colourless oil.

^1H NMR (400 MHz, CDCl_3) δ 7.64 (bs, 1H), 7.58–7.51 (m, 2H), 7.42–7.33 (m, 2H), 7.18 (td, $J=7.3, 1.2$ Hz, 1H), 2.95 (s, 1H).

General procedure (IV) for the synthesis of (aryl)(1,2,3-Triazolyl)methanol

Ethynylmagnesium bromide solution (1.2 eq, 0.5 M solution in THF) was added dropwise to a stirred solution of aldehydes (**90**) (1 eq) in anhydrous THF (6 mL) at 0°C . The mixture was kept stirring at 0°C for 20 min, then warmed to rt and stirred for an additional 2 h. The reaction mixture was quenched with a saturated NH_4Cl solution (6 mL) and extracted with EtOAc (3×8 mL). The organic layers were combined, dried over anhydrous Na_2SO_4 , filtered, and concentrated under reduced pressure to give the intermediate 1-aryl propargyl alcohols (**91**), which were directly used in next step. Alcohols (**91**) (1 eq), TMSN_3 (1.5 eq), and CuI (0.05 eq) in DMF/MeOH solution (9:1) were stirred at 100°C for 10–12 h. After consumption of the ethynyl substrate, the mixture was cooled to rt, the precipitate was filtered off, and the solution was concentrated under reduced pressure. The crude residue was purified by FC (SiO_2 , EtOAc/petroleum ether) to afford compounds **92a–92u** in 55–85% yields.

Synthesis of (aryl)(1,2,3-Triazolyl)methanol (92a–92u)

Phenyl(1,2,3-triazol-4-yl)methanol (**92a**)¹¹²: Synthesised from benzaldehyde (212 mg, 2.0 mmol), ethynylmagnesium bromide solution (4.8 mL, 0.5 M in THF, 2.4 mmol), and TMSN_3 (345 mg, 3.0 mmol) according to the general procedure (IV) to afford **92a** (297 mg, 85%) as a white solid. ^1H NMR (400 MHz, CDCl_3) δ 7.57 (s, 1H), 7.51–7.31 (m, 5H), 6.08 (s, 1H).

(2-Chlorophenyl)(1,2,3-triazol-4-yl)methanol (**92b**, CAS [1511220–63-5]): Synthesised from 2-chlorobenzaldehyde (422 mg, 3.0 mmol) ethynylmagnesium bromide solution (7.2 mL, 0.5 M in THF, 3.6 mmol) and TMSN_3 (518 mg, 4.5 mmol) according to the general procedure (IV) to afford **92b** (470 mg, 75%) as a white solid. ^1H NMR (400 MHz, MeOD) δ 7.74 (dd, $J=8.0, 1.7$ Hz, 1H), 7.57 (s, 1H), 7.44–7.37 (m, 2H), 7.41–7.27 (m, 1H), 6.36 (s, 1H).

(3-Chlorophenyl)(1,2,3-triazol-4-yl)methanol (**92c**, CAS [1511815–17-0]): Synthesised from 3-chlorobenzaldehyde (422 mg, 3.0 mmol), ethynylmagnesium bromide solution (7.2 mL, 0.5 M in THF, 3.6 mmol) and TMSN_3 (518 mg, 4.5 mmol) according to the general procedure (IV) to afford **92c** (501 mg, 75%) as a white solid. ^1H NMR (400 MHz, CDCl_3) δ 7.48 (s, 1H), 7.42 (q, $J=2.0$ Hz, 1H), 7.27 (ddd, $J=9.5, 5.1, 1.5$ Hz, 4H), 5.95 (t, $J=3.2$ Hz, 1H).

(4-Chlorophenyl)(1,2,3-triazol-4-yl)methanol (**92d**, CAS [1429056–35-8]): Synthesised from 4-chlorobenzaldehyde (422 mg, 3.0 mmol), ethynylmagnesium bromide solution (7.2 mL, 0.5 M in THF, 3.6 mmol) and TMSN_3 (518 mg, 4.5 mmol) according to the general procedure (IV) to afford **92d** (501 mg, 70%) as a white solid. ^1H NMR (400 MHz, MeOD) δ 7.66 (s, 1H), 7.47–7.33 (m, 4H), 5.98 (s, 1H).

(2-Methoxyphenyl)(1,2,3-triazol-4-yl)methanol (**92e**, CAS [1518311–97-1]): Synthesised from 2-methoxybenzaldehyde (408 mg, 3.0 mmol), ethynylmagnesium bromide solution (7.2 mL, 0.5 M in THF, 3.6 mmol) and TMSN_3 (518 mg, 4.5 mmol) according to the general procedure (IV) to afford **92e** (399 mg, 65%) as a white solid. ^1H NMR (400 MHz, CDCl_3) δ 7.52 (s, 1H), 7.40–7.27 (m, 2H), 7.04–6.90 (m, 2H), 6.21 (s, 1H), 3.84 (s, 3H).

(3-Methoxyphenyl)(1,2,3-triazol-4-yl)methanol (**92f**, CAS [1541589–58-5]): Synthesised from 3-methoxybenzaldehyde (408 mg, 3.0 mmol), ethynylmagnesium bromide solution (7.2 mL, 0.5 M in THF, 3.6 mmol) and TMSN_3 (518 mg, 4.5 mmol) according

to the general procedure (IV) to afford **92f** (338 mg, 55%) as a white solid. ^1H NMR (400 MHz, MeOD) δ 7.63 (s, 1H), 7.27 (t, $J=7.9$ Hz, 1H), 7.07–6.96 (m, 2H), 6.86 (dd, $J=8.3, 2.6$ Hz, 1H), 5.95 (s, 1H), 3.80 (s, 3H).

(4-Methoxyphenyl)(1,2,3-triazol-4-yl)methanol (**92g**, CAS [1526953–98-9]): Synthesised from 4-methoxybenzaldehyde (408 mg, 3.0 mmol), ethynylmagnesium bromide solution (7.2 mL, 0.5 M in THF, 3.6 mmol) and TMSN_3 (518 mg, 4.5 mmol) according to the general procedure (IV) to afford **92g** (338 mg, 55%) as a white solid. ^1H NMR (400 MHz, MeOD) δ 7.62 (s, 1H), 7.38–7.30 (m, 2H), 6.99–6.88 (m, 2H), 5.93 (s, 1H), 3.80 (s, 3H).

(4-Bromophenyl)(1,2,3-triazol-4-yl)methanol (**92h**, CAS [1934702–39-2]): Synthesised from 4-bromobenzaldehyde (555 mg, 3.0 mmol), ethynylmagnesium bromide solution (7.2 mL, 0.5 M in THF, 3.6 mmol) and TMSN_3 (518 mg, 4.5 mmol) according to the general procedure (IV) to afford **92h** (546 mg, 72%) as a white solid. ^1H NMR (400 MHz, MeOD) δ 7.66 (s, 1H), 7.56–7.49 (m, 2H), 7.42–7.34 (m, 2H), 5.96 (s, 1H).

(4-Fluorophenyl)(1,2,3-triazol-4-yl)methanol (**92i**, CAS [1517879–10-5]): Synthesised from 4-fluorobenzaldehyde (372 mg, 3.0 mmol), ethynylmagnesium bromide solution (7.2 mL, 0.5 M in THF, 3.6 mmol) and TMSN_3 (518 mg, 4.5 mmol) according to the general procedure (IV) to afford **92i** (359 mg, 62%) as a white solid. ^1H NMR (400 MHz, MeOD) δ 7.66 (s, 1H), 7.50–7.41 (m, 2H), 7.15–7.04 (m, 2H), 5.98 (s, 1H).

(5-Chloro-2-hydroxyphenyl)(1,2,3-triazol-4-yl)methanol (**92j**): Synthesised from 5-chloro-2-methoxybenzaldehyde (513 mg, 3.0 mmol), ethynylmagnesium bromide solution (7.2 mL, 0.5 M in THF, 3.6 mmol) and TMSN_3 (518 mg, 4.5 mmol) according to the general procedure (IV) to afford **92j** (499 mg, 74%) as a white solid. ^1H NMR (400 MHz, MeOD) δ 7.59 (s, 1H), 7.43 (d, $J=2.7$ Hz, 1H), 7.11 (dd, $J=8.6, 2.7$ Hz, 1H), 6.77 (d, $J=8.6$ Hz, 1H), 6.24 (s, 1H).

(4-Chloro-2-hydroxyphenyl)(1,2,3-triazol-4-yl)methanol (**92k**): Synthesised from 4-chloro-2-methoxybenzaldehyde (513 mg, 3.0 mmol), ethynylmagnesium bromide solution (7.2 mL, 0.5 M in THF, 3.6 mmol) and TMSN_3 (518 mg, 4.5 mmol) according to the general procedure (IV) to afford **92k** (466 mg, 69%) as a white solid. ^1H NMR (400 MHz, MeOD) δ 7.58–7.48 (m, 2H), 7.02 (dd, $J=6.0, 2.2$ Hz, 2H), 6.25 (s, 1H), 3.82 (s, 3H).

(4-Bromo-2-hydroxyphenyl)(1,2,3-triazol-4-yl)methanol (**92l**): Synthesised from 4-bromo-2-methoxybenzaldehyde (403 mg, 2.0 mmol), ethynylmagnesium bromide solution (4.8 mL, 0.5 M in THF, 2.4 mmol), and TMSN_3 (345 mg, 3.0 mmol) according to the general procedure (IV) to afford **92l** (371 mg, 69%) as a white solid. ^1H NMR (400 MHz, CDCl_3) δ 7.66 (s, 1H), 7.11–6.96 (m, 3H), 5.72 (s, 1H).

Furan-2-yl(1,2,3-triazol-4-yl)methanol (**92m**, CAS [1519476–28-8]): Synthesised from 2-furaldehyde (289 mg, 3.0 mmol), ethynylmagnesium bromide solution (7.2 mL, 0.5 M in THF, 3.6 mmol) and TMSN_3 (518 mg, 4.5 mmol) according to the general procedure (IV) to afford **92m** (297 mg, 60%) as a white solid. ^1H NMR (400 MHz, CDCl_3) δ 8.05 (s, 1H), 7.94–7.74 (m, 1H), 7.51–7.37 (m, 1H), 6.45–6.25 (m, 1H), 6.12–5.99 (m, 1H).

Furan-3-yl(1,2,3-triazol-4-yl)methanol (**92n**, CAS [1500898–43-0]): Synthesised from 3-furaldehyde (289 mg, 3.0 mmol), ethynylmagnesium bromide solution (7.2 mL, 0.5 M in THF, 3.6 mmol) and TMSN_3 (518 mg, 4.5 mmol) according to the general procedure (IV) to afford **92n** (352 mg, 71%) as a white solid. ^1H NMR (400 MHz, MeOD) δ 7.73 (s, 1H), 7.49 (d, $J=1.5$ Hz, 2H), 6.47 (d, $J=2.9$ Hz, 1H), 5.96 (s, 1H).

Thiophen-2-yl(1,2,3-triazol-4-yl)methanol (**92o**, CAS [1542859–11-9]): Synthesised from thiophene-2-carbaldehyde

(224 mg, 2.0 mmol), ethynylmagnesium bromide solution (4.8 mL, 0.5 M in THF, 2.4 mmol), and TMSN₃ (345 mg, 3.0 mmol) according to the general procedure (IV) to afford **92o** (239 mg, 66%) as a white solid. ¹H NMR (400 MHz, MeOD) δ 7.75–7.70 (s, 1H), 7.37 (dd, *J* = 5.0, 1.4 Hz, 1H), 7.08–6.95 (m, 2H), 6.24 (s, 1H).

Thiophen-3-yl(1,2,3-triazol-4-yl)methanol (**92p**, CAS [1522175–89-8]): Synthesised from thiophene-3-carbaldehyde (336 mg, 3.0 mmol), ethynylmagnesium bromide solution (7.2 mL, 0.5 M in THF, 3.6 mmol) and TMSN₃ (518 mg, 4.5 mmol) according to the general procedure (IV) to afford **92p** (396 mg, 73%) as a white solid. ¹H NMR (400 MHz, MeOD) δ 7.68 (s, 1H), 7.40 (dd, *J* = 5.1, 3.0 Hz, 1H), 7.36–7.31 (m, 1H), 7.11 (dd, *J* = 5.0, 1.3 Hz, 1H), 6.07 (s, 1H).

Thiazol-4-yl(1,2,3-triazol-4-yl)methanol (**92q**, CAS [1935872–98-2]): Synthesised from thiazole-4-carbaldehyde (326 mg, 2.0 mmol), ethynylmagnesium bromide solution (4.8 mL, 0.5 M in THF, 2.4 mmol), and TMSN₃ (345 mg, 3.0 mmol) according to the general procedure (IV) to afford **92q** (272 mg, 73%) as a white solid. ¹H NMR (400 MHz, MeOD) δ 8.99 (s, 1H), 8.00 (s, 1H), 7.81 (s, 1H), 6.35 (s, 1H).

(1,2,3-Thiadiazol-4-yl)(1,2,3-triazol-4-yl)methanol (**92r**): Synthesised from 1,2,3-thiadiazole-4-carbaldehyde (228 mg, 2.0 mmol), ethynylmagnesium bromide solution (4.8 mL, 0.5 M in THF, 2.4 mmol), and TMSN₃ (345 mg, 3.0 mmol) according to the general procedure (IV) to afford **92r** (260 mg, 71%) as a white solid. ¹H NMR (400 MHz, MeOD) δ 8.95 (s, 1H), 7.84 (s, 1H), 6.60 (s, 1H).

Pyridin-2-yl(1,2,3-triazol-4-yl)methanol (**92s**): Synthesised from picolinaldehyde (322 mg, 3.0 mmol), ethynylmagnesium bromide solution (7.2 mL, 0.5 M in THF, 3.6 mmol) and TMSN₃ (518 mg, 4.5 mmol) according to the general procedure (IV) to afford **92s** (370 mg, 70%) as a yellow solid. ¹H NMR (400 MHz, CDCl₃) δ 8.68–8.58 (m, 1H), 8.24 (dt, *J* = 7.8, 1.1 Hz, 1H), 7.99 (s, 1H), 7.89 (td, *J* = 7.7, 1.8 Hz, 1H), 7.48 (ddd, *J* = 7.6, 4.8, 1.3 Hz, 1H), 5.60 (s, 1H).

Pyridin-3-yl(1,2,3-triazol-4-yl)methanol (**92t**, CAS [1508769–16-1]): Synthesised from nicotinaldehyde (322 mg, 3.0 mmol), ethynylmagnesium bromide solution (7.2 mL, 0.5 M in THF, 3.6 mmol) and TMSN₃ (518 mg, 4.5 mmol) according to the general procedure (IV) to afford **92t** (396 mg, 75%) as a yellow solid. ¹H NMR (400 MHz, MeOD) δ 8.64 (d, *J* = 2.2 Hz, 1H), 8.49 (dd, *J* = 4.9, 1.6 Hz, 1H), 7.93 (dt, *J* = 8.1, 2.0 Hz, 1H), 7.75 (s, 1H), 7.46 (dd, *J* = 8.0, 4.9 Hz, 1H), 6.08 (s, 1H).

Pyridin-4-yl(1,2,3-triazol-4-yl)methanol (**92u**): Synthesised from isonicotinaldehyde (322 mg, 3.0 mmol), ethynylmagnesium bromide solution (7.2 mL, 0.5 M in THF, 3.6 mmol) and TMSN₃ (518 mg, 4.5 mmol) according to the general procedure (IV) to afford **92u** (359 mg, 68%) as a yellow solid. ¹H NMR (400 MHz, CDCl₃) δ 8.67–8.51 (m, 2H), 7.57–7.49 (m, 2H), 7.34 (s, 1H), 5.51 (s, 1H).

Synthesis of 5-Aroyl and 5-Hetaroyl-1,2,3-Triazoles

Phenyl(1*H*-1,2,3-triazol-5-yl)methanone (**99**)¹¹³: A solution of phenyl(1,2,3-triazol-4-yl)methanol (**92a**) (88 mg, 0.5 mmol) in CH₂Cl₂ (3 mL) was treated with PCC (162 mg, 0.75 mmol). After stirring at rt for 2 h, the reaction was complete as determined by TLC. Excess PCC was removed by filtration of the reaction mixture through a pad of celite. The filtrate was sequentially washed with brine, dried over Na₂SO₄, filtered, and concentrated under reduced pressure. The residue as purified by FC (SiO₂, EtOAc/petroleum ether) giving **99** (63 mg, 73%) as a oily solid. ¹H NMR (400 MHz, CDCl₃) δ 8.39 (s, 1H), 8.33 (d, *J* = 7.7 Hz, 1H), 7.71–7.64 (m, 1H), 7.57 (tt, *J* = 6.6, 1.2 Hz, 3H), ¹³C NMR (101 MHz, MeOD) δ 186.20, 136.83,

133.07, 129.76, 128.16, HRMS (ESI/QTOF) *m/z*: calcd for [M + Na]⁺ C₉H₇N₃O₂Na⁺ 196.0481; found, 196.0481.

(2-Chlorophenyl)(1*H*-1,2,3-triazol-5-yl)methanone (**100**)¹¹⁷: Prepared the same way as **99** from (2-chlorophenyl)(1,2,3-triazol-4-yl)methanol (**92b**) (250 mg, 1.2 mmol) and PCC (389 mg, 1.8 mmol) in CH₂Cl₂ (8 mL), giving **100** (137 mg, 55% yield) as a white solid. ¹H NMR (400 MHz, CDCl₃) δ 8.32 (s, 1H), 7.64–7.58 (m, 1H), 7.55–7.46 (m, 2H), 7.43 (ddd, *J* = 7.6, 6.2, 2.3 Hz, 1H), ¹³C NMR (101 MHz, MeOD) δ 187.13, 145.63, 137.95, 131.76, 130.96, 129.95, 129.37, 126.64, HRMS (ESI/QTOF) *m/z*: calcd for [M + Na]⁺ C₉H₆ClN₃O₂Na⁺ 230.0092; found, 230.0090.

(3-Chlorophenyl)(1*H*-1,2,3-triazol-5-yl)methanone (**101**)¹¹⁸: Prepared the same way as **99** from (3-chlorophenyl)(1,2,3-triazol-4-yl)methanol (**92c**) (320 mg, 1.5 mmol) and PCC (486 mg, 2.25 mmol) in CH₂Cl₂ (10 mL), giving **101** (186 mg, 60% yield) as white solid. ¹H NMR (400 MHz, CDCl₃) δ 8.47–8.21 (m, 3H), 7.64 (ddd, *J* = 8.0, 2.2, 1.1 Hz, 1H), 7.51 (t, *J* = 7.9 Hz, 1H), ¹³C NMR (101 MHz, MeOD) δ 184.44, 145.54, 138.36, 134.22, 132.76, 129.74, 129.58, 128.20, HRMS (ESI/QTOF) *m/z*: calcd for [M + Na]⁺ C₉H₆ClN₃O₂Na⁺ 230.0097; found, 230.0096.

(4-Chlorophenyl)(1*H*-1,2,3-triazol-5-yl)methanone (**102**)¹¹⁸: Prepared the same way as **99** from (4-chlorophenyl)(1,2,3-triazol-4-yl)methanol (**92d**) (105 mg, 0.5 mmol) and PCC (162 mg, 0.75 mmol) in CH₂Cl₂ (3 mL) giving **102** (68 mg, 65% yield) as white solid. ¹H NMR (400 MHz, MeOD) δ 8.48 (s, 1H), 8.38–8.27 (m, 2H), 7.66–7.54 (m, 2H), ¹³C NMR (101 MHz, MeOD) δ 184.67, 139.36, 135.21, 131.49, 128.38, HRMS (ESI/QTOF) *m/z*: calcd for [M + Na]⁺ C₉H₆ClN₃O₂Na⁺ 230.0097; found, 230.0105.

(2-Methoxyphenyl)(1*H*-1,2,3-triazol-5-yl)methanone (**103**, CAS [1541622–39-2]): Prepared the same way as **99** from (2-methoxyphenyl)(1,2,3-triazol-5-yl)methanol (**92e**) (205 mg, 1.0 mmol) and PCC (324 mg, 1.5 mmol) in CH₂Cl₂ (5 mL) giving **103** (142 mg, 70% yield) as white solid. ¹H NMR (400 MHz, CDCl₃) δ 8.21 (s, 1H), 7.64–7.49 (m, 2H), 7.16–6.99 (m, 2H), 3.83 (s, 1H), ¹³C NMR (101 MHz, MeOD) δ 187.99, 157.89, 132.87, 129.44, 128.22, 120.16, 111.72, 54.77, HRMS (ESI/QTOF) *m/z*: calcd for [M + Na]⁺ C₁₀H₉N₃O₂Na⁺ 226.0587; found, 226.0589.

(3-Methoxyphenyl)(1*H*-1,2,3-triazol-5-yl)methanone (**104**)¹¹⁸: Prepared the same way as **99** from (3-methoxyphenyl)(1,2,3-triazol-5-yl)methanol (**92f**) (205 mg, 1.0 mmol) and PCC (324 mg, 1.5 mmol) in CH₂Cl₂ (5 mL) giving **104** (122 mg, 60% yield) as white solid. ¹H NMR (400 MHz, MeOD) δ 8.46 (s, 1H), 7.87 (d, *J* = 7.6 Hz, 1H), 7.79 (d, *J* = 2.7 Hz, 1H), 7.49 (t, *J* = 8.0 Hz, 1H), 7.26 (dd, *J* = 8.1, 2.6 Hz, 1H), 3.90 (s, 3H), ¹³C NMR (101 MHz, MeOD) δ 185.82, 159.76, 138.00, 129.23, 122.35, 119.20, 114.25, 54.52, HRMS (ESI/QTOF) *m/z*: calcd for [M + Na]⁺ C₁₀H₉N₃O₂Na⁺ 226.0587; found, 226.0584.

(4-Methoxyphenyl)(1*H*-1,2,3-triazol-5-yl)methanone (**105**)¹¹⁷: Prepared the same way as **99** from (4-methoxyphenyl)(1,2,3-triazol-5-yl)methanol (**92g**) (240 mg, 1.2 mmol) and PCC (389 mg, 1.8 mmol) in CH₂Cl₂ (8 mL) giving **105** (171 mg, 70% yield) as white solid. ¹H NMR (400 MHz, MeOD) δ 8.48–8.28 (m, 3H), 7.15–7.01 (m, 2H), 3.93 (s, 3H), ¹³C NMR (101 MHz, MeOD) δ 184.65, 164.23, 132.35, 129.34, 113.45, 54.70, HRMS (ESI/QTOF) *m/z*: calcd for [M + Na]⁺ C₁₀H₉N₃O₂Na⁺ 226.0587; found, 226.0590.

(2-Hydroxyphenyl)(1*H*-1,2,3-triazol-5-yl)methanone (**106**, CAS [2294215–75-9]): Synthesised from compound **103** (102 mg, 0.5 mmol) and 48% HBr in water (2 mL) using the general procedure (III) to give **106** (42 mg, 45%) as a yellow solid. ¹H NMR (400 MHz, MeOD) δ 8.82 (d, *J* = 8.1 Hz, 1H), 8.52 (s, 1H), 7.59 (ddd, *J* = 8.7, 7.2, 1.7 Hz, 1H), 7.07–6.99 (m, 2H), ¹³C NMR (101 MHz, MeOD) δ 189.62, 163.06, 136.31, 132.91, 119.17, 118.80, 117.52,

HRMS (ESI/QTOF) m/z : calcd for $[M + Na]^+ C_9H_7N_3O_2Na^+$ 212.0436; found, 212.0439.

(3-Hydroxyphenyl)(1*H*-1,2,3-triazol-5-yl)methanone (**107**, CAS [2294564–32-0]): Synthesised from compound **104** (102 mg, 0.5 mmol) and 48% HBr in water (2 mL) using the general procedure (**III**) to give **107** (46 mg, 49%) as a fluffy yellow powder. 1H NMR (400 MHz, MeOD) δ 8.43 (s, 1H), 7.72 (d, $J=7.7$ Hz, 1H), 7.65 (s, 1H), 7.39 (t, $J=7.9$ Hz, 1H), 7.10 (ddd, $J=8.1, 2.6, 1.0$ Hz, 1H), ^{13}C NMR (101 MHz, MeOD) δ 186.16, 157.44, 138.09, 129.24, 121.09, 120.24, 115.99, HRMS (ESI/QTOF) m/z : calcd for $[M + Na]^+ C_9H_7N_3O_2Na^+$ 212.0430; found, 212.0429.

(4-Hydroxyphenyl)(1*H*-1,2,3-triazol-5-yl)methanone (**108**, CAS [2296580–04-4]): Synthesised from compound **105** (102 mg, 0.5 mmol) and 48% HBr in water (2 mL) using the general procedure (**III**) to give **108** (49 mg, 50%) as a yellow solid. 1H NMR (400 MHz, MeOD) δ 8.39 (s, 1H), 8.24 (d, $J=8.4$ Hz, 2H), 6.99–6.82 (m, 2H), ^{13}C NMR (101 MHz, MeOD) δ 162.87, 132.64, 128.22, 114.86, HRMS (ESI/QTOF) m/z : calcd for $[M + Na]^+ C_9H_7N_3O_2Na^+$ 212.0430; found, 212.0438.

(4-Bromophenyl)(1*H*-1,2,3-triazol-5-yl)methanone (**109**)¹¹⁸: Prepared the same way as **99** from (4-bromophenyl)(1,2,3-triazol-4-yl)methanol (**92h**) (253 mg, 1.0 mmol) and PCC (324 mg, 1.5 mmol) in CH_2Cl_2 (5 mL) giving **109** (148 mg, 59% yield) as white solid. 1H NMR (400 MHz, $CDCl_3$) δ 8.33 (s, 1H), 8.24 (d, $J=8.2$ Hz, 2H), 7.76–7.61 (m, 2H), ^{13}C NMR (101 MHz, MeOD) δ 184.88, 135.64, 131.56, 131.45, 127.99, HRMS (ESI/QTOF) m/z : calcd for $[M + Na]^+ C_9H_6BrN_3ONa^+$ 273.9586; found, 273.9587.

(4-Fluorophenyl)(1*H*-1,2,3-triazol-5-yl)methanone (**110**)¹¹³: Prepared the same way as **99** from (4-fluorophenyl)(1,2,3-triazol-4-yl)methanol (**92i**) (193 mg, 1.0 mmol) and PCC (324 mg, 1.5 mmol) in CH_2Cl_2 (5 mL) giving **110** (86 mg, 45% yield) as white solid. 1H NMR (400 MHz, MeOD) δ 8.48 (s, 1H), 8.45–8.37 (m, 2H), 7.35–7.27 (m, 2H), ^{13}C NMR (101 MHz, MeOD) δ 184.37, 167.18, 164.66, 145.64, 133.18, 133.15, 132.84, 132.74, 115.20, 114.98, HRMS (ESI/QTOF) m/z : calcd for $[M + Na]^+ C_9H_6FN_3ONa^+$ 214.0387; found, 214.0386.

(5-Chloro-2-hydroxyphenyl)(1*H*-1,2,3-triazol-5-yl)methanone (**111**): Prepared the same way as **99** from (5-chloro-2-hydroxyphenyl)(1,2,3-triazol-4-yl)methanol (**92j**) (125 mg, 0.6 mmol) and PCC (194 mg, 1.5 mmol) in CH_2Cl_2 (4 mL) giving **111** (48 mg, 39% yield) as white solid, m.p. 186–188 °C. 1H NMR (400 MHz, MeOD) δ 8.95 (s, 1H), 8.55 (s, 1H), 7.56 (dd, $J=9.0, 2.7$ Hz, 1H), 7.04 (d, $J=8.9$ Hz, 1H), ^{13}C NMR (101 MHz, MeOD) δ 188.32, 161.52, 135.86, 131.84, 123.48, 119.95, 119.34, HRMS (ESI/QTOF) m/z : calcd for $[M + Na]^+ C_9H_6ClN_3O_2Na^+$ 246.0046; found, 246.0051.

(4-Chloro-2-hydroxyphenyl)(1*H*-1,2,3-triazol-5-yl)methanone (**112**): Prepared the same way as **99** from (4-chloro-2-hydroxyphenyl)(1,2,3-triazol-4-yl)methanol (**92k**) (96 mg, 0.5 mmol) and PCC (162 mg, 0.75 mmol) in CH_2Cl_2 (3 mL) giving **112** (53 mg, 55% yield) as oily solid. 1H NMR (400 MHz, MeOD) δ 8.92 (d, $J=8.8$ Hz, 1H), 8.55 (s, 1H), 7.12–6.99 (m, 2H), ^{13}C NMR (101 MHz, MeOD) δ 188.61, 163.74, 141.90, 134.34, 119.32, 118.00, 117.42, HRMS (ESI/QTOF) m/z : calcd for $[M + Na]^+ C_9H_6ClN_3O_2Na^+$ 246.0041; found, 246.0038.

(4-Bromo-2-hydroxyphenyl)(1*H*-1,2,3-triazol-5-yl)methanone (**113**): Prepared the same way as **99** from (4-bromo-2-hydroxyphenyl)(1,2,3-triazol-4-yl)methanol (**92l**) (200 mg, 0.75 mmol) and PCC (243 mg, 1.13 mmol) in CH_2Cl_2 (5 mL) giving **113** (100 mg, 50% yield) as yellow solid, m.p. 192–194 °C. 1H NMR (400 MHz, MeOD) δ 8.79 (d, $J=8.7$ Hz, 1H), 8.52 (s, 1H), 7.21 (d, $J=1.9$ Hz, 1H), 7.16 (dd, $J=8.7, 2.0$ Hz, 1H), ^{13}C NMR (101 MHz, MeOD) δ 188.84, 163.46, 145.87, 134.20, 132.23, 130.50, 122.24, 120.58, 118.23, HRMS (ESI/

QTOF) m/z : calcd for $[M-H]^- C_9H_6BrN_3O_2^-$ 267.9545; found, 267.9543.

Furan-2-yl(1*H*-1,2,3-triazol-5-yl)methanone (**114**)¹¹⁸: Prepared the same way as **99** from furan-2-yl(1,2,3-triazol-4-yl)methanol (**92m**) (165 mg, 1.0 mmol) and PCC (324 mg, 1.5 mmol) in CH_2Cl_2 (6 mL) giving **114** (57 mg, 35% yield) as white solid. 1H NMR (400 MHz, MeOD) δ 8.57 (s, 1H), 8.01 (s, 1H), 7.97–7.93 (m, 1H), 6.77 (dd, $J=3.6, 1.7$ Hz, 1H), ^{13}C NMR (101 MHz, MeOD) δ 175.43, 151.23, 148.25, 121.80, 112.39, HRMS (ESI/QTOF) m/z : calcd for $[M + Na]^+ C_7H_5N_3O_2Na^+$ 186.0274; found, 186.0271.

Furan-3-yl(1*H*-1,2,3-triazol-5-yl)methanone (**115**, CAS [1522300–51-1]): Prepared the same way as **99** from furan-3-yl(1,2,3-triazol-4-yl)methanol (**92n**) (165 mg, 1.0 mmol) and PCC (324 mg, 1.5 mmol) in CH_2Cl_2 (6 mL) giving **115** (83 mg, 51% yield) as white solid. 1H NMR (400 MHz, MeOD) δ 8.89 (s, 1H), 8.43 (s, 1H), 7.68 (t, $J=1.7$ Hz, 1H), 7.05 (d, $J=1.8$ Hz, 1H), ^{13}C NMR (101 MHz, MeOD) δ 179.64, 150.59, 143.92, 125.78, 108.79, HRMS (ESI/QTOF) m/z : calcd for $[M + Na]^+ C_7H_5N_3O_2Na^+$ 186.0274; found, 186.0274.

Thiophen-2-yl(1*H*-1,2,3-triazol-5-yl)methanone (**116**, CAS [1540541–16-9]): Prepared the same way as **99** from thiophen-2-yl(1,2,3-triazol-4-yl)methanol (**92o**) (200 mg, 1.1 mmol) and PCC (356 mg, 1.65 mmol) in CH_2Cl_2 (6 mL) giving **116** (69 mg, 35% yield) as white solid. 1H NMR (400 MHz, MeOD) δ 8.60 (d, $J=3.8$ Hz, 1H), 8.47 (s, 1H), 7.97 (dd, $J=4.9, 1.2$ Hz, 1H), 7.30 (dd, $J=5.0, 3.9$ Hz, 1H), ^{13}C NMR (101 MHz, MeOD) δ 177.70, 145.71, 142.24, 135.64, 135.19, 128.14, HRMS (ESI/QTOF) m/z : calcd for $[M + Na]^+ C_7H_5N_3OSNa^+$ 202.0046; found, 202.0042.

Thiophen-3-yl(1*H*-1,2,3-triazol-5-yl)methanone (**117**)¹¹⁸: Prepared the same way as **99** from thiophen-3-yl(1,2,3-triazol-4-yl)methanol (**92p**) (200 mg, 1.1 mmol) and PCC (356 mg, 1.65 mmol) in CH_2Cl_2 (6 mL) giving **117** (81 mg, 41% yield) as white solid. 1H NMR (400 MHz, MeOD) δ 8.99 (s, 1H), 8.46 (s, 1H), 7.86 (d, $J=5.1$ Hz, 1H), 7.55 (dd, $J=5.2, 2.9$ Hz, 1H), ^{13}C NMR (101 MHz, MeOD) δ 179.25, 147.86, 140.32, 135.87, 127.67, 125.82, HRMS (ESI/QTOF) m/z : calcd for $[M + Na]^+ C_7H_5N_3OSNa^+$ 202.0046; found, 202.0044.

Thiazol-4-yl(1*H*-1,2,3-triazol-5-yl)methanone (**118**, CAS [1935572–44-3]): Prepared the same way as **99** from thiazol-4-yl(1,2,3-triazol-4-yl)methanol (**92q**) (225 mg, 1.25 mmol) and PCC (405 mg, 1.88 mmol) in CH_2Cl_2 (8 mL) giving **118** (143 mg, 64% yield) as white solid. 1H NMR (400 MHz, MeOD) δ 9.35 (s, 1H), 9.23 (s, 1H), 8.53 (s, 1H), ^{13}C NMR (101 MHz, DMSO) δ 177.42, 162.18, 149.95, 145.47, 137.72, 131.16, HRMS (ESI/QTOF) m/z : calcd for $[M + H]^+ C_6H_5N_4OS^+$ 181.0179; found, 181.0175.

(1,2,3-Thiadiazol-4-yl)(1*H*-1,2,3-triazol-5-yl)methanone (**119**): Prepared the same way as **99** from (1,2,3-thiadiazol-4-yl)(1,2,3-triazol-4-yl)methanol (**92r**) (275 mg, 1.5 mmol) and PCC (486 mg, 2.25 mmol) in CH_2Cl_2 (8 mL) giving **119** (117 mg, 43% yield) as white solid, m.p. 170–172 °C. 1H NMR (400 MHz, MeOD) δ 10.10 (s, 1H), 8.99 (s, 1H), ^{13}C NMR (101 MHz, MeOD) δ 175.58, 160.36, 145.03, HRMS (ESI/QTOF) m/z : calcd for $[M + Na]^+ C_5H_3N_5NaOSNa^+$ 203.9951; found, 203.9947.

Pyridin-2-yl(1*H*-1,2,3-triazol-5-yl)methanone (**120**): Prepared the same way as **99** from pyridin-2-yl(1,2,3-triazol-4-yl)methanol (**92s**) (240 mg, 1.2 mmol) and PCC (389 mg, 1.8 mmol) in CH_2Cl_2 (8 mL) giving **120** (114 mg, 55% yield) as white solid, m.p. 161–163 °C. 1H NMR (400 MHz, MeOD) δ 9.00 (s, 1H), 8.85–8.74 (m, 1H), 8.27 (dt, $J=7.8, 1.2$ Hz, 1H), 8.07 (td, $J=7.7, 1.7$ Hz, 1H), 7.69 (ddd, $J=7.6, 4.8, 1.2$ Hz, 1H), ^{13}C NMR (101 MHz, MeOD) δ 182.94, 153.16, 148.91, 137.36, 133.15, 127.47, 123.57, HRMS (ESI/QTOF) m/z : calcd for $[M + Na]^+ C_8H_6N_4ONa^+$ 197.0434; found, 197.0432.

Pyridin-3-yl(1*H*-1,2,3-triazol-5-yl)methanone (**121**, CAS [1523140–26-2]): Prepared the same way as **99** from pyridin-3-yl(1,2,3-triazol-4-yl)methanol (**92t**) (270 mg, 1.5 mmol) and PCC (486 mg, 2.25 mmol) in CH₂Cl₂ (10 mL) giving **121** (104 mg, 40% yield) as white solid. ¹H NMR (400 MHz, MeOD) δ 9.45 (d, *J* = 2.2 Hz, 1H), 8.81 (dd, *J* = 5.0, 1.7 Hz, 1H), 8.73 (d, *J* = 8.1 Hz, 1H), 8.51 (brs, 1H), 7.66 (dd, *J* = 8.0, 4.9 Hz, 1H), ¹³C NMR (101 MHz, MeOD) δ 184.19, 152.35, 150.31, 138.15, 132.93, 123.80, HRMS (ESI/QTOF) *m/z*: calcd for [M + H]⁺ C₈H₇N₄O⁺ 175.0614; found, 175.0613.

Pyridin-4-yl(1*H*-1,2,3-triazol-5-yl)methanone (**122**): Prepared the same way as **99** from pyridin-4-yl(1,2,3-triazol-4-yl)methanol (**92u**) (165 mg, 1.0 mmol) and PCC (324 mg, 1.5 mmol) in CH₂Cl₂ (6 mL) giving **122** (96 mg, 52% yield) as white solid, m.p. 221–223 °C. ¹H NMR (400 MHz, MeOD) δ 8.89–8.76 (m, 2H), 8.57 (s, 1H), 8.25–8.12 (m, 2H), ¹³C NMR (101 MHz, MeOD) δ 184.76, 149.70, 145.27, 143.91, 132.09, 123.40, HRMS (ESI/QTOF) *m/z*: calcd for [M + H]⁺ C₈H₇N₄O⁺ 175.0614; found, 175.0613.

(4-Bromophenyl)(4-(hydroxymethyl)-1*H*-1,2,3-triazol-5-yl)methanone (**123**) and (4-(Bromomethyl)-1*H*-1,2,3-triazol-5-yl)(4-bromophenyl)methanone (**124**): To a solution of 2-(prop-2-ynyloxy)-tetrahydro-2*H*-pyran (**93**) (1.43 g, 7.7 mmol) in THF (15 mL), *n*-BuLi (1.6 M, 4.82 mL, 7.7 mmol) was added at –78 °C. The reaction mixture was kept at –78 °C for 1 h, then 4-bromobenzaldehyde (982 mg, 7.0 mmol) was added at –78 °C. The reaction mixture was stirred for 2 h, then slowly warmed to –30 °C before being poured into an aqueous solution of NaHCO₃ (10 mL). After extraction with EtOAc (3 × 100 mL), the organic layer was collected, dried over anhyd. Na₂SO₄, filtered, and concentrated under reduced pressure to afford (1-(4-bromophenyl)-4-((tetrahydro-2*H*-pyran-2-yl)oxy)but-2-yn-1-ol (**94**) (2.1 g, 88%) as colourless oil. ¹H NMR (400 MHz, CDCl₃) δ 7.56–7.41 (m, 4H), 5.50 (dd, *J* = 4.8, 3.0 Hz, 1H), 4.83 (t, *J* = 3.4 Hz, 1H), 4.37 (qt, *J* = 15.7, 1.6 Hz, 2H), 3.86 (ddd, *J* = 11.5, 9.0, 3.1 Hz, 1H), 3.55 (ddt, *J* = 12.6, 5.3, 2.8 Hz, 1H), 2.30 (d, *J* = 6.0 Hz, 1H), 1.93–1.59 (m, 4H), 1.56 (ddd, *J* = 11.6, 5.3, 3.0 Hz, 2H). To a solution of compound **94** (1.3 g, 4.0 mmol) in CH₂Cl₂ (50 mL), MnO₂ (3.6 g, 41.2 mmol) was added. The suspension was stirred at rt for 5 h and then filtered over a pad of celite. After removing the solvent under reduced pressure, the crude product was filtered over a pad of silica gel and washed with petroleum ether:EtOAc (10:1) to afford (1-(4-bromophenyl)-4-((tetrahydro-2*H*-pyran-2-yl)oxy)but-2-yn-1-one (**95**) (1.25 g, 97%) as yellow oil. ¹H NMR (400 MHz, CDCl₃) δ 8.14–8.17 (m, 2H), 7.61–7.66 (m, 1H), 7.48–7.53 (m, 1H), 4.90–4.92 (m, 1H), 4.57 (s, 2H), 3.86–3.92 (m, 1H), 3.58–3.61 (m, 1H), 1.55–1.86 (m, 6H). To a solution of compound **95** (970 mg, 3.0 mmol) in EtOH (10 mL), pyridinium *p*-toluenesulfonate (158 mg, 0.63 mmol) was added. The resulting solution was stirred for 4 h at 50 °C before being poured into water (30 mL). After extraction with Et₂O (3 × 50 mL), the organic layer was collected, dried over anhyd. Na₂SO₄, filtered, and concentrated under reduced pressure. The residue was purified by FC to afford (1-(4-bromophenyl)-4-hydroxybut-2-yn-1-one (**96**) (534 mg, 75%) as white solid. ¹H NMR (400 MHz, CDCl₃) δ 8.06–7.99 (m, 2H), 7.71–7.63 (m, 2H), 4.60 (d, *J* = 6.4 Hz, 2H). Compound **123** was synthesised from **96** (400 mg, 1.7 mmol) and TMSN₃ according to the general procedure (II) to give **123** (239 mg, 50%) as a brown fluffy powder, m.p. 240–242 °C. ¹H NMR (400 MHz, MeOD) δ 8.26 (d, *J* = 8.3 Hz, 2H), 7.81–7.68 (m, 2H), 5.02 (s, 2H), ¹³C NMR (101 MHz, MeOD) δ 186.07, 135.94, 131.74, 131.27, 127.73, 55.27, HRMS (ESI/QTOF) *m/z*: calcd for [M + Na]⁺ C₁₀H₈BrN₃O₂Na⁺ 303.9698; found, 303.9713. A solution of PPh₃ (135 mg, 0.52 mmol) and CBr₄ (173 mg, 0.52 mmol) in dry DMF (4 mL) was stirred for 10 min before adding compound **123** (121 mg, 0.43 mmol) and

monitoring the reaction by TLC. After completion, the reaction was quenched with an aq. solution of sodium metabisulfite and extracted with EtOAc (3 × 5 mL). The organic layers were collected, dried over Na₂SO₄, filtered, and concentrated under reduced pressure. The crude product was purified by FC (silica gel, EtOAc/hexane, 1:3) to afford **124** (125 mg, 85%) as white solid, m.p. 121–123 °C. ¹H NMR (400 MHz, CDCl₃) δ 8.23 (d, *J* = 8.3 Hz, 2H), 7.69 (d, *J* = 8.5 Hz, 2H), 4.93 (s, 2H), ¹³C NMR (101 MHz, MeOD) δ 185.65, 135.72, 131.70, 131.34, 127.99, 22.80, HRMS (ESI/QTOF) *m/z*: calcd for [M + Na]⁺ C₁₀H₈BrN₃O₂Na⁺ 367.8833; found, 367.8830.

(4-(Aminomethyl)-1*H*-1,2,3-triazol-5-yl)(4-bromophenyl)methanone (**126**): To a solution of 4-bromobenzoyl chloride (1.32 g, 6.0 mmol) and *t*-butyl prop-2-yn-1-ylcarbamate (**97**) (621 mg, 4.0 mmol) in anhydrous THF (10 mL), PdCl₂(PPh₃)₂ (26 mg, 0.04 mmol) and CuI (23 mg, 0.12 mmol) were added under a nitrogen atmosphere. After 1 min of stirring, Et₃N (0.6 mL, 5.0 mmol) was added, and the reaction was stirred for 40 min at rt. During this time, Et₃NHCl precipitated, and the solution assumed a dark orange/brown colour. The reaction was diluted with Et₂O (30 mL) and washed with H₂O (30 mL). After extraction with CH₂Cl₂ (3 × 50 mL), the organic layers were combined, dried over Na₂SO₄, filtered, and concentrated under reduced pressure. The residue was purified by FC to afford (*tert*-butyl (4-(4-bromophenyl)-4-oxobut-2-yn-1-yl)carbamate (**98**) (1.82 g, 90%) as colourless oil. ¹H NMR (400 MHz, CDCl₃) δ 8.05–7.92 (m, 2H), 7.74–7.58 (m, 2H), 4.90 (bs, 1H), 4.24 (d, *J* = 5.9 Hz, 2H), 1.51 (s, 9H). *Tert*-butyl ((5-(4-bromobenzoyl)-1*H*-1,2,3-triazol-5-yl)methyl)carbamate (**125**) was synthesised from **98** (500 mg, 1.5 mmol) and TMSN₃ according to the general procedure (II) to afford **125** (257 mg, 45%) as solid. ¹H NMR (400 MHz, CDCl₃) δ 8.31 (d, *J* = 8.3 Hz, 2H), 7.73–7.65 (m, 2H), 5.57 (s, 1H), 4.73 (d, *J* = 6.2 Hz, 2H), 1.48 (s, 9H). To a solution of compound **125** (190 mg, 0.5 mmol) in CH₂Cl₂ (4 mL), trifluoroacetic acid (0.37 mL, 5 mmol) was added and the mixture was stirred overnight at rt. The solution was concentrated, basified with NaHCO₃ solution, and extracted with EtOAc. The organic layer was dried over Na₂SO₄, filtered, concentrated under reduced pressure and triturated with Et₂O to afford **126** (105 mg, 75%) as white solid, m.p. 190–192 °C. ¹H NMR (400 MHz, MeOD) δ 8.25–8.18 (m, 2H), 7.75–7.69 (m, 2H), 4.36 (s, 2H), ¹³C NMR (101 MHz, DMSO) δ 185.98, 138.22, 132.82, 131.42, 126.27, HRMS (ESI/QTOF) *m/z*: calcd for [M + H]⁺ C₁₀H₁₀BrN₄O⁺ 281.0032; found, 281.0038.

General procedure (V) for the synthesis of 3-Aryl-1*H*-1,2,4-Triazoles

The commercially available or synthetically prepared aryl nitriles (**130**) (1 mmol) were dissolved in DMF (3 mL), and formic acid (1.0 mL/mmol) and hydrazine hydrate (1.0 mL) were added. The reaction mixture was heated under reflux (90 °C) for 12 h. Upon completion of the reaction as determined by TLC, the reaction mixture was cooled to rt and poured into ice-water slurry (5 mL). After extraction with EtOAc (3 × 10 mL), the organic phases were collected, washed with brine solution (2 × 5 mL), dried over Na₂SO₄, filtered and concentrated under reduced pressure. The residue was purified by FC (SiO₂, EtOAc/petroleum ether) to afford aryl 1*H*-1,2,4-triazoles (**134–154** and **158–161**). Overall yields 20–45%.

Synthesis of 3-Aryl-1*H*-1,2,4-Triazoles (134–154 and 158–161)

3-(4-Fluorophenyl)-1*H*-1,2,4-triazole (**134**)^{B1}: Synthesised from 4-fluorobenzonitrile (**130a**) (123 mg, 1 mmol) according to the general procedure (V) to afford **134** (43 mg, 30%) as a white solid. ¹H NMR (400 MHz, CDCl₃) δ 8.35 (s, 1H), 8.11–8.00 (m, 2H),

7.22–7.13 (m, 2H), ^{13}C NMR (101 MHz, MeOD) δ 164.98, 162.51, 128.28, 128.20, 125.72, 115.51, 115.29, HRMS (ESI/QTOF) m/z : calcd for $[\text{M} + \text{H}]^+ \text{C}_8\text{H}_7\text{FN}_3^+$ 164.0619; found, 164.0619.

3-(3-Bromophenyl)-1*H*-1,2,4-triazole (**135**)¹¹⁹: Synthesised from 3-bromobenzonitrile (**130b**) (181 mg, 1 mmol) according to the general procedure (**V**) to afford **135** (55 mg, 25%) as a white solid. ^1H NMR (400 MHz, MeOD) δ 8.46 (s, 1H), 8.22 (t, $J=1.8$ Hz, 1H), 8.02 (dt, $J=7.9, 1.3$ Hz, 1H), 7.63 (dt, $J=8.1, 1.3$ Hz, 1H), 7.43 (t, $J=7.9$ Hz, 1H), ^{13}C NMR (101 MHz, MeOD) δ 134.46, 132.22, 130.32, 128.90, 124.69, 122.40, HRMS (ESI/QTOF) m/z : calcd for $[\text{M} + \text{H}]^+ \text{C}_8\text{H}_7\text{BrN}_3^+$ 223.9818; found, 223.9815.

3-(3-Fluorophenyl)-1*H*-1,2,4-triazole (**137**)¹²⁰: Synthesised from 3-fluorobenzonitrile (**130c**) (121 mg, 1 mmol) according to the general procedure (**V**) to afford **137** (49 mg, 30%) as white solid. ^1H NMR (400 MHz, CDCl_3) δ 8.33 (d, $J=8.9$ Hz, 1H), 7.84 (dt, $J=7.4, 1.3$ Hz, 1H), 7.75 (ddd, $J=9.7, 2.7, 1.5$ Hz, 1H), 7.44 (td, $J=8.0, 5.8$ Hz, 1H), 7.13 (tdd, $J=8.4, 2.6, 1.1$ Hz, 1H), ^{13}C NMR (101 MHz, MeOD) δ 164.28, 161.85, 130.47, 130.39, 121.87, 121.84, 112.85, 112.61, HRMS (ESI/QTOF) m/z : calcd for $[\text{M} + \text{H}]^+ \text{C}_8\text{H}_7\text{FN}_3^+$ 164.0619; found, 164.0620.

2-Fluoro-6-(1*H*-1,2,4-triazol-3-yl)aniline (**140**, CAS [1503176-05-3]): Synthesised from 2-amino-3-fluorobenzonitrile (**130d**) (136 mg, 1 mmol) according to the general procedure (**V**) to afford **140** (44 mg, 25%) as white solid. ^1H NMR (400 MHz, MeOD) δ 8.46 (brs, 1H), 7.71 (brs, 1H), 7.12–6.94 (m, 1H), 6.69 (td, $J=8.0, 5.2$ Hz, 1H), ^{13}C NMR (101 MHz, MeOD) δ 153.20, 150.84, 115.43, 115.35, HRMS (ESI/QTOF) m/z : calcd for $[\text{M} + \text{H}]^+ \text{C}_8\text{H}_8\text{FN}_4^+$ 179.0728; found, 179.0732.

2-Chloro-6-(1*H*-1,2,4-triazol-3-yl)aniline (**141**, CAS [1698578-50-5]): Synthesised from 2-amino-3-chlorobenzonitrile (**130e**) (152 mg, 1 mmol) according to the general procedure (**V**) to afford **141** (77 mg, 40%) as white solid. ^1H NMR (400 MHz, MeOD) δ 8.44 (s, 1H), 7.99 (d, $J=2.6$ Hz, 1H), 7.31 (dd, $J=8.8, 2.6$ Hz, 1H), 6.99 (d, $J=8.8$ Hz, 1H), ^{13}C NMR (101 MHz, MeOD) δ 155.11, 130.65, 125.97, 123.92, 118.28, HRMS (ESI/QTOF) m/z : calcd for $[\text{M} + \text{H}]^+ \text{C}_8\text{H}_8\text{ClN}_4^+$ 195.0432; found, 195.0431.

2-(1*H*-1,2,4-triazol-3-yl)benzene-1,3-diamine (**142**): Synthesised from 2,6-dinitrobenzonitrile (**130f**) (193 mg, 1 mmol) according to the general procedure (**V**) to afford 3-(2,6-dinitrophenyl)-1*H*-1,2,4-triazole **142a** (77 mg, 40%) as yellow solid. ^1H NMR (400 MHz, MeOD) δ 8.60 (s, 1H), 8.33 (d, $J=8.2$ Hz, 2H), 7.98 (t, $J=8.2$ Hz, 1H). Following the same procedure as used for **155**, 3-(2,6-dinitrophenyl)-1*H*-1,2,4-triazole (**142a**) (60 mg, 0.25 mmol) was mixed with $\text{SnCl}_2 \cdot 2\text{H}_2\text{O}$ (281 mg, 1.25 mmol) to obtain **142** (20 mg, 45%) as white solid, m.p. 152–154 °C. ^1H NMR (400 MHz, MeOD) δ 8.50 (s, 1H), 6.89 (t, $J=7.9$ Hz, 1H), 6.22 (d, $J=7.9$ Hz, 2H), ^{13}C NMR (101 MHz, MeOD) δ 147.47, 147.41, 142.49, 129.70, 129.59, 105.78, 100.52, HRMS (ESI/QTOF) m/z : calcd for $[\text{M} + \text{H}]^+ \text{C}_8\text{H}_{10}\text{N}_5^+$ 176.0931; found, 176.0936.

4-Fluoro-2-(1*H*-1,2,4-triazol-3-yl)aniline (**143**, CAS [147004-95-3]): Synthesised from 2-amino-5-fluorobenzonitrile (**130g**) (136 mg, 1 mmol) according to the general procedure (**V**) to afford **143** (44 mg, 25%) as white solid. ^1H NMR (400 MHz, MeOD) δ 8.46 (brs, 1H), 7.63 (brs, 1H), 6.95 (td, $J=8.5, 3.0$ Hz, 1H), 6.85 (dd, $J=8.9, 4.9$ Hz, 1H), ^{13}C NMR (101 MHz, MeOD) δ 156.18, 153.86, 142.73, 117.67, 117.59, 113.12, HRMS (ESI/QTOF) m/z : calcd for $[\text{M} + \text{H}]^+ \text{C}_8\text{H}_8\text{FN}_4^+$ 179.0728; found, 179.0732.

4-Bromo-5-fluoro-2-(1*H*-1,2,4-triazol-3-yl)aniline (**144**): Synthesised from 2-amino-5-bromo-4-fluorobenzonitrile (**130h**) (214 mg, 1 mmol) according to the general procedure (**V**) to afford **144** (72 mg, 28%) as a white solid, m.p. 243–246 °C. ^1H NMR (400 MHz, CDCl_3) δ 8.47 (s, 1H), 8.05 (dd, $J=7.5, 2.0$ Hz, 1H), 6.58 (dd, $J=10.4, 1.9$ Hz, 1H), ^{13}C NMR (101 MHz, MeOD) δ 160.95,

148.13, 132.07, 102.62, 102.37, 93.00, 92.79, HRMS (ESI/QTOF) m/z : calcd for $[\text{M} + \text{H}]^+ \text{C}_8\text{H}_7\text{BrFN}_4^+$ 256.9833; found, 256.9834.

4-Chloro-*N*-methyl-2-(1*H*-1,2,4-triazol-3-yl)aniline (**145**): Synthesised from 5-chloro-2-(methylamino)benzonitrile (**130an**) (166 mg, 1 mmol) according to the general procedure (**V**) to afford **145** (52 mg, 25%) as white solid, m.p. 207–209 °C. ^1H NMR (400 MHz, CDCl_3) δ 8.24 (s, 1H), 7.89 (s, 1H), 7.54 (s, 1H), 6.70 (d, $J=8.9$ Hz, 1H), 2.98 (s, 3H), ^{13}C NMR (101 MHz, MeOD) δ 150.42, 129.22, 125.32, 121.42, 120.07, 117.27, 29.27, HRMS (ESI/QTOF) m/z : calcd for $[\text{M} + \text{H}]^+ \text{C}_9\text{H}_{10}\text{ClN}_4^+$ 209.0589; found, 209.0587.

N-(4-Chloro-2-(1*H*-1,2,4-triazol-3-yl)phenyl)acetamide (**146**): Synthesised from *N*-(4-chloro-2-cyanophenyl)acetamide (**130aa**) (194 mg, 1 mmol) according to the general procedure (**V**) to afford **146** (62 mg, 26%) as yellow amorphous solid. ^1H NMR (400 MHz, MeOD) δ 8.63–8.46 (m, 2H), 8.15 (d, $J=2.5$ Hz, 1H), 7.39 (dd, $J=9.0, 2.5$ Hz, 1H), 2.25 (s, 3H), ^{13}C NMR (101 MHz, MeOD) δ 169.95, 135.41, 129.27, 128.19, 127.03, 121.97, 23.47, HRMS (ESI/QTOF) m/z : calcd for $[\text{M} + \text{Na}]^+ \text{C}_{10}\text{H}_9\text{ClN}_4\text{ONa}^+$ 259.0357; found, 259.035.

N-(4-Chloro-2-(1*H*-1,2,4-triazol-3-yl)phenyl)propionamide (**147**): Synthesised from *N*-(4-chloro-2-cyanophenyl)propionamide (**130ab**) (208 mg, 1 mmol) according to the general procedure (**V**) to afford **147** (75 mg, 30%) as yellow solid, m.p. 168–171 °C. ^1H NMR (400 MHz, DMSO) δ 8.66 (s, 1H), 8.54 (d, $J=8.9$ Hz, 1H), 8.11 (d, $J=2.6$ Hz, 1H), 7.45 (dd, $J=9.1, 2.6$ Hz, 1H), 2.43 (q, $J=7.5$ Hz, 2H), 1.15 (t, $J=7.5$ Hz, 2H), ^{13}C NMR (101 MHz, MeOD) δ 173.64, 135.49, 131.91, 129.26, 128.03, 127.01, 121.90, 30.85, 8.63, HRMS (ESI/QTOF) m/z : calcd for $[\text{M} + \text{Na}]^+ \text{C}_{11}\text{H}_{11}\text{ClN}_4\text{ONa}^+$ 273.0514; found, 273.0521.

N-(4-Chloro-2-(1*H*-1,2,4-triazol-3-yl)phenyl)butyramide (**148**): Synthesised from *N*-(4-chloro-2-cyanophenyl)butyramide (**130ac**) (222 mg, 1 mmol) according to the general procedure (**V**) to afford **148** (76 mg, 29%) as white solid, m.p. 156–158 °C. ^1H NMR (400 MHz, MeOD) δ 8.59 (d, $J=8.9$ Hz, 2H), 8.18 (s, 1H), 7.41 (dd, $J=9.0, 2.6$ Hz, 1H), 2.48 (dd, $J=8.4, 6.6$ Hz, 2H), 1.87–1.74 (m, 2H), 1.04 (dd, $J=8.4, 6.5$ Hz, 3H), ^{13}C NMR (101 MHz, MeOD) δ 172.85, 135.44, 129.25, 128.09, 127.04, 121.93, 39.78, 18.68, 12.59, HRMS (ESI/QTOF) m/z : calcd for $[\text{M} + \text{Na}]^+ \text{C}_{12}\text{H}_{13}\text{ClN}_4\text{ONa}^+$ 287.0670; found, 287.0675.

N-(4-Chloro-2-(1*H*-1,2,4-triazol-3-yl)phenyl)cyclopropanecarboxamide (**149**): Synthesised from *N*-(4-chloro-2-cyanophenyl)cyclopropanecarboxamide (**130ad**) (220 mg, 1 mmol) according to the general procedure (**V**) to afford **149** (71 mg, 27%) as white solid, m.p. 183–186 °C. ^1H NMR (400 MHz, DMSO) δ 8.60 (brs, 1H), 8.43 (d, $J=9.0$ Hz, 1H), 8.08 (d, $J=2.6$ Hz, 1H), 7.42 (dd, $J=8.9, 2.6$ Hz, 1H), 1.72 (td, $J=7.4, 3.8$ Hz, 1H), 0.89 (dt, $J=8.6, 3.0$ Hz, 6H), ^{13}C NMR (101 MHz, MeOD) δ 173.32, 143.18, 134.08, 135.61, 129.13, 127.87, 127.09, 121.82, 15.74, 7.02, HRMS (ESI/QTOF) m/z : calcd for $[\text{M} + \text{Na}]^+ \text{C}_{12}\text{H}_{11}\text{ClN}_4\text{ONa}^+$ 285.0514; found, 285.0518.

N-(4-Chloro-2-(1*H*-1,2,4-triazol-3-yl)phenyl)cyclobutanecarboxamide (**150**): Synthesised from *N*-(4-chloro-2-cyanophenyl)cyclobutanecarboxamide (**130ae**) (234 mg, 1 mmol) according to the general procedure (**V**) to afford **150** (69 mg, 25%) as a white solid, m.p. 201–203 °C. ^1H NMR (400 MHz, MeOD) δ 8.68–8.52 (m, 1H), 8.18 (d, $J=2.6$ Hz, 1H), 7.41 (dd, $J=9.0, 2.6$ Hz, 1H), 3.39 (qd, $J=8.7, 1.1$ Hz, 1H), 2.50–2.27 (m, 4H), 2.18–2.00 (m, 1H), 1.99–1.88 (m, 1H), ^{13}C NMR (101 MHz, MeOD) δ 174.81, 138.39, 128.01, 121.80, 41.39, 25.06, 17.41, HRMS (ESI/QTOF) m/z : calcd for $[\text{M} + \text{Na}]^+ \text{C}_{13}\text{H}_{13}\text{ClN}_4\text{ONa}^+$ 299.0670; found, 299.0677.

N-(4-Chloro-2-(1*H*-1,2,4-triazol-3-yl)phenyl)cyclopentanecarboxamide (**151**): Synthesised from *N*-(4-chloro-2-cyanophenyl)cyclopentanecarboxamide (**130af**) (248 mg, 1 mmol) according to the general procedure (**V**) to afford **151** (96 mg, 33%) as white solid,

m.p. 197–199 °C. ^1H NMR (400 MHz, DMSO) δ 11.63 (brs, 1H), 8.84 (brs, 1H), 8.63 (d, $J=9.0$ Hz, 1H), 8.14 (d, $J=2.6$ Hz, 1H), 7.48 (dd, $J=8.9, 2.6$ Hz, 1H), 2.85 (p, $J=8.1$ Hz, 1H), 2.06–1.89 (m, 2H), 1.80 (dq, $J=11.4, 6.9$ Hz, 2H), 1.74–1.61 (m, 2H), 1.68–1.54 (m, 2H), ^{13}C NMR (101 MHz, MeOD) δ 175.97, 135.64, 129.28, 127.95, 127.03, 121.90, 29.99, 25.48, HRMS (ESI/QTOF) m/z : calcd for $[\text{M} + \text{Na}]^+ \text{C}_{14}\text{H}_{15}\text{ClN}_4\text{ONa}^+$ 313.0827; found, 313.0825.

N-(2-(1*H*-1,2,4-triazol-3-yl)phenyl)benzamide (**152**, CAS [2428213–63-0]): Synthesised from *N*-(2-cyanophenyl)benzamide (**130bg**) (222 mg, 1 mmol) according to the general procedure (**V**) to afford **152** (92 mg, 35%) as a white solid. ^1H NMR (400 MHz, MeOD) δ 8.81 (d, $J=8.4$ Hz, 1H), 8.59 (s, 1H), 8.21 (s, 1H), 8.15 (dd, $J=8.1, 1.6$ Hz, 2H), 7.70–7.54 (m, 3H), 7.55–7.44 (m, 1H), 7.27 (t, $J=7.6$ Hz, 1H), ^{13}C NMR (101 MHz, MeOD) δ 166.35, 137.00, 134.84, 131.72, 129.91, 128.47, 127.47, 127.19, 123.36, 120.51, HRMS (ESI/QTOF) m/z : calcd for $[\text{M} + \text{Na}]^+ \text{C}_{15}\text{H}_{12}\text{N}_4\text{ONa}^+$ 287.0903; found, 287.0903.

N-(4-Chloro-2-(1*H*-1,2,4-triazol-3-yl)phenyl)benzamide (**153**): Synthesised from *N*-(4-chloro-2-cyanophenyl)benzamide (**130ag**) (256 mg, 1 mmol) according to the general procedure (**V**) to afford **153** (95 mg, 32%) as white solid, m.p. 213–216 °C. ^1H NMR (400 MHz, MeOD) δ 8.85 (d, $J=9.0$ Hz, 1H), 8.67 (s, 1H), 8.27 (s, 1H), 8.18–8.11 (m, 2H), 7.68–7.55 (m, 3H), 7.48 (dd, $J=9.0, 2.5$ Hz, 1H), ^{13}C NMR (101 MHz, MeOD) δ 166.29, 143.40, 134.54, 131.88, 129.30, 128.54, 128.30, 127.22, 121.84, HRMS (ESI/QTOF) m/z : calcd for $[\text{M} + \text{Na}]^+ \text{C}_{15}\text{H}_{11}\text{ClN}_4\text{ONa}^+$ 321.0514; found, 321.0517.

N-(2-Chloro-6-(1*H*-1,2,4-triazol-3-yl)phenyl)benzamide (**154**): Synthesised from *N*-(2-chloro-6-cyanophenyl)benzamide (**130cg**) (256 mg, 1 mmol) according to the general procedure (**V**) to afford **154** (101 mg, 34%) as amorphous solid. ^1H NMR (400 MHz, CDCl_3) δ 10.16 (s, 1H), 8.18–8.03 (m, 3H), 7.79–7.46 (m, 5H), 7.10 (t, $J=8.0$ Hz, 1H), ^{13}C NMR (101 MHz, CDCl_3) δ 166.58, 133.46, 133.01, 132.90, 132.48, 131.58, 128.84, 127.89, 127.10, 127.00, HRMS (ESI/QTOF) m/z : calcd for $[\text{M} + \text{Na}]^+ \text{C}_{15}\text{H}_{11}\text{ClN}_4\text{ONa}^+$ 321.0519; found, 321.0524.

4-(1*H*-1,2,4-Triazol-3-yl)pyridine (**158**)⁸¹: Synthesised from isonicotinonitrile (**130i**) (104 mg, 1 mmol) according to the general procedure (**V**) to afford **158** (59 mg, 40%) as white solid. ^1H NMR (400 MHz, CDCl_3) δ 8.71–8.58 (m, 1H), 8.15 (d, $J=6.8$ Hz, 2H), 7.88 (tt, $J=7.8, 1.8$ Hz, 1H), 7.40 (t, $J=6.3$ Hz, 1H), ^{13}C NMR (101 MHz, MeOD) δ 149.41, 137.37, 124.59, 121.31, HRMS (ESI/QTOF) m/z : calcd for $[\text{M} + \text{H}]^+ \text{C}_7\text{H}_7\text{N}_4^+$ 147.0665; found, 147.0660.

2-(1*H*-1,2,4-Triazol-3-yl)pyridine (**159**)⁸¹: Synthesised from picolinonitrile (**130j**) (104 mg, 1 mmol) according to the general procedure (**V**) to afford **159** (61 mg, 41%) as white solid. ^1H NMR (400 MHz, CDCl_3) δ 8.71–8.62 (m, 2H), 8.29 (s, 1H), 8.03–7.93 (m, 2H), ^{13}C NMR (101 MHz, MeOD) δ 170.82, 149.45, 145.46, 120.68, HRMS (ESI/QTOF) m/z : calcd for $[\text{M} + \text{H}]^+ \text{C}_7\text{H}_7\text{N}_4^+$ 147.0665; found, 147.0665.

2-(1*H*-1,2,4-Triazol-3-yl)pyridine-3-amine (**160**, CAS [53511–60-7]): Synthesised from 3-aminopicolinonitrile (**130k**) (119 mg, 1 mmol) according to the general procedure (**V**) to afford **160** (64 mg, 40%) as white solid. ^1H NMR (400 MHz, MeOD) δ 9.28 (s, 1H), 8.76 (s, 1H), 8.57 (brs, 1H), ^{13}C NMR (101 MHz, MeOD) δ 148.91, 147.21, 140.28, HRMS (ESI/QTOF) m/z : calcd for $[\text{M} + \text{H}]^+ \text{C}_6\text{H}_5\text{ClN}_5^+$ 182.0228; found, 182.0223.

2-(1*H*-1,2,4-Triazol-3-yl)thiophen-3-amine (**161**, CAS [1250372–48-5]): Synthesised from 3-aminothiophene-2-carbonitrile (**130l**) (124 mg, 1 mmol) according to the general procedure (**V**) to afford **161** (66 mg, 40%) as yellow solid. ^1H NMR (400 MHz, MeOD) δ 8.70 (s, 1H), 7.66 (d, $J=5.4$ Hz, 1H), 7.14 (d, $J=5.4$ Hz, 1H), ^{13}C NMR (101 MHz, MeOD) δ 154.71, 143.76, 129.26, 127.55,

123.03, 121.36, HRMS (ESI/QTOF) m/z : calcd for $[\text{M} + \text{H}]^+ \text{C}_6\text{H}_7\text{N}_4\text{S}^+$ 167.0386; found, 167.0379.

2-Chloro-6-(1*H*-1,2,4-triazol-3-yl)pyrazine (**162**, CAS [1472615–55-6]): Synthesised from 6-chloropyrazine-2-carbonitrile (**130m**) (139 mg, 1 mmol) according to the general procedure (**V**) to afford **162** (76 mg, 42%) as white solid. ^1H NMR (400 MHz, MeOD) δ 8.15 (s, 1H), 7.96 (dd, $J=4.3, 1.5$ Hz, 1H), 7.28–7.13 (m, 2H), ^{13}C NMR (101 MHz, MeOD) δ 143.31, 137.23, 125.05, 123.33, HRMS (ESI/QTOF) m/z : calcd for $[\text{M} + \text{H}]^+ \text{C}_7\text{H}_8\text{N}_5^+$ 162.0774; found, 162.0770.

Synthesis of 3-Aryl-1*H*-1,2,4-Triazoles (132a–132c) and (155–157)

3-(3-Bromo-2-methyl-6-nitrophenyl)-1*H*-1,2,4-triazole (**132a**)⁸¹: A solution of 3-bromo-2-methyl-6-nitrobenzamide (**131a**) (387 mg, 1.5 mmol) and *N,N*-dimethylformamide-dimethyl acetal (DMF-DMA) (3.0 mL) was heated under reflux for 1 h under a nitrogen atmosphere. The mixture was cooled, concentrated under reduced pressure, and the residue was washed with hexane. After drying *in vacuo*, a white solid was obtained and used in the next step without purification. The crude product was dissolved in acetic acid (2 mL), and hydrazine hydrate (90 mg, 1.65 mmol) was added dropwise to the stirred solution. The mixture was stirred at 90 °C for 2 h. After cooling to rt, the solvent was removed under reduced pressure. The mixture was dissolved in diethyl ether (5 mL) and stirred at 0 °C for 30 min. The precipitate was collected, dried under reduced pressure, and purified by FC (SiO_2 , EtOAc/petroleum ether) to give **132a** (304 mg, 72%) as white solid. ^1H NMR (400 MHz, MeOD) δ 8.70 (s, 1H), 7.99 (d, $J=8.3$ Hz, 1H), 7.84 (m, 1H), 2.31 (s, 3H).

3-(3-Chloro-2-methyl-6-nitrophenyl)-1*H*-1,2,4-triazole (**132b**): Synthesised from 3-chloro-2-methyl-6-nitrobenzamide (**131b**) (214 mg, 1.0 mmol) according to the procedure used for **132a** to afford **132b** (167 mg, 70%) as white solid. ^1H NMR (400 MHz, MeOD) δ 9.19 (s, 1H), 8.09 (d, $J=8.8$ Hz, 1H), 7.91 (d, $J=8.8$ Hz, 1H), 2.30 (s, 3H).

3-(3-Chloro-2,6-dinitrophenyl)-1*H*-1,2,4-triazole (**132c**): Synthesised from 3-chloro-2,6-dinitrobenzamide (**131c**) (244 mg, 1.0 mmol) according to the procedure used for **132a** to afford **132c** (214 mg, 80%) as white solid. ^1H NMR (400 MHz, MeOD) δ 8.60 (s, 1H), 8.24 (d, $J=8.9$ Hz, 1H), 8.06 (d, $J=8.8$ Hz, 1H).

4-Bromo-3-methyl-2-(1*H*-1,2,4-triazol-3-yl)aniline (**155**)⁸²: A mixture of **132a** (141 mg, 0.5 mmol) and $\text{SnCl}_2 \cdot 2\text{H}_2\text{O}$ (560 mg, 2.5 mmol) in absolute EtOH (3 mL) was heated to 70 °C under a nitrogen atmosphere. The progress of the reaction was monitored by TLC. After 1.5 h the starting material has disappeared. The solution was cooled to rt and poured into ice. The pH was adjusted to a slightly basic value (7–8) by addition of 5% NaHCO_3 before extraction with EtOAc (3 \times 5 mL). The collected organic phases were washed with brine, treated with charcoal and filtered. After drying over Na_2SO_4 , the solvent was removed under reduced pressure and the residue was purified by FC (silica gel, EtOAc/hexanes) to give **155** (83 mg, 66%) as white solid, m.p. 201–204 °C. ^1H NMR (400 MHz, MeOD) δ 8.45 (brs, 1H), 7.37 (d, $J=8.8$ Hz, 1H), 6.63 (d, $J=8.6$ Hz, 1H), ^{13}C NMR (101 MHz, MeOD) δ 146.79, 137.07, 133.60, 114.57, 19.63, HRMS (ESI/QTOF) m/z : calcd for $[\text{M} + \text{H}]^+ \text{C}_9\text{H}_9\text{BrN}_4$ + 253.0089; found, 253.0092.

4-Chloro-3-methyl-2-(1*H*-1,2,4-triazol-3-yl)aniline (**156**): Prepared from **132b** (119 mg, 0.5 mmol) and $\text{SnCl}_2 \cdot 2\text{H}_2\text{O}$ (560 mg, 2.5 mmol) according to the procedure used for **155** to afford **156** (62 mg, 59%) as white solid, m.p. 208–210 °C. ^1H NMR (400 MHz, MeOD) δ 8.46 (brs, 1H), 7.20 (d, $J=8.8$ Hz, 1H), 6.69 (d, $J=8.7$ Hz, 1H), ^{13}C NMR (101 MHz, MeOD) δ 146.21, 130.54, 135.42, 114.22, 16.55.

HRMS (ESI/QTOF) m/z : calcd for $[M + H]^+$ $C_9H_9ClN_4^+$ 209.0594; found, 209.0597.

4-Chloro-2-(1*H*-1,2,4-triazol-3-yl)benzene-1,3-diamine (**157**): Prepared from **132c** (135 mg, 0.5 mmol) and $SnCl_2 \cdot H_2O$ (560 mg, 2.5 mmol) according to the procedure used for **155** to afford **157** (63 mg, 60%) as brown solid, m.p. 212–214 °C. 1H NMR (400 MHz, MeOD) δ 7.96 (s, 1H), 7.46 (d, $J=8.9$ Hz, 1H), 6.98 (d, $J=8.9$ Hz, 1H).

Synthesis of aryl carbonitriles

5-Chloro-2-(methylamino)benzonitrile (**130an**)¹²¹: A mixture of 2-amino-5-chlorobenzonitrile (**127a**) (458 mg, 3.0 mmol), dimethyl oxalate (532 mg, 4.5 mmol) and *t*-BuOK (421 mg, 3.75 mmol) in DMA (6 mL) was heated under a nitrogen atmosphere to 130–140 °C for 5 h. The mixture was poured into ice water and extracted with EtOAc (3 \times 10 mL). After concentration of the organic layers under reduced pressure, the crude product was purified by FC (silica gel, EtOAc/hexane) to afford **130an** (345 mg, 70%) as white solid. 1H NMR (400 MHz, $CDCl_3$) δ 7.42–7.34 (m, 2H), 6.65–6.58 (m, 1H), 4.68 (brs, 1H), 2.94 (dd, $J=5.1$, 1.8 Hz, 3H).

N-(4-Chloro-2-cyanophenyl)acetamide (**130aa**)¹²²: To a stirred mixture of 2-amino-5-chlorobenzonitrile (**127a**) (456 mg, 3.0 mmol) in CH_2Cl_2 (6 mL), pyridine (260 mg, 3.3 mmol), DMAP (18 mg, 0.15 mmol), and acetyl chloride (**128a**) (351 mg, 4.5 mmol) were added. The reaction mixture was stirred at rt for 3 h, then diluted with CH_2Cl_2 (10 mL) and washed with H_2O (2 \times 5 mL) and brine (2 \times 5 mL). The combined organic phases were dried over Na_2SO_4 , filtered, and concentrated under reduced pressure. The residue was triturated with pentane and dried under air to afford **130aa** (436 mg, 75%) as an oil. 1H NMR (400 MHz, DMSO) δ 10.28 (bs, 1H), 7.97 (d, $J=2.5$ Hz, 1H), 7.74 (dd, $J=8.8$, 2.6 Hz, 1H), 7.58 (d, $J=8.8$ Hz, 2H), 2.09 (s, 3H).

N-(4-Chloro-2-cyanophenyl)propionamide (**130ab**)¹²³: Synthesised the same way as **130aa** from 2-amino-5-chlorobenzonitrile (**127a**) (456 mg, 3.0 mmol) and propionyl chloride (**128b**) (304 mg, 3.3 mmol) to afford **130ab** (530 mg, 85%) as a colourless oil. 1H NMR (400 MHz, $CDCl_3$) δ 8.51–8.43 (m, 1H), 7.61–7.53 (m, 2H), 2.52 (q, $J=7.5$ Hz, 2H), 1.30 (td, $J=7.5$, 1.1 Hz, 3H).

N-(4-Chloro-2-cyanophenyl)butyramide (**130ac**, CAS [53313–24–9]): Synthesised the same way as **130aa** from 2-amino-5-chlorobenzonitrile (**127a**) (456 mg, 3.0 mmol) and butyryl chloride (**128c**) (350 mg, 3.3 mmol) to afford **130ac** (566 mg, 85%) as a colourless oil. 1H NMR (400 MHz, $CDCl_3$) δ 8.50–8.42 (m, 1H), 7.57 (dq, $J=4.6$, 2.5 Hz, 2H), 2.46 (t, $J=7.4$ Hz, 2H), 1.81 (h, $J=7.4$ Hz, 2H), 1.06 (t, $J=7.4$ Hz, 3H).

N-(4-Chloro-2-cyanophenyl)cyclopropanecarboxamide (**130ad**): Synthesised the same way as **130aa** from 2-amino-5-chlorobenzonitrile (**127a**) (456 mg, 3.0 mmol) and cyclopropanecarbonyl chloride (**128d**) (343 mg, 3.3 mmol) to afford **130ad** (528 mg, 80%) as a colourless oil. 1H NMR (400 MHz, $CDCl_3$) δ 8.50–8.40 (m, 1H), 7.61–7.53 (m, 1H), 7.56 (bs, 1H), 7.50 (s, 1H), 3.22 (pd, $J=8.5$, 1.1 Hz, 1H), 2.15–1.85 (m, 4H).

N-(4-Chloro-2-cyanophenyl)cyclobutanecarboxamide (**130ae**, CAS [2147559–95–1]): Synthesised the same way as **130aa** from 2-amino-5-chlorobenzonitrile (**127a**) (456 mg, 3.0 mmol) and cyclobutanecarbonyl chloride (**128e**) (390 mg, 3.3 mmol) to afford **130ae** (597 mg, 80%) as an oil. 1H NMR (400 MHz, $CDCl_3$) δ 8.52–8.45 (m, 1H), 7.61–7.53 (m, 1H), 7.56 (s, 1H), 7.50 (s, 1H), 3.27 (pd, $J=8.5$, 1.1 Hz, 1H), 2.50–2.25 (m, 4H), 2.18–1.91 (m, 2H).

N-(4-chloro-2-cyanophenyl)cyclopentanecarboxamide (**130af**, CAS [2242379–82–2]): Synthesised the same way as **130aa** from 2-

amino-5-chlorobenzonitrile (**127a**) (456 mg, 3.0 mmol) and cyclopentanecarbonyl chloride (**128f**) (436 mg, 3.3 mmol) to afford **130af** (632 mg, 85%) as a colourless oil. 1H NMR (400 MHz, $CDCl_3$) δ 8.52–8.45 (m, 1H), 7.61–7.53 (m, 1H), 7.56 (s, 1H), 7.50 (s, 1H), 3.27 (pd, $J=8.5$, 1.1 Hz, 1H), 2.50–2.25 (m, 4H), 2.18–1.91 (m, 4H).

N-(4-chloro-2-cyanophenyl)benzamide (**130ag**)¹²⁴: Synthesised the same way as **130aa** from 2-amino-5-chlorobenzonitrile (**127a**) (456 mg, 3.0 mmol) and benzoyl chloride (**128g**) (462 mg, 3.3 mmol) to afford **130ag** (600 mg, 78%) as an amorphous solid. 1H NMR (400 MHz, $CDCl_3$) δ 8.64 (d, $J=8.8$ Hz, 1H), 8.40 (s, 1H), 7.99–7.92 (m, 2H), 7.75–7.52 (m, 5H).

N-(2-cyanophenyl)benzamide (**130bg**)¹²⁵: Synthesised the same way as **130aa** from 2-aminobenzonitrile (**127b**) (354 mg, 3.0 mmol) and benzoyl chloride (**128g**) (462 mg, 3.3 mmol) to afford **130bg** (566 mg, 85%) as an oil. 1H NMR (400 MHz, $CDCl_3$) δ 8.65 (d, $J=8.5$ Hz, 1H), 8.45–8.40 (m, 1H), 8.01–7.93 (m, 2H), 7.73–7.52 (m, 5H), 7.25 (td, $J=7.7$, 1.1 Hz, 1H).

N-(2-chloro-6-cyanophenyl)-benzamide (**130cg**): Synthesised the same way as **130aa** from 2-amino-3-chloro-benzonitrile (**127c**) (456 mg, 3.0 mmol) and benzoyl chloride (**128g**) (462 mg, 3.3 mmol) to afford **130cg** (614 mg, 80%) as a colourless oil. 1H NMR (400 MHz, $CDCl_3$) δ 8.04–7.97 (m, 2H), 7.93 (bs, 1H), 7.77–7.68 (m, 2H), 7.67–7.62 (m, 1H), 7.59–7.52 (m, 2H), 7.37 (t, $J=8.0$ Hz, 1H).

Synthesis of aryl carboxamides

3-Bromo-2-methyl-6-nitrobenzamide (**131a**, CAS [110127–08–7]): A solution of 3-bromo-2-methylbenzoic acid (**129a**) (1.07 g, 5 mmol) in H_2SO_4 (98%, 1.1 mL) was treated with fuming nitric acid (1.1 mL) at rt. The reaction mixture was stirred for 3 h, cooled and poured into ice water (10 mL). The white precipitate was collected and dried. The aqueous filtrate was extracted with EtOAc (3 \times 10 mL) and concentrated under reduced pressure. The residue was combined with the previously collected precipitate and used in the next step without further purification. To a slurry of crude compound in CH_2Cl_2 (20 mL) at 0 °C, oxalyl chloride (661 mg, 5.25 mmol) was added under a nitrogen atmosphere, followed by dropwise addition of DMF (2.5 mmol). The mixture was stirred 5 min at 0 °C, 15 min at rt, and then heated to reflux under N_2 for 1 h. The mixture was cooled and poured into NH_4OH (15 mL, ca. 30% NH_3). Precipitated solids were collected by filtration and purified by FC to afford **131a** (903 mg, 70%) as a yellow oil. 1H NMR (400 MHz, MeOD) δ 7.96 (d, $J=8.8$ Hz, 1H), 7.89 (d, $J=8.8$ Hz, 1H), 2.55 (s, 3H).

3-Chloro-2-methyl-6-nitrobenzamide (**131b**, CAS [51123–60–5]): Synthesised the same way as **131a** from 3-chloro-2-methylbenzoic acid (**129b**) (850 mg, 5 mmol) to afford **131b** (760 mg, 71%) as a yellow oil. 1H NMR (400 MHz, MeOD) δ 8.06 (d, $J=8.8$ Hz, 1H), 7.70 (d, $J=8.8$ Hz, 1H), 2.51 (s, 3H).

3-Chloro-2-6-dinitrobenzamide (**131c**): Synthesised the same way as **131a** from 3-chloro-2-nitrobenzoic acid (**129c**) (1 g, 5 mmol) to afford **131c** (920 mg, 75%) as an oil. 1H NMR (400 MHz, MeOD) δ 8.38 (d, $J=8.9$ Hz, 1H), 8.00 (d, $J=8.9$ Hz, 1H).

Synthesis of other 1,2,4-Triazoles

N-(4-Bromophenyl)-4*H*-1,2,4-triazol-3-amine (**166**): 1-Bromo-4-iodobenzene (283 mg, 1.0 mmol) was dissolved in *N,N*-dimethylacetamide and 4*H*-1,2,4-triazol-3-amine (**163**) (168 mg, 2.0 mmol), K_2CO_3 (207 mg, 1.5 mmol), and CuI (19.1 mg, 0.1 mmol) were added under a nitrogen atmosphere. The mixture was stirred at 90 °C for 48 h. After cooling to rt, the solids were filtered and washed with

CH₂Cl₂ (2 × 10 mL). The combined organic phases were concentrated under reduced pressure and the residue was purified by FC (silica gel, EtOAc/hexane) to give **166** (93 mg, 39%) as a white solid, m.p. 190–192 °C. ¹H NMR (400 MHz, CDCl₃) δ 7.88 (s, 1H), 7.73 (d, *J* = 8.4 Hz, 2H), 7.44 (d, *J* = 8.4 Hz, 2H), ¹³C NMR (101 MHz, MeOD) δ 148.90, 135.93, 132.49, 125.22, 121.28, HRMS (ESI/QTOF) *m/z*: calcd for [M + H]⁺ C₈H₈BrN₄⁺ 238.9927; found, 238.9929.

2-((1,9a-Dihydrobenzo[4,5]thiazolo[2,3-c][1,2,4]triazol-3-yl)thio)acetamide (**168**): To the solution of (1,9a-dihydrobenzo[4,5]thiazolo[2,3-c][1,2,4]triazol-3-yl)thiol (**164**) (207 mg, 1.0 mmol) in acetone (5 mL), K₂CO₃ (138 mg, 1.0 mmol) and 2-chloroacetamide (**165**) (191 mg, 1.0 mmol) were added. The reaction mixture was heated under reflux for 9 h, then cooled to rt, filtered, and acidified with aq. 2 N HCl solution. The precipitate was filtered, washed with cold water (2 mL), and recrystallized from aqueous ethanol to afford **168** (160 mg, 60%) as white solid. ¹H NMR (400 MHz, CDCl₃) δ 7.92–7.77 (m, 2H), 7.10 (td, *J* = 8.5, 4.3 Hz, 2H), 6.91–6.73 (m, 2H), 4.54 (brs, 1H), ¹³C NMR (101 MHz, CDCl₃) δ 154.81, 152.73, 132.28, 132.26, 127.32, 127.30, 124.37, 118.59, 118.56, 110.64, HRMS (ESI/QTOF) *m/z*: calcd for [M + Na]⁺ C₁₀H₈N₄O₂Na⁺ 287.0032; found, 287.0037.

Protein expression and purification

Full-length human IDO1 gene was cloned into the pET-28a vector and expressed in *E. coli* Rosetta (DE3) cells. Protein was produced in LB medium supplemented with 0.5 mM dALA (5-aminolevulinic acid) and was induced by addition of 0.1 mM isopropylthio-β-galactoside overnight at 16 °C. The culture was harvested and frozen at –80 °C until further use. The frozen cells were lysed by sonication in 20 mM Tris pH 7, 400 mM NaCl, 1 mM MgCl₂, 20 mM imidazole, 1 mM DTT, 0.5 mg/mL Lysozyme and Protease inhibitor. After centrifugation, the supernatant was loaded into a HisTrap HP column pre-equilibrated with buffer containing 20 mM Tris pH 7, 500 mM NaCl and 20 mM imidazole, and eluted with the same buffer containing 500 mM imidazole. Fractions containing IDO1 were pooled, concentrated, and injected on a size exclusion chromatography column (HiLoad Superdex S75 16/60) to increase purity. hIDO1 fractions were concentrated to 20 mg/mL in 20 mM Tris pH 7 and 150 mM NaCl.

Protein crystallisation, data collection, structure determination and model refinement

hIDO1 protein at 20 mg/mL was mixed with compound MMG-0472 at a final concentration of 5 mM, and co-crystallized by sitting drop vapour diffusion method. Crystals formed in a couple of days in 15% PEG 4000, 0.2 M lithium sulphate, and 0.1 M Tris pH 7.5. The crystals were cryoprotected with 25% glycerol. Diffraction data were collected at the Paul Scherrer Institute (SLS, Villigen) at PXII-X06DA beamline. Data were processed with the XDS Program Package¹²⁶. Structures were solved by molecular replacement using Phaser-MR and chain A of PDB entry 2d0t⁴⁰ as the model. Manual model building and structure refinement were carried out in Phenix Suite¹²⁷ using coot software¹²⁸ and phenix-refine, respectively. After validation, the ligand bound IDO1 model was deposited in the PDB database under PDB code 7zv3. Data collection and refinement statistics are summarised in the Supplementary Information (Table S1). The structures were displayed with PyMOL (<http://www.pymol.org/>) and UCSF Chimera¹²⁹. Authors will release the atomic coordinates and experimental data upon article publication.

Enzymatic assays

The enzymatic inhibition assays were performed as described by Takikawa et al.¹³⁰ with some modifications. Briefly, the reaction mixture (100 μL) contained potassium phosphate buffer (100 mM, pH 6.5) ascorbic acid (20 mM), catalase (400 units/mL), methylene blue (10 μM), purified recombinant IDO1 (2.5 ng/μL), L-Trp (100 μM), Triton X-100 (0.01%) and DMSO (5 μL). The inhibitors were serially diluted 3-fold for at least 8 different concentrations. After incubation at room temperature for 20 min, the reaction was stopped in its linear phase by addition of trichloroacetic acid solution (40 mL, 30% w/v), and the samples were incubated at 50 °C for 30 min. After centrifugation, 80 μL of supernatant from each well were used for HPLC analysis. The mobile phase for HPLC analysis was composed of 50% (v/v) of methanol and 50% of sodium citrate buffer (40 mM, pH 2.4) containing 400 μM sodium dodecyl sulphate. An Agilent Zorbax Eclipse XDB C18 column (150 × 4.6 mm) was used at 23 °C with a flow rate of 1 mL/min and an injection volume of 20 μL. For detection of kynurenine, absorption at 365 nm was measured, while remaining L-Trp was detected at a wavelength of 280 nm. All assays were carried out in duplicates. The activity (Act) of each compound was calculated as $Act = RT \log(IC_{50})$ in analogy to the relation between the binding free energy and the K_i value. The ligand efficiency (LE) was calculated as $LE = -Act/N_{HA}$, where N_{HA} is the number of non-hydrogen atoms (heavy atoms) in the compound.

Cellular assays

The cDNA encoding hIDO1 (NCBI, NM 0021464.3) was purchased from Origene as pCMV6-Entry vector (RC206592). The full ORF of hIDO1 was cloned into the mammalian expression vector pcDNA6/myc-His from Invitrogen. Human embryonic kidney 293 T (HEK 293 T) cells were transiently transfected with the plasmid construct encoding hIDO1. A 75 cm² flask containing HEK 293 T cells at a confluency of 70% was transfected with jetPEI DNA transfection reagent (Polyplus-transfection), according to manufacturer's protocol. A total of 20 μg of pcDNA-IDO1 along with 5 μg of pcDNA-GFP plasmid were used for the transfection; GFP was used to evaluate transfection efficiency prior to the cellular assays. 16–18 h post-transfection the 293 T cells were detached with trypsin, centrifuged, and re-suspended in 25 mL of DMEM medium without phenol red, supplemented with penicillin and streptomycin, 10% foetal bovine serum and 1 mM pyruvate (Gibco). Subsequently, 100 μL of cells were distributed to each well of two 96-well round-bottom plates that had been pre-loaded with 100 μL DMEM and the small organic test molecule in DMSO (for a final DMSO concentration of 2%). DMEM medium contains 78 μM L-Trp and was supplemented with 500 μM of L-Trp. Cells transfected with hIDO1 were incubated for 7 h at 37 °C in a CO₂ incubator. The reaction was stopped in its linear phase by adding trichloroacetic acid (TCA) to the medium at a final concentration of 4%. Plates were centrifuged for 15 min at 4,000 rpm. 100 μL of supernatant was added to 100 μL of 2% (w/v) DMAB in glacial acetic acid. After 10 min the absorbance was measured at a wavelength of 480 nm to detect kynurenine formation⁸⁵. Alternatively, kynurenine content was determined by HPLC as done for the enzymatic assay.

Cell viability

Following DMSO (negative control) or inhibitor treatments, apoptotic cells were detected by 4',6-diamidino-2-phenylindole (DAPI)

staining. Briefly, after 7 h of incubation, cells were washed with PBS, resuspended in PBS with 1 µg/mL DAPI and immediately analysed using a BD LSR II cytometer. A 405 nm laser with 450/50 nm bandpass filter was used to collect data.

Acknowledgements

We thank Bili Seijo from the Melita Irving and George Coukos laboratory for providing the IDO1 construct and Jean Philippe Gaudry from the Protein Production and Structure Core Facility for rhIDO1 production and purification. We would like to thank Ganesh Kumar Mothukuri for help with the analytical HPLC analysis for purity of the compounds. We acknowledge computational resources from Vital-IT (SIB Swiss Institute of Bioinformatics) and the Scientific Computing and Research Support Unit (University of Lausanne). We thank the local contacts of the Swiss Light Source beamline (SLS-PSI) for their support. We are grateful to Antoine Daina for fruitful discussions. MarvinSketch 21.15, 2021, and InstantJChem 21.2.0, 2020, ChemAxon (<http://www.chemaxon.com>), were used for displaying and handling chemical structures.

Author contributions

U.F.R. designed the compounds, performed the enzymatic assays and the HPLC analysis of enzymatic and cellular samples, performed docking calculations, determined the X-ray crystallographic protein structures with F.P., analysed and interpreted the data. S.M.R. and P.V. planned, carried out, and documented chemical synthesis and characterisation. A.R. and F.P. performed protein expression and crystallography. N.D., P.R., and K.A. carried out the cellular assays under supervision of M.I. and G.C. O.M. and V.Z. initiated the project, provided critical feedback, and contributed to compound design. U.F.R., S.M.R., P.V., and V.Z. wrote the manuscript.

Disclosure statement

No potential conflict of interest was reported by the author(s).

Supporting information

X-ray data collection and refinement statistics, previously determined cellular inhibition and toxicity data, binding poses of 5-substituted 4-aryl-1,2,3-triazoles, enzymatic dose-response curves of all compounds, HPLC purity traces, NMR spectra.

Accession codes

Compound MMG-0472, PDB ID 7zv3. Authors will release the atomic coordinates upon article publication.

Funding

The author(s) reported there is no funding associated with the work featured in this article.

ORCID

Ute F. Röhrig <http://orcid.org/0000-0002-4676-4087>
Somi Reddy Majjigapu <http://orcid.org/0000-0001-6422-5223>
Pierre Vogel <http://orcid.org/0000-0002-7399-2341>

Aline Reynaud <http://orcid.org/0000-0002-9694-7383>
Florence Pojer <http://orcid.org/0000-0002-9183-7206>
Nahzli Dilek <http://orcid.org/0000-0002-3375-2773>
Kelly Ascensão <http://orcid.org/0000-0001-6693-6897>
Melita Irving <http://orcid.org/0000-0002-6849-7194>
George Coukos <http://orcid.org/0000-0001-8813-7367>
Olivier Michielin <http://orcid.org/0000-0003-4926-6355>
Vincent Zoete <http://orcid.org/0000-0002-2336-6537>

References

- Kraehenbuehl L, Weng C-H, Eghbali S, et al. Enhancing immunotherapy in cancer by targeting emerging immunomodulatory pathways. *Nat Rev Clin Oncol* 2022;19:37–50.
- Uyttenhove C, Pilotte L, Théate I, et al. Evidence for a tumoral immune resistance mechanism based on tryptophan degradation by indoleamine 2,3-dioxygenase. *Nat Med* 2003;9:1269–74.
- Platten M, Nollen EAA, Röhrig UF, et al. Tryptophan metabolism as a common therapeutic target in cancer, neurodegeneration and beyond. *Nat Rev Drug Discov* 2019;18:379–401.
- Mondanelli G, Mandarano M, Belladonna ML, et al. Current challenges for IDO2 as target in cancer immunotherapy. *Front Immunol* 2021;12:679953.
- Yuasa HJ, Stocker R. Methylene blue and ascorbate interfere with the accurate determination of the kinetic properties of IDO2. *FEBS J* 2021;288:4892–904.
- Munn DH, Mellor AL. Indoleamine 2,3-dioxygenase and tumor-induced tolerance. *J Clin Invest* 2007;117:1147–54.
- Spranger S, Spaapen RM, Zha Y, et al. Up-regulation of PD-L1, IDO, and Tregs in the melanoma tumor microenvironment is driven by CD⁸⁺ T cells. *Sci Transl Med* 2013;5:200–ra116.
- Spranger S, Koblisch HK, Horton B, et al. Mechanism of tumor rejection with doublets of CTLA-4, PD-1/PD-L1, or IDO blockade involves restored IL-2 production and proliferation of CD8(+) T cells directly within the tumor microenvironment. *J Immunother Cancer* 2014;2:3.
- Long GV, Dummer R, Hamid O, et al. Efficacy of pembrolizumab versus placebo plus pembrolizumab in patients with unresectable or metastatic melanoma (ECHO-301/KEYNOTE-252): a phase 3, randomised, double-blind study. *Lancet Oncol* 2019;20:1083–97.
- Muller AJ, Manfredi MG, Zakharia Y, Prendergast GC. Inhibiting IDO pathways to treat cancer: lessons from the ECHO-301 trial and beyond. *Semin Immunopathol* 2019;41:41–8.
- Van den Eynde BJ, van Baren N, Baurain J-f. Is there a clinical future for IDO1 inhibitors after the failure of epacadostat in Melanoma? *Annu Rev Cancer Biol* 2020;4:241–256.
- Pallotta MT, Orabona C, Volpi C, et al. Indoleamine 2,3-dioxygenase is a signaling protein in long-term tolerance by dendritic cells. *Nat Immunol* 2011;12:870–8.
- Albini E, Rosini V, Gargaro M, et al. Distinct roles of immunoreceptor tyrosine-based motifs in immunosuppressive indoleamine 2,3-dioxygenase 1. *J Cell Mol Med* 2017;21:165–76.
- Albini E, Coletti A, Greco F, et al. Identification of a 2-propanol analogue modulating the nonenzymatic function of indoleamine 2,3-dioxygenase 1. *Biochem Pharmacol* 2018;158:286–97.

15. Nelp MT, Kates PA, Hunt JT, et al. Immune-modulating enzyme indoleamine 2,3-dioxygenase is effectively inhibited by targeting its apo-form. *Proc Natl Acad Sci USA* 2018;115:3249–54.
16. Lim YJ, Foo TC, Yeung AWS, et al. Human indoleamine 2,3-dioxygenase 1 is an efficient Mammalian nitrite reductase. *Biochemistry* 2019;58:974–86.
17. Stanley CP, Maghzal GJ, Ayer A, et al. Singlet molecular oxygen regulates vascular tone and blood pressure in inflammation. *Nature* 2019;566:548–52.
18. Nelp MT, Zheng V, Davis KM, et al. Potent activation of indoleamine 2,3-dioxygenase by polysulfides. *J Am Chem Soc* 2019;141:15288–300.
19. Feng X, Liao D, Liu D, et al. Development of indoleamine 2,3-dioxygenase 1 inhibitors for cancer therapy and beyond: a recent perspective. *J Med Chem* 2020;63:15115–39.
20. Tang K, Wu Y-H, Song Y, Yu B. Indoleamine 2,3-dioxygenase 1 (IDO1) inhibitors in clinical trials for cancer immunotherapy. *J Hematol Oncol* 2021;14:68.
21. wwPDB c. Protein Data Bank: the single global archive for 3D macromolecular structure data. *Nucleic Acids Res* 2019;47:D520–D528.
22. Röhrig UF, Reynaud A, Majjigapu SR, et al. Inhibition mechanisms of indoleamine 2,3-Dioxygenase 1 (IDO1). *J Med Chem* 2019;62:8784–95.
23. Yue EW, Sparks R, Polam P, et al. INCB24360 (Epacadostat), a highly potent and selective indoleamine-2,3-dioxygenase 1 (IDO1) inhibitor for immuno-oncology. *ACS Med Chem Lett* 2017;8:486–91.
24. Kumar S, Waldo JP, Jaipuri FA, et al. Discovery of clinical candidate (1R,4r)-4-((R)-2-((S)-6-Fluoro-5H-imidazo[5,1-a]isoindol-5-yl)-1-hydroxyethyl)cyclohexan-1-ol (Navoximod), a potent and selective inhibitor of indoleamine 2,3-dioxygenase 1. *J Med Chem* 2019;62:6705–33.
25. Crosignani S, Bingham P, Botteman P, et al. Discovery of a Novel and selective indoleamine 2,3-dioxygenase (IDO-1) inhibitor 3-(5-Fluoro-1H-indol-3-yl)pyrrolidine-2,5-dione (EOS200271/PF-06840003) and its characterization as a potential clinical candidate. *J Med Chem* 2017;60:9617–29.
26. Balog A, Lin T-a, Maley D, et al. Preclinical characterization of linrodostat mesylate, a Novel, potent, and selective oral indoleamine 2,3-dioxygenase 1 inhibitor. *Mol Cancer Ther* 2021;20:467–76.
27. Röhrig UF, Michielin O, Zoete V. Structure and plasticity of indoleamine 2,3-dioxygenase 1 (IDO1). *J Med Chem* 2021;64:17690–705.
28. Röhrig UF, Majjigapu SR, Reynaud A, et al. Azole-based indoleamine 2,3-dioxygenase 1 (IDO1) inhibitors. *J Med Chem* 2021;64:2205–27.
29. Röhrig UF, Awad L, Grosdidier A, et al. Rational design of indoleamine 2,3-dioxygenase inhibitors. *J Med Chem* 2010;53:1172–89.
30. Yue EW, Douty B, Wayland B, et al. Discovery of potent competitive inhibitors of indoleamine 2,3-dioxygenase with *in vivo* pharmacodynamic activity and efficacy in a mouse melanoma model. *J Med Chem* 2009;52:7364–7.
31. Paul S, Roy A, Deka SJ, et al. Nitrobenzofurazan derivatives of N'-hydroxyamidines as potent inhibitors of indoleamine-2,3-dioxygenase 1. *Eur J Med Chem* 2016;121:364–75.
32. Zhang H, Liu K, Pu Q, et al. Discovery of amino-cyclobutane-derived indoleamine-2,3-dioxygenase 1 (IDO1) inhibitors for cancer immunotherapy. *ACS Med Chem Lett* 2019;10:1530–6.
33. Du Q, Feng X, Wang Y, et al. Discovery of phosphonamide IDO1 inhibitors for the treatment of non-small cell lung cancer. *Eur J Med Chem* 2019;182:111629.
34. Chen S, Guo W, Liu X, et al. Design, synthesis and antitumor study of a series of N-Cyclic sulfamoylaminoethyl substituted 1,2,5-oxadiazol-3-amines as new indoleamine 2,3-dioxygenase 1 (IDO1) inhibitors. *Eur J Med Chem* 2019;179:38–55.
35. Liu C, Nan Y, Xia Z, et al. Discovery of novel hydroxyamidine derivatives as indoleamine 2,3-dioxygenase 1 inhibitors with *in vivo* anti-tumor efficacy. *Bioorg Med Chem Lett* 2020;30:127038.
36. Steeneck C, Kinzel O, Anderhub S, et al. Discovery of hydroxyamidine based inhibitors of IDO1 for cancer immunotherapy with reduced potential for glucuronidation. *ACS Med Chem Lett* 2020;11:179–87.
37. Song X, Sun P, Wang J, et al. Design, synthesis, and biological evaluation of 1,2,5-oxadiazole-3-carboximidamide derivatives as Novel indoleamine-2,3-dioxygenase 1 inhibitors. *Eur J Med Chem* 2020;189:112059.
38. Jin F, Hu Q, Fei H, et al. Discovery of hydroxyamidine derivatives as highly potent, selective indoleamine-2,3-dioxygenase 1 Inhibitors. *ACS Med Chem Lett* 2021;12:195–201.
39. Sono M, Cady SG. Enzyme kinetic and spectroscopic studies of inhibitor and effector interactions with indoleamine 2,3-dioxygenase. 1. Norharman and 4-phenylimidazole binding to the enzyme as inhibitors and heme ligands. *Biochemistry* 1989;28:5392–9.
40. Sugimoto H, Oda S-i, Otsuki T, et al. Crystal structure of human indoleamine 2,3-dioxygenase: catalytic mechanism of O₂ incorporation by a heme-containing dioxygenase. *Proc Natl Acad Sci USA* 2006;103:2611–6.
41. Kumar S, Jaller D, Patel B, et al. Structure based development of phenylimidazole-derived inhibitors of indoleamine 2,3-dioxygenase. *J Med Chem* 2008;51:4968–77.
42. Fallarini S, Massarotti A, Gesù A, et al. In silico-driven multi-component synthesis of 4,5- and 1,5-disubstituted imidazoles as indoleamine 2,3-dioxygenase inhibitors. *MedChemComm* 2016;7:409–19.
43. Brant MG, Goodwin-Tindall J, Stover KR, et al. Identification of potent indoleamine 2,3-dioxygenase 1 (IDO1) inhibitors based on a phenylimidazole scaffold. *ACS Med Chem Lett* 2018;9:131–6.
44. Zheng Y, Stafford PM, Stover KR, et al. A series of 2-((1-Phenyl-1H-imidazol-5-yl)methyl)-1H-indoles as Indoleamine 2,3-Dioxygenase 1 (IDO1) Inhibitors. *ChemMedChem* 2021;16:2195–205.
45. Peng Y-H, Ueng S-H, Tseng C-T, et al. Important hydrogen bond networks in indoleamine 2,3-Dioxygenase 1 (IDO1) inhibitor design revealed by crystal structures of imidazoleisoindole derivatives with IDO1. *J Med Chem* 2016;59:282–93.
46. Zou Y, Wang F, Wang Y, et al. Discovery of imidazoleisoindole derivatives as potent IDO1 inhibitors: design, synthesis, biological evaluation and computational studies. *Eur J Med Chem* 2017;140:293–304.
47. Tu W, Yang F, Xu G, et al. Discovery of imidazoisoindole derivatives as highly potent and orally active indoleamine-2,3-dioxygenase Inhibitors. *ACS Med Chem Lett* 2019;10:949–53.

48. Parr BT, Pastor R, Sellers BD, et al. Implementation of the CYP index for the design of selective tryptophan-2,3-dioxygenase inhibitors. *ACS Med Chem Lett* 2020;11:541–9.
49. Crescenzi C, Fuchss T, Ippoliti D, et al. Reiterative chiral resolution/racemization/recycle (RRR synthesis) for an effective and scalable process for the enantioselective synthesis of a dual IDO1/TDO2 inhibitor imidazoisoindole derivative. *Org Process Res Dev* 2020;24:1018–23.
50. Tojo S, Kohno T, Tanaka T, et al. Crystal structures and structure–activity relationships of imidazothiazole derivatives as IDO1 inhibitors. *ACS Med Chem Lett* 2014;5:1119–23.
51. Peng Y-h, Liao F-y, Tseng C-t, et al. Unique sulfur–aromatic interactions contribute to the binding of potent imidazothiazole indoleamine 2,3-dioxygenase inhibitors. *J Med Chem* 2020;63:1642–59.
52. Griglio A, Torre E, Serafini M, et al. A multicomponent approach in the discovery of indoleamine 2,3-dioxygenase 1 inhibitors: synthesis, biological investigation and docking studies. *Bioorg Med Chem Lett* 2018;28:651–7.
53. Serafini M, Torre E, Aprile S, et al. Synthesis, docking and biological evaluation of a novel class of imidazothiazoles as IDO1 inhibitors. *Molecules* 2019;24:1874.
54. Cowley P, Wise A, Pharmaceutical compound. 2016; Patent WO 2016/071293.
55. Qian S, He T, Wang W, et al. Discovery and preliminary structure–activity relationship of 1H-indazoles with promising indoleamine-2,3-dioxygenase 1 (IDO1) inhibition properties. *Bioorg Med Chem* 2016;24:6194–205.
56. Yang L, Chen Y, He J, et al. 4,6-Substituted-1H-indazoles as potent IDO1/TDO dual inhibitors. *Bioorg Med Chem* 2019;27:1087–98.
57. Ning X-L, Li Y-Z, Huo C, et al. X-ray structure-guided discovery of a potent, orally bioavailable, dual human indoleamine/tryptophan 2,3-dioxygenase (hIDO/hTDO) inhibitor that shows activity in a mouse model of Parkinson's Disease. *J Med Chem* 2021;64:8303–32.
58. Röhrig UF, Majjigapu SR, Grosdidier A, et al. Rational design of 4-aryl-1,2,3-triazoles for indoleamine 2,3-dioxygenase 1 inhibition. *J Med Chem* 2012;55:5270–90.
59. Panda S, Pradhan N, Chatterjee S, et al. Manna, D. 4,5-disubstituted 1,2,3-triazoles: effective inhibition of indoleamine 2,3-dioxygenase 1 enzyme regulates t cell activity and mitigates tumor growth. *Sci Rep* 2019;9:18455.
60. Alexandre JAC, Swan MK, Latchem MJ, et al. New 4-Amino-1,2,3-triazole inhibitors of indoleamine 2,3-dioxygenase form a long-lived complex with the enzyme and display exquisite cellular potency. *ChemBioChem* 2018;19:552–61.
61. Röhrig UF, Majjigapu SR, Chambon M, et al. Detailed analysis and follow-up studies of a high-throughput screening for indoleamine 2,3-dioxygenase 1 (IDO1) inhibitors. *Eur J Med Chem* 2014;84:284–301.
62. Röhrig UF, Majjigapu SR, Caldelari D, et al. Michielin, O. 1,2,3-triazoles as inhibitors of indoleamine 2,3-dioxygenase 2 (IDO2). *Bioorg Med Chem Lett* 2016;26:4330–3.
63. Jin T, Kamijo S, Yamamoto Y. Copper-catalyzed synthesis of N-unsubstituted 1,2,3-triazoles from nonactivated terminal alkynes. *Eur J Org Chem* 2004;2004:3789–91.
64. Arcadi A, Cacchi S, Del Rosario M, et al. Palladium catalyzed reaction of o-ethynylphenols, o-((trimethylsilyl)ethynyl)phenyl acetates, and o-alkynylphenols with unsaturated triflates or halides: a route to 2-substituted-, 2,3-disubstituted-, and 2-substituted-3-acylbenzo[b]furans. *J Org Chem* 1996;61:9280–8.
65. Cheng Z-y, Li W-j, He F, et al. Synthesis and biological evaluation of 4-aryl-5-cyano-2H-1,2,3-triazoles as inhibitor of HER2 tyrosine kinase. *Bioorg Med Chem* 2007;15:1533–8.
66. Quan X; Ren Z-h, Wang Y-y, Guan Z-h. p-toluenesulfonic acid mediated 1,3-dipolar cycloaddition of nitroolefins with NaN_3 for synthesis of 4Aryl-NH-1,2,3-triazoles. *Org Lett* 2014;16:5728–31.
67. Panda S, Maity P, Manna D. Transition metal, azide, and oxidant-free homo- and heterocoupling of ambiphilic tosylhydrazones to the regioselective triazoles and pyrazoles. *Org Lett* 2017;19:1534–7.
68. Lai Q, Liu Q, He Y, et al. Triazoleimidazole (TA-IM) derivatives as ultrafast fluorescent probes for selective Ag⁺ detection. *Org Biomol Chem* 2018;16:7801–5.
69. Ponpandian T, Muthusubramanian S. Tandem Knoevenagel-[3 + 2] cycloaddition-elimination reactions: one-pot synthesis of 4,5-disubstituted 1,2,3-(NH)-triazoles. *Tetrahedron Lett* 2012;53:59–63.
70. Boyall D, Davis C, Dodd J, et al. Compounds useful as inhibitors of indoleamine 2,3-dioxygenase. 2014; Patent WO 2014/081689.
71. Boyall D, Davis C, Dodd J, et al. Compounds useful as inhibitors of indoleamine 2,3-dioxygenase, WO/2014/081689. 2014.
72. Zoller T, Uguen D, De Clan A, Flischer J. Efficient preparation of E- β -iodovinyl phenylsulfone by Finkelstein reaction at a vinylic center. *Tetrahedron Lett* 1998;39:8089–92.
73. Tsai AS, Brasse M, Bergman RG, Ellman JA. Rh(III)-catalyzed oxidative coupling of unactivated alkenes via C–H activation. *Org Lett* 2011;13:540–2.
74. Tomé AC, Science of synthesis, 13: category 2, hetarenes and related ring systems. Stuttgart, New York, Delhi, Rio: Thieme Verlagsgruppe; 2004:415–601.
75. Liu Y-L, Xu X-H, Qing F-L. Regioselective dehydroxytrifluoromethylthiolation of allylic and propargylic alcohols with AgSCF_3 . *Tetrahedron Lett* 2019;60:953–6.
76. Koniev O, Leriche G, Nothisen M, et al. Selective irreversible chemical tagging of cysteine with 3-arylpropionitriles. *Bioconjug Chem* 2014;25:202–6.
77. Pauli L, Tannert R, Scheil R, Pfaltz A. Asymmetric hydrogenation of furans and benzofurans with iridium-pyridine-phosphinite catalysts. *Chem- A Eur J* 2015;21:1482–7.
78. Lanni TB, Greene KL, Kolz CN, et al. Design and synthesis of phenethyl benzo[1,4]oxazine-3-ones as potent inhibitors of PI3Kinase γ . *Bioorg Med Chem Lett* 2007;17:756–60.
79. Cox RJ, Ritson DJ, Dane TA, et al. Room temperature palladium catalysed coupling of acyl chlorides with terminal alkynes. *Chem Commun* 2005;1037–9.
80. Shechter S, Kauffmann M, Sandanyaka VP, Shacham S, Nuclear transport modulators and uses thereof, WO/2011/109799. 2011.
81. Sun X, Hong Z, Liu M, et al. Design, synthesis, and biological activity of novel tetrahydropyrazolopyridone derivatives as FXa inhibitors with potent anticoagulant activity. *Bioorg Med Chem* 2017;25:2800–10.
82. Bellamy F, Ou K. Selective reduction of aromatic nitro compounds with stannous chloride in non acidic and non aqueous medium. *Tetrahedron Lett* 1984;25:839–42.
83. Panigrahi R, Panda S, Behera PK, et al. Recyclable bimetallic CuMoO_4 nanoparticles for C–N cross-coupling reaction under mild conditions. *New J Chem* 2019;43:19274–8.

84. Aboelmagd A, Ali IA, Salem EM, Abdel-Razik M. Synthesis and antifungal activity of some S-mercaptotriazolobenzothiazolyl amino acid derivatives. *Eur J Med Chem* 2013;60:503–11.
85. Littlejohn TK, Takikawa O, Skylas D, et al. Expression and purification of recombinant human indoleamine 2,3-dioxygenase. *Protein Expr Purif* 2000;19:22–9.
86. Boyall D, Davis C, Dodd J, et al. Compounds useful as inhibitors of indoleamine 2,3-dioxygenase. 2015; Patent US 2015/0336903.
87. Zoete V, Schuepbach T, Bovigny C, et al. Attracting cavities for docking: replacing the rough energy landscape of the protein by a smooth attracting landscape. *J Comput Chem* 2016;37:437–47.
88. Mackerell AD, Bashford D, Bellott M, et al. All-atom empirical potential for molecular modeling and dynamics studies of proteins. *J Phys Chem B* 1998;102:3586–616.
89. Mackerell AD, Feig M, Brooks CL. Extending the treatment of backbone energetics in protein force fields: limitations of gas-phase quantum mechanics in reproducing protein conformational distributions in molecular dynamics simulations. *J Comput Chem* 2004;25:1400–15.
90. Haberthür U, Caflisch A. FACTS: fast analytical continuum treatment of solvation. *J Comput Chem* 2008;29:701–15.
91. Zoete V, Grosdidier A, Cuendet M, Michielin O. Use of the FACTS solvation model for protein-ligand docking calculations: application to EADock. *J Mol Recognit* 2010;23:457–61.
92. Zoete V, Cuendet MA, Grosdidier A, Michielin O. SwissParam: a fast force field generation tool for small organic molecules. *J Comput Chem* 2011;32:2359–68.
93. Röhrig UF, Grosdidier A, Zoete V, Michielin O. Docking to heme proteins. *J Comput Chem* 2009;30:2305–15.
94. Luo S, Xu K, Xiang S, et al. High-resolution structures of inhibitor complexes of human indoleamine 2,3-dioxygenase 1 in a new crystal form. *Acta Crystallogr Sect F Struct Biol Commun* 2018;74:717–24.
95. Adamo C, Cossi M, Barone V. An accurate density functional method for the study of magnetic properties: the PBE0 model. *J Mol Struct Theochem* 1999;493:145–57.
96. Frisch MJ, Trucks GW, Schlegel HB, et al. Gaussian 16 Revision C.01. 2016; Gaussian Inc. Wallingford CT.
97. Schäfer A, Huber C, Ahlrichs R. Fully optimized contracted Gaussian basis sets of triple zeta valence quality for atoms Li to Kr. *J Chem Phys* 1994;100:5829–35.
98. Tomasi J, Mennucci B, Cammi R. Quantum mechanical continuum solvation models. *Chem Rev* 2005;105:2999–3094.
99. Cowart M, Bennani YL, Faghieh R, et al. Novel amines as Histamine-3 receptor ligands and their therapeutic applications. *WO/2002/074758*. 2002.
100. Chao MN, Lorenzo-Ocampo MV, Szajnman SH, et al. Further insights of selenium-containing analogues of WC-9 against *Trypanosoma cruzi*. *Bioorg Med Chem* 2019;27:1350–61.
101. Zhu X, Li W, Luo X, et al. A catalyst-free and additive-free method for the synthesis of benzothiazolethiones from oidoanilines, DMSO and potassium sulfide. *Green Chem* 2018;20:1970–4.
102. Naidu A, Ganapathy D, Sekar G. Copper(I)-catalyzed intramolecular C_{aryl}-O bond-forming cyclization for the synthesis of 1,4-benzodioxines and its application in the total synthesis of sweetening isovanillins. *Synthesis* 2010;2010:3509–19.
103. Xie S, Li Y, Liu P, Sun P. Visible light-induced radical addition/annulation to construct phenylsulfonyl-functionalized dihydrobenzofurans involving an intramolecular 1,5-hydrogen atom transfer process. *Org Lett* 2020;22:8774–9.
104. Rong Z, Hu W, Dai N, Qian G. A Hg(OTf)₂-catalyzed enolate umpolung reaction enables the synthesis of coumaran-3-ones and Indolin-3-ones. *Org Lett* 2020;22:3286–90.
105. Lee H, Torres J, Truong L, et al. Reducing agents affect inhibitory activities of compounds: results from multiple drug targets. *Anal Biochem* 2012;423:46–53.
106. Miller D, Bailey C, Sammelton R. Synthesis of isoxazolines and isoxazoles inspired by fipronil. *Synthesis* 2015;47:2791–8.
107. Li D, Liu L, Tian Y, et al. A flow strategy for the rapid, safe and scalable synthesis of N-H 1,2,3-triazoles via acetic acid mediated cycloaddition between nitroalkene and NaN₃. *Tetrahedron* 2017;73:3959–65.
108. Kallander LS, Ryan MD, Thompson SK. Compounds and Methods, WO/2003/031434. 2003.
109. Lee H, Lee JK, Min S-J, et al. Copper(I)-catalyzed synthesis of 1,4-disubstituted 1,2,3-triazoles from azidoformates and aryl terminal alkynes. *J Org Chem* 2018;83:4805–11.
110. Yan S, Gao Y, Xing R, et al. An efficient synthesis of (E)-nitroalkenes catalyzed by recoverable diamino-functionalized mesostructured polymers. *Tetrahedron* 2008;64:6294–9.
111. Maiorana S, Pocar D, Dalla Croce P. Dalla Croce, P. Studies in the enamine field reactions of sulfonyl- and nitro-enamines with azides. *Tetrahedron Lett* 1966;7:6043–5.
112. Adibekian A, Martin BR, Wang C, et al. Click-generated triazole ureas as ultrapotent *in vivo*-active serine hydrolase inhibitors. *Nat Chem Biol* 2011;7:469–78.
113. Efimov I, Bakulev V, Beliaev N, et al. Reactions of β -azolylenamines with sulfonyl azides as an approach to N-unsubstituted 1,2,3-triazoles and ethene-1,2-diamines. *Eur J Org Chem* 2014;2014:3684–9.
114. Polo EC, Wang MF, Angnes RA, et al. Enantioselective heck arylation of acyclic alkenol aryl ethers: synthetic applications and DFT investigation of the stereoselectivity. *Adv Synth Catal* 2020;362:884–92.
115. Eller C, Kehr G, Daniliuc CG, et al. Facile 1,1-carboboration reactions of acetylenic thioethers. *Organometallics* 2013;32:384–6.
116. Al-Awadi NA, Mohamed AS, Habib OM, et al. Flash vacuum pyrolysis of acetylenic amides: a mechanistic study. *J Anal Appl Pyrolysis* 2020;150:104894.
117. Blass BE, Coburn K, Lee W, et al. Synthesis and evaluation of (2-phenethyl-2H-1,2,3-triazol-4-yl)(phenyl)methanones as Kv1.5 channel blockers for the treatment of atrial fibrillation. *Bioorg Med Chem Lett* 2006;16:4629–32.
118. Yang L, Wu Y, Yang Y, et al. Catalyst-free synthesis of 4-acyl-NH-1,2,3-triazoles by water-mediated cycloaddition reactions of enaminones and tosyl azide. *Beilstein J Org Chem* 2018;14:2348–53.
119. Cowan DJ, Larkin AL, Zhang C, et al. Novel compounds as antagonists or inverse agonists at opioid receptors, WO/2008/021849. 2008.
120. Guirado A, López-Caracena L, López-Sánchez JI, et al. A new, high-yield synthesis of 3-aryl-1,2,4-triazoles. *Tetrahedron* 2016;72:8055–60.
121. Bergman J, Brynolf A, Vuorinen E. A new synthesis of 4-amino-2-quinolinones. *Tetrahedron* 1986;42:3689–96.
122. Aradi K, Novák Z. Copper-catalyzed oxidative ring closure of ortho cyanoanilides with hypervalent iodonium salts:

- arylation-ring closure approach to iminobenzoxazines. *Adv Synth Catal* 2015;357:371–6.
123. Yoshida M, Sakauchi N, Sato A, Iminopyridine derivatives and use thereof, WO/2009/131245. 2009.
 124. Sturnio C, Deroy P, Duplessis M, et al. Inhibitors of HIV replication, WO/2010/115264. 2010.
 125. O'Broin CQ, Guiry PJ. Synthesis of 2-Amino-1,3-dienes from propargyl carbonates via palladium-catalyzed carbon–nitrogen bond formation. *Org Lett* 2020;22:879–83.
 126. Kabsch W. *Acta crystallographica Section D. Biol Crystallogr.* 2010;66:125–132.
 127. Adams PD, Afonine PV, Bunkóczi G, et al. PHENIX: a comprehensive Python-based system for macromolecular structure solution. *Acta Crystallogr Sect D Biol Crystallogr* 2010;66:213–21.
 128. Emsley P, Lohkamp B, Scott WG, Cowtan K. Features and development of Coot. *Acta Crystallogr Sect D Biol Crystallogr* 2010;66:486–501.
 129. Pettersen EF, Goddard TD, Huang CC, et al. UCSF Chimera—A visualization system for exploratory research and analysis. *J Comput Chem* 2004;25:1605–12.
 130. Takikawa O, Kuroiwa T, Yamazaki F, Kido R. Mechanism of interferon-gamma action. Characterization of indoleamine 2,3-dioxygenase in cultured human cells induced by interferon-gamma and evaluation of the enzyme-mediated tryptophan degradation in its anticellular activity. *J Biol Chem* 1988;263:2041–8.